



NAT meeting

27.2.2018

agenda



9.00- 9.50:

F. Zonca: “The fishbone paradigm and the beam plasma system” with contributions from N. Carlevaro and G. Montani

9.50-10.30:

Z. Lu: “Study of EP driven Alfvén eigenmode using theoretical tools and ORB5”

10:30-10.50: coffee break

10.50- 11.20:

A. Biancalani: WP4 (global modes with turbulence and EP, with ORB5): “main results of 2017, and plans for 2018” with contributions from A. Bottino, N. Carlevaro, A. Di Siena, A. Mishchenko, I. Novikau, F. Vannini and D. Zarzoso

11:20 -12.10:

Ph. Lauber: “Update on NAT related AUG experiments and planned WP6 activities, Kinetic GAM physics (LIGKA) for AUG experiments, Progress on HAGIS wave-wave model (WP2)”

12.10 -12.30:

General discussion, other informal updates, planning for 2018 collaborations and related travel, conferences in 2018 etc...

overall goal: predict behaviour of burning fusion plasma

meso-scale structures driven by EPs
and
micro-scale turbulence
can efficiently interact via zonal structures

some of the theoretically predicted physics elements concerning their non-linear interaction have not yet been identified in experiments or simulations with respect to their importance in various regimes and with respect to other competing non-linear processes:

wave-wave interaction processes such as forced excitation, spontaneous excitation of modulational instabilities, parametric decay

present day NBI experiments: low β -EP, small $v_{EP}/v_{thi,e}$
sub-Alfvénic resonances, large orbits, low-n modes

→ small amplitudes of perturbations;

for identification and code validation: strong mode dynamics is helpful

outline

- new AUG experiments and WP6 plans
- kinetic (k)GAM simulations with LIGKA for NLED/
NAT AUG reference case (WP2)
- progress report: HAGIS wave-wave model
- WP3 report (prepared by X. Wang)

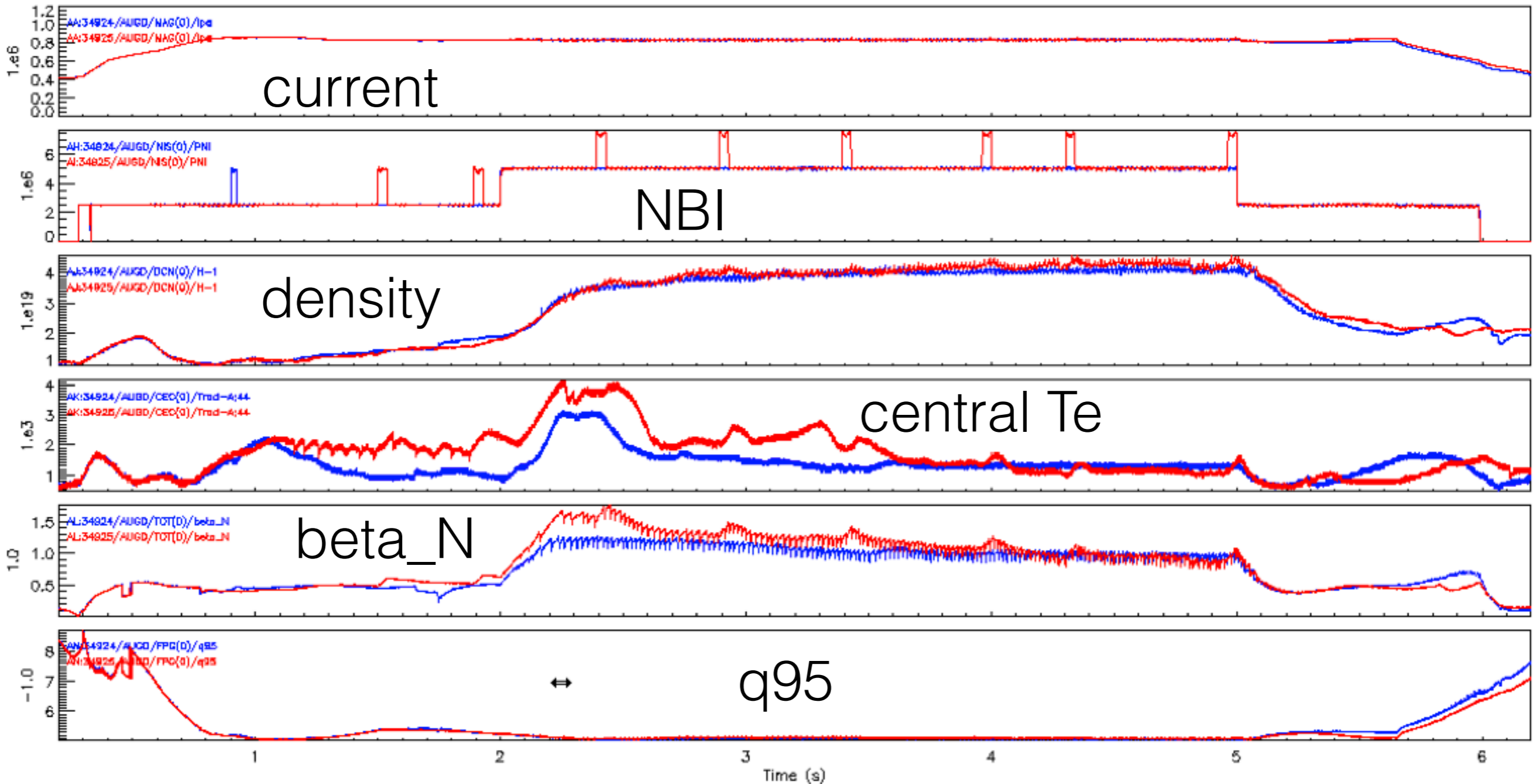
new AUG experiments - WG 6

Inspired by analysis of NLED/NAT base case, new experiments have been planned and conducted on ASDEX Upgrade (Oct 2017)

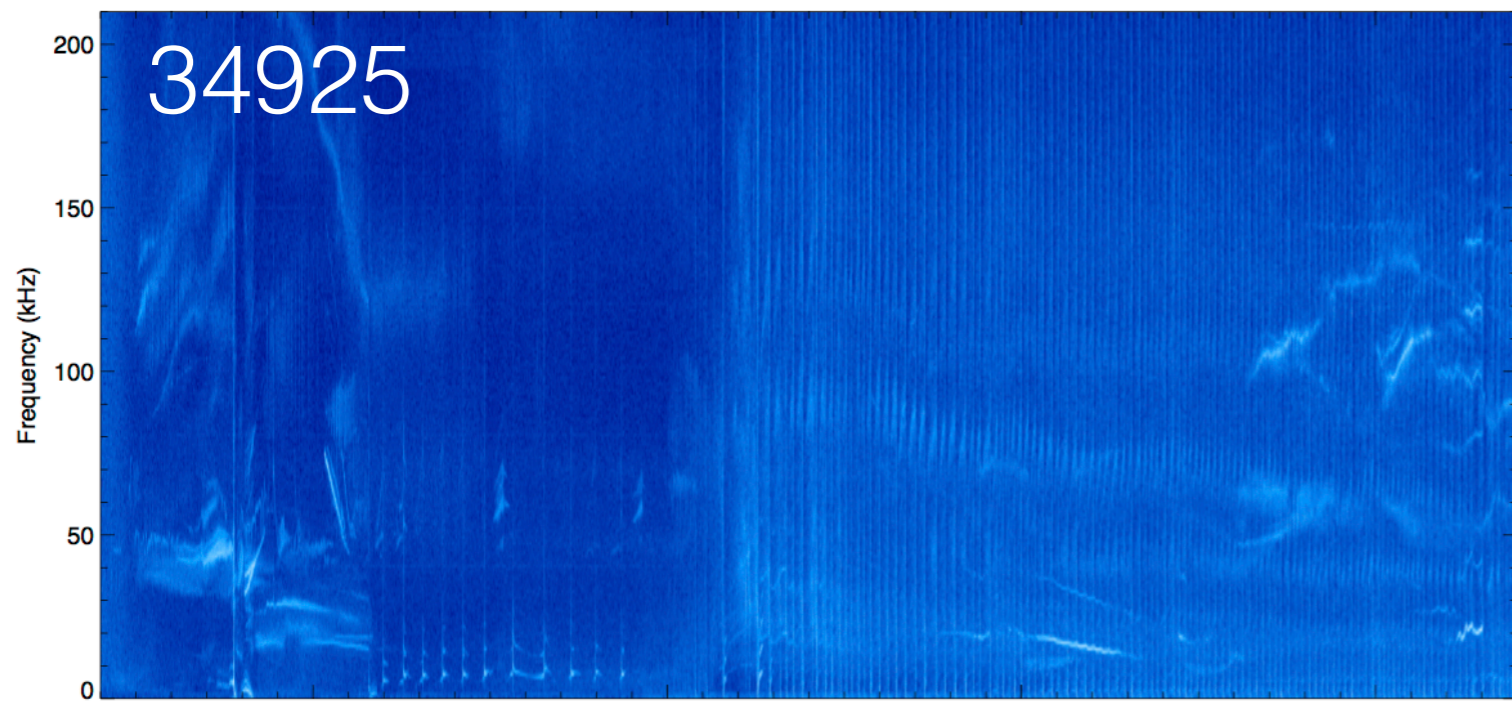


ASDEX Upgrade

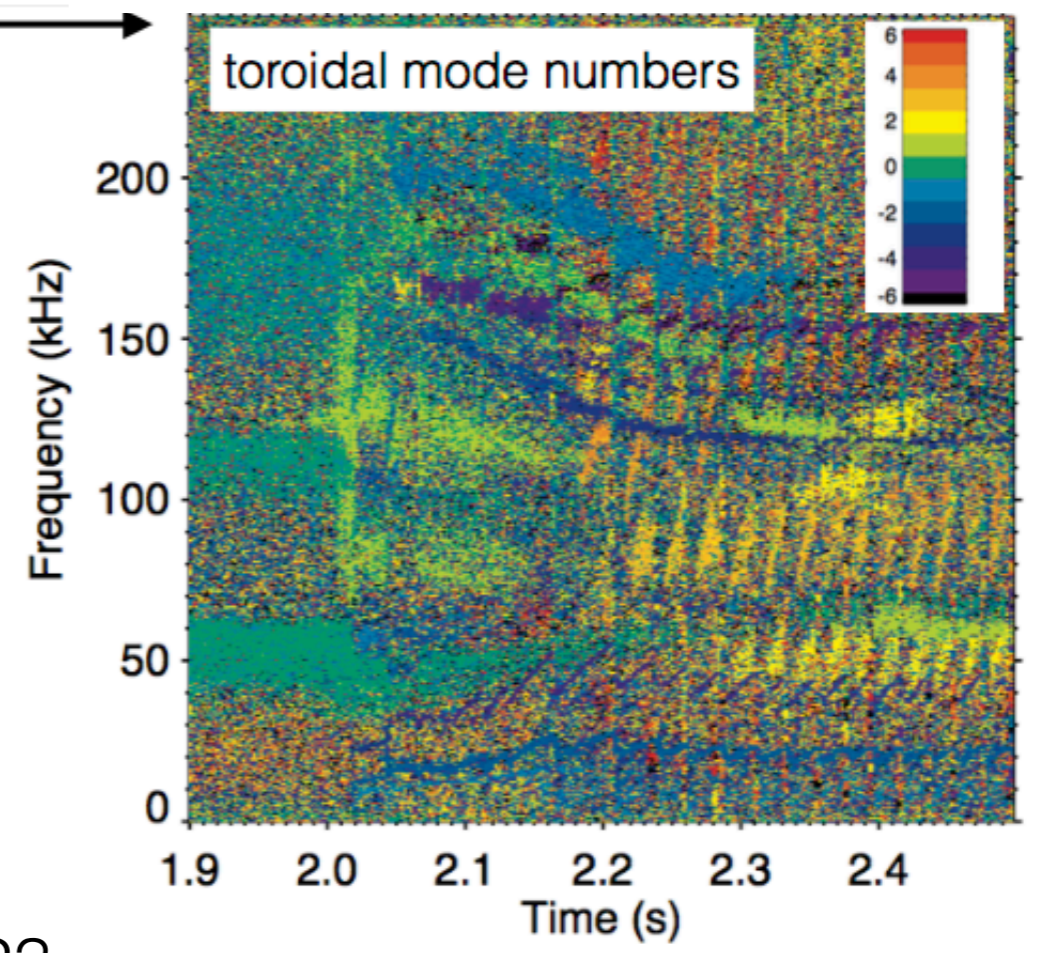
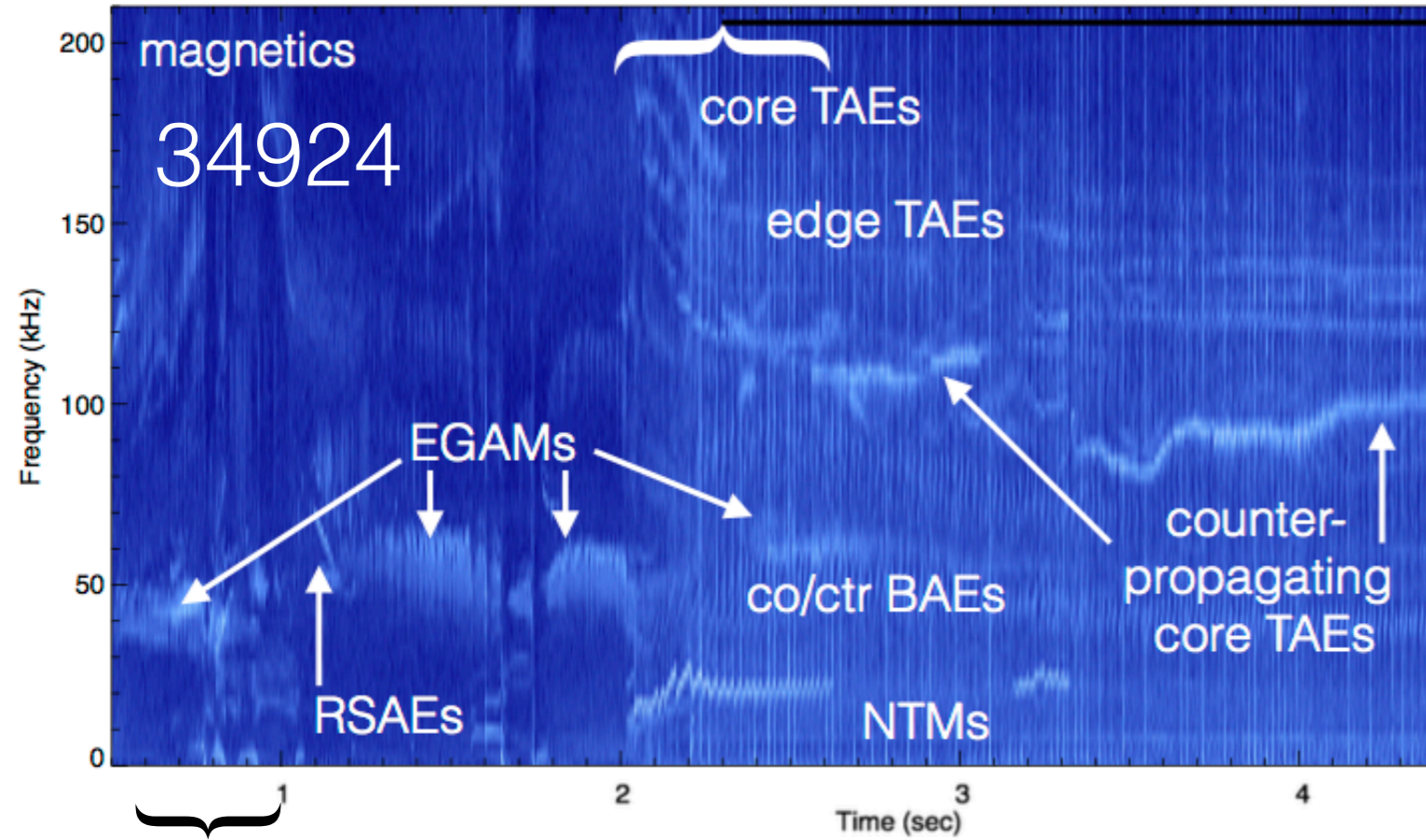
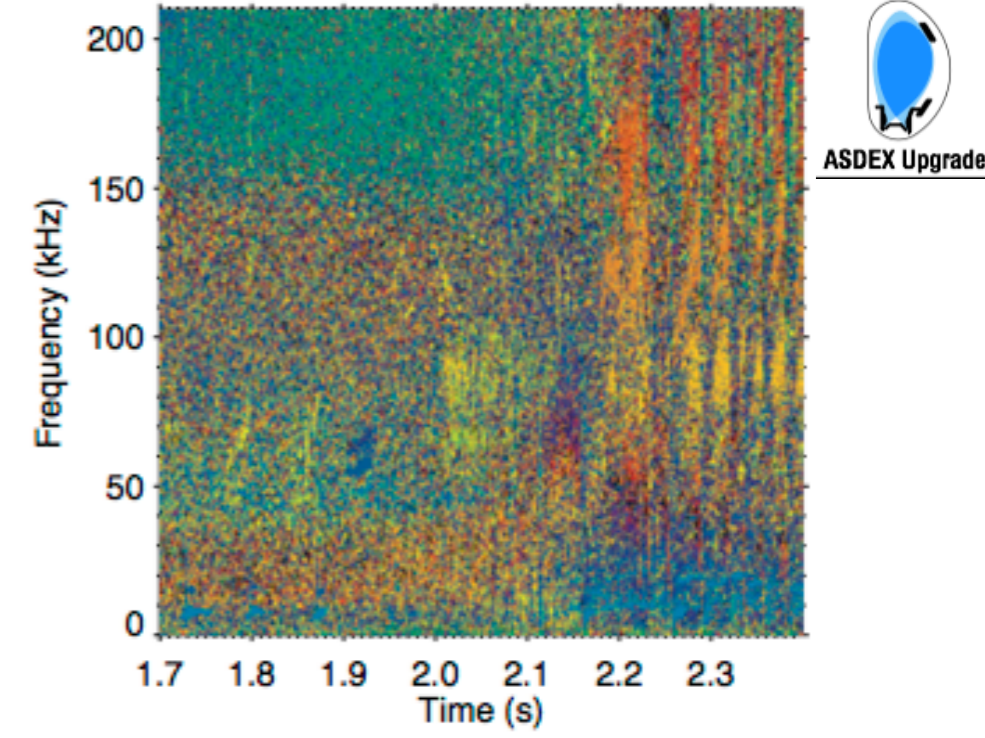
#34924/34925



high-core-radiation 'recipe' successful for reaching large β_{EP}/β_{th} : strong and 'non-linear' mode activity, stable discharge phases for EP transport studies



Toroidal mode numbers of AUGD 34925



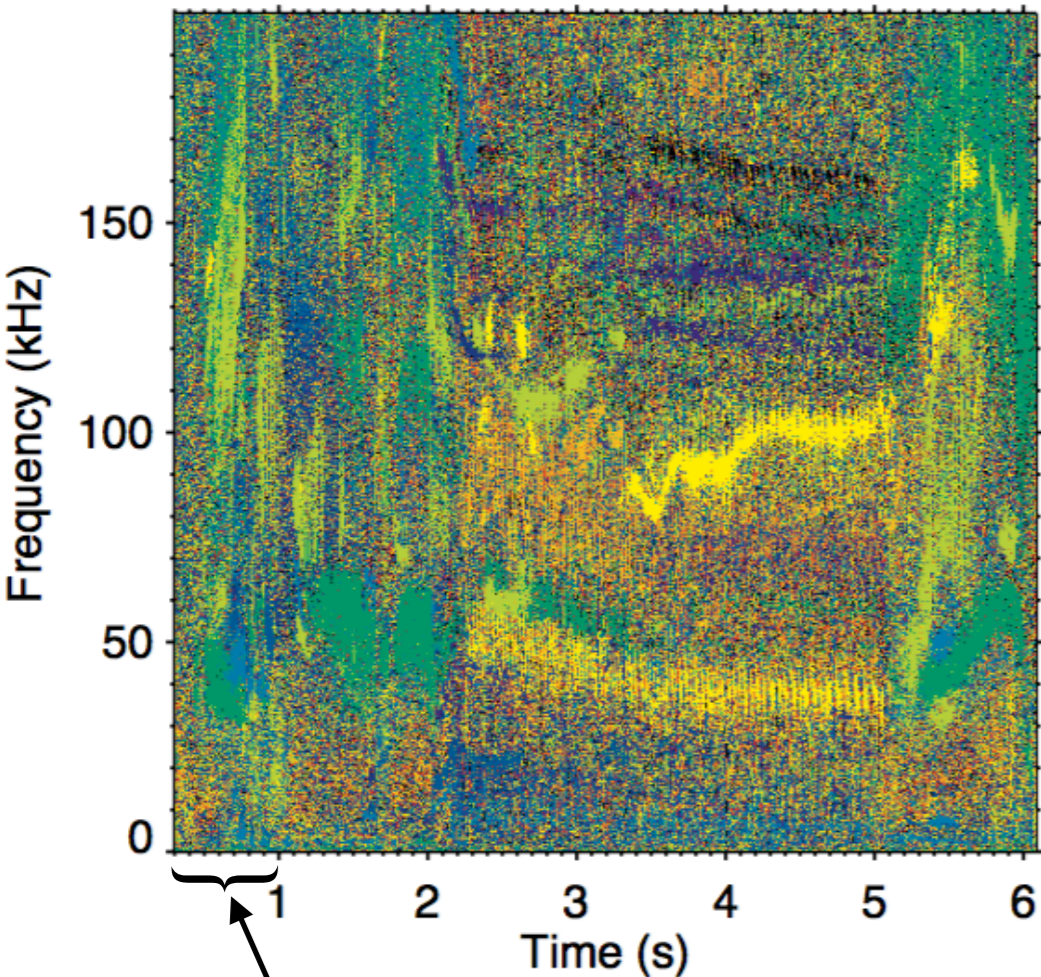
#34924: 'conditioned' with W by #34923

previous NLED base case

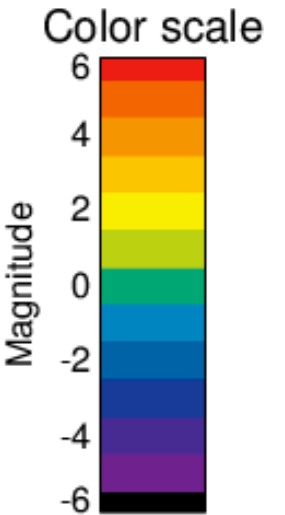
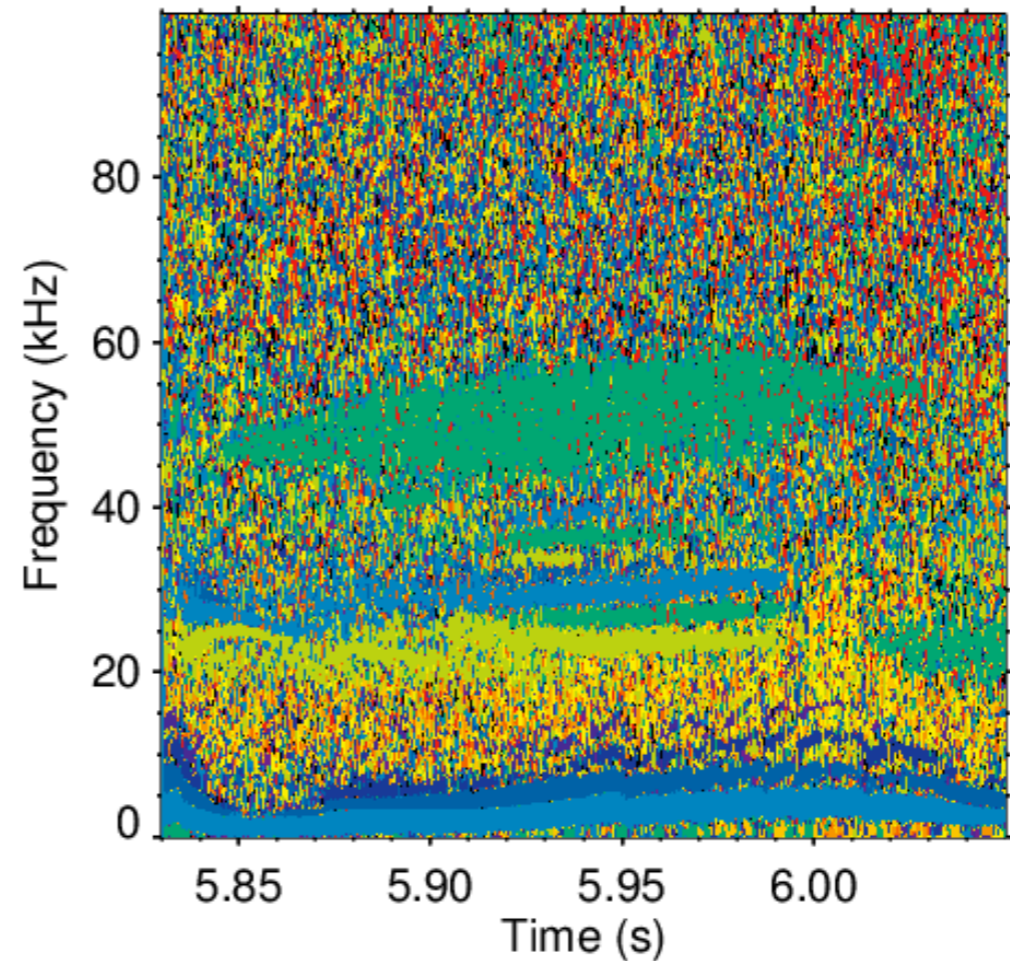
various indications for nl particle-wave and wave-wave coupling processes

strong co- and counter-propagating modes observed
most modes show non-linear evolution (chirping/bursting)

Toroidal mode numbers of AUGD 34924



Toroidal mode numbers of AUGD 34925

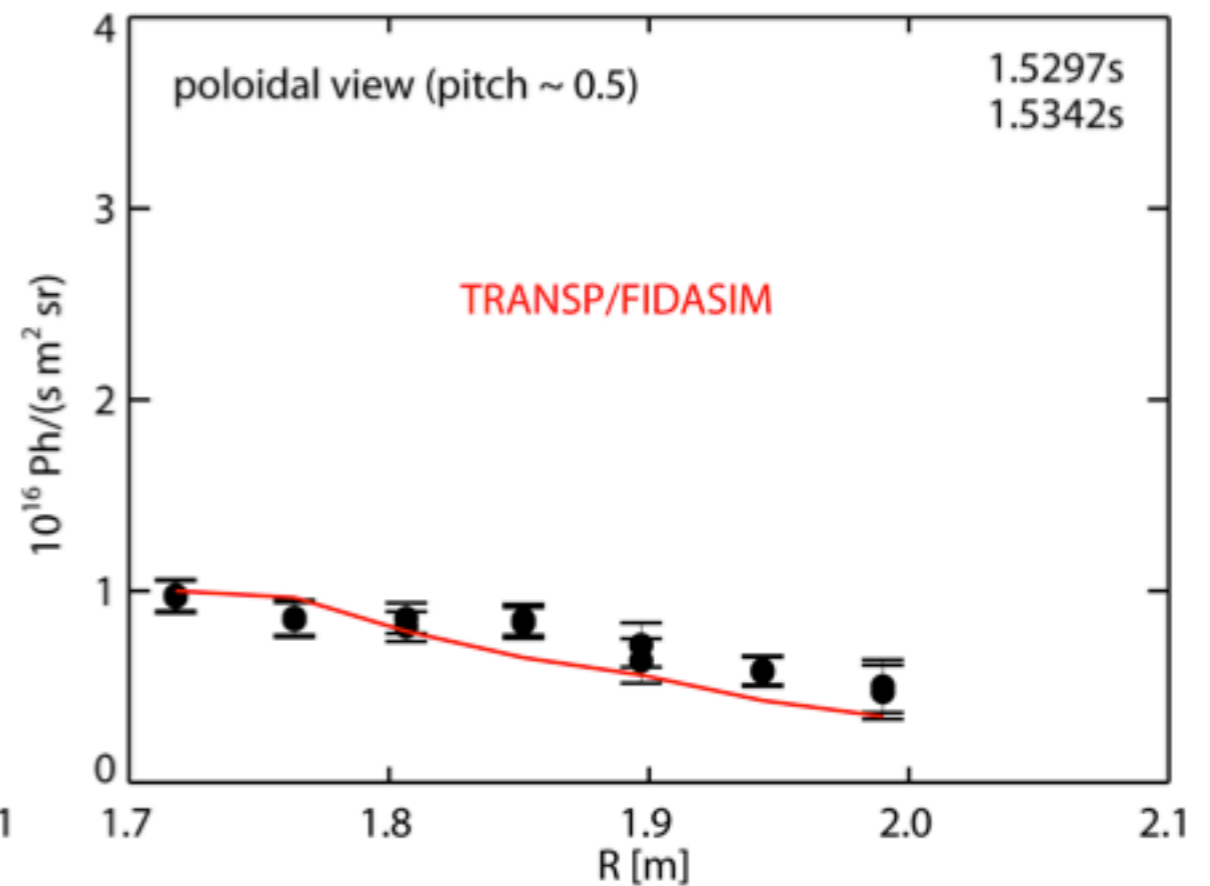
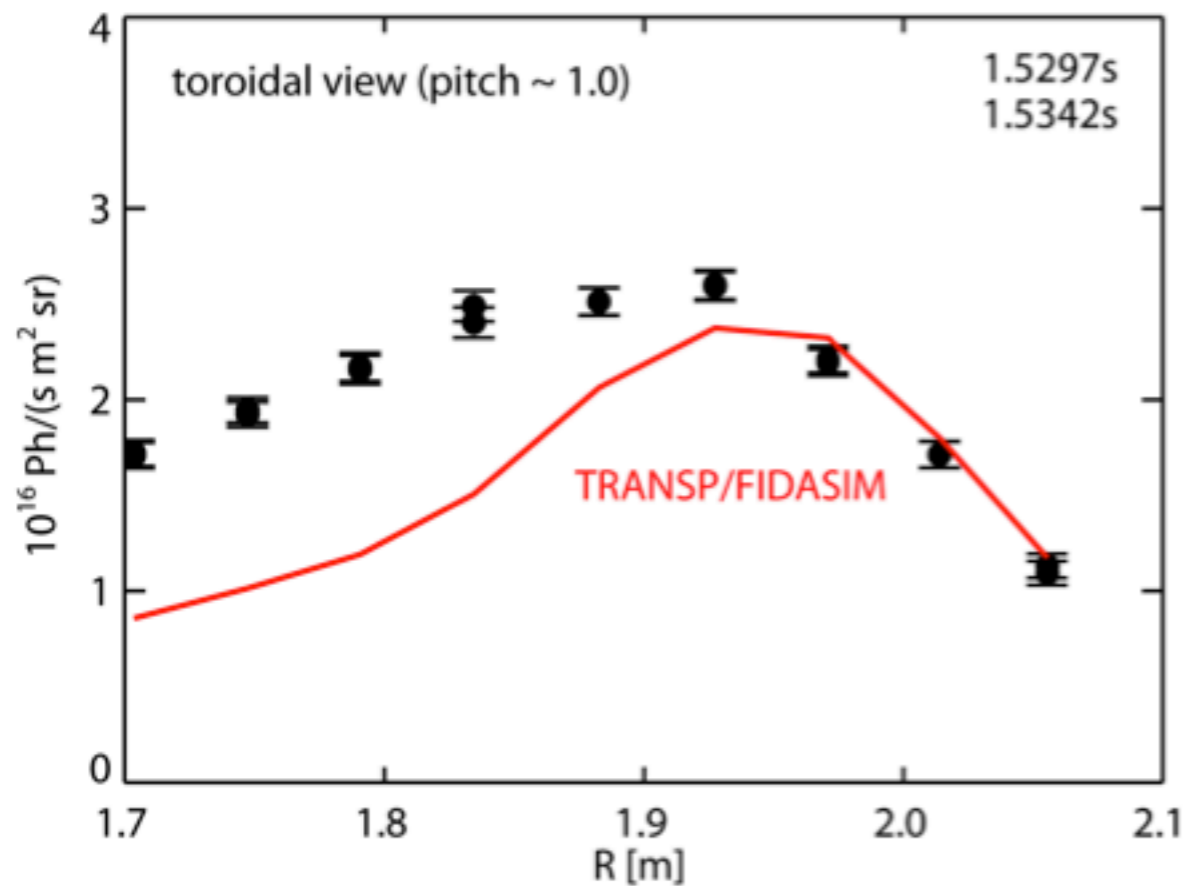


Time stamp: /afs/ipp-garching.mpg.de/hc
version: 1.8.0
shot: AUGD 34925
window: Gauss
wsize: 100
tsize: 0.0005000479s
fres: 400
step: 10
averages: 0
filter: Rel_pos
mode steps: 1.000
Coherence limit: 0.00000 %
Power limit: 0.00000 %
Q limit: 100 %
channel pairs: 28
MHI-B31-14-MHI-B31-14
MHI-B31-14-MHI-B31-03
MHI-B31-14-MHI-B31-01
MHI-B31-14-MHI-B31-02
MHI-B31-14-MHI-B31-12
MHI-B31-14-MHI-B31-22
MHI-B31-14-MHI-B31-13
MHI-B31-14-MHI-B31-03
MHI-B31-14-MHI-B31-01

various indications for nl particle-wave and
wave-wave₇ coupling processes

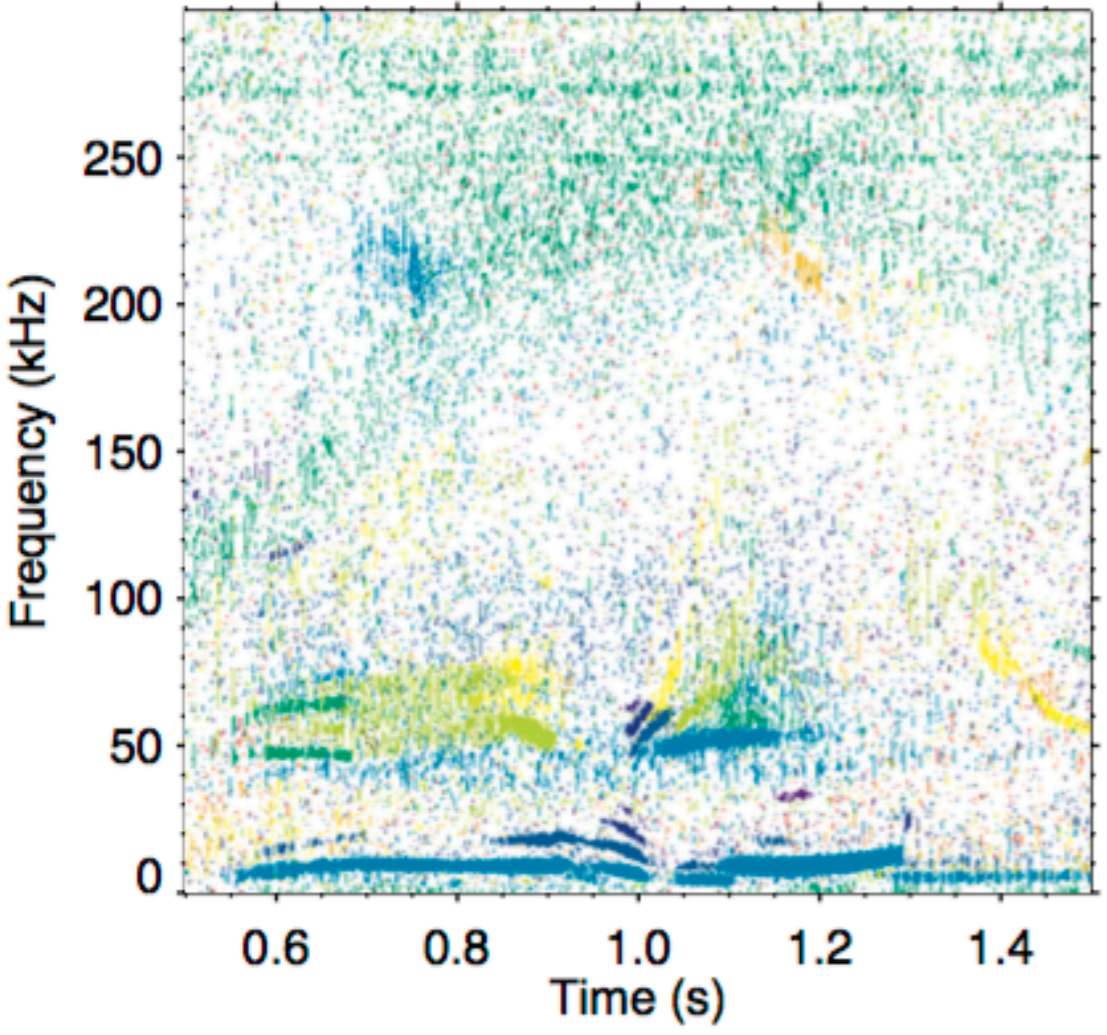


indication for strong EP transport

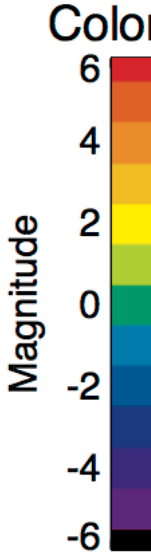
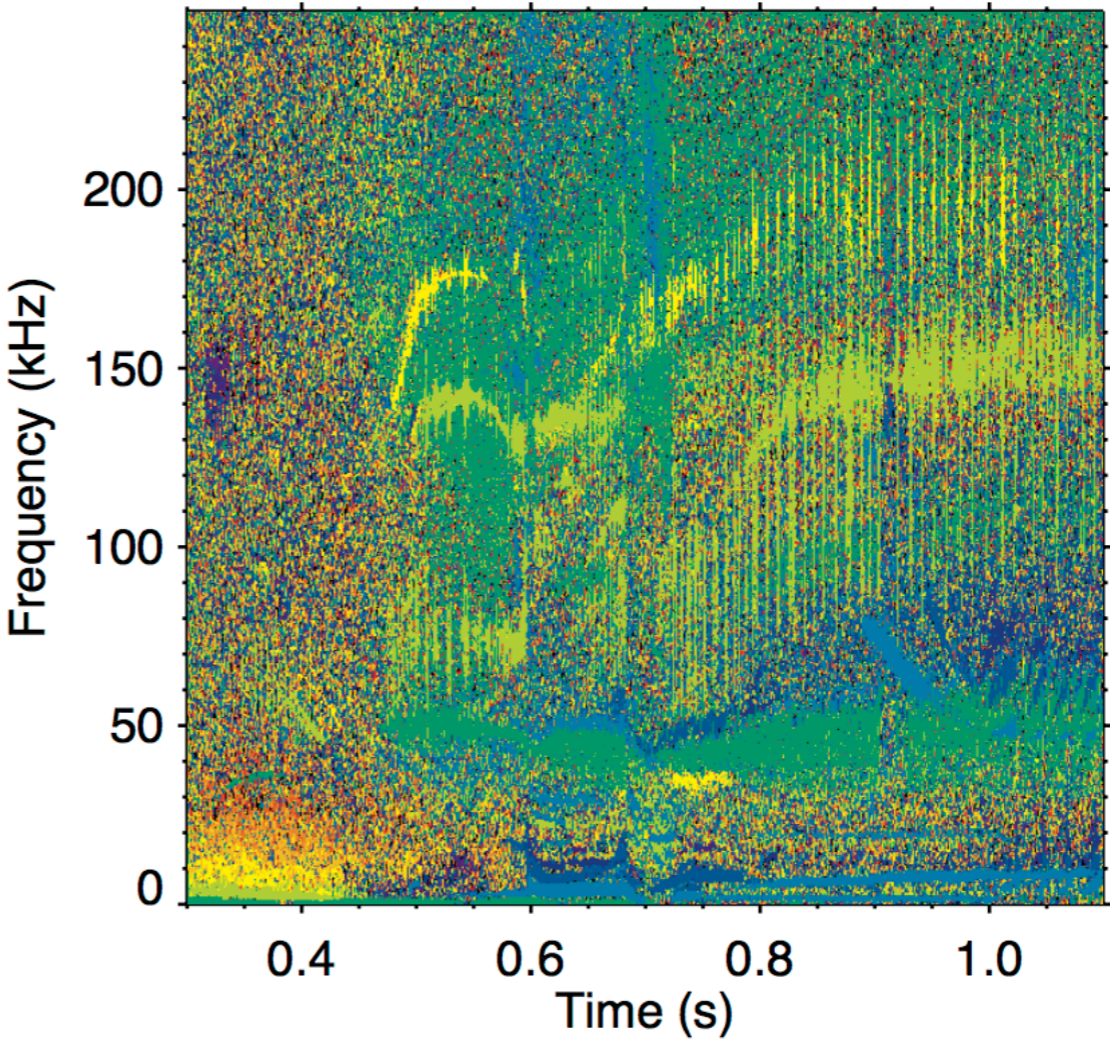


instability threshold for EGAM clearly observed

Toroidal mode numbers of AUGD 33872

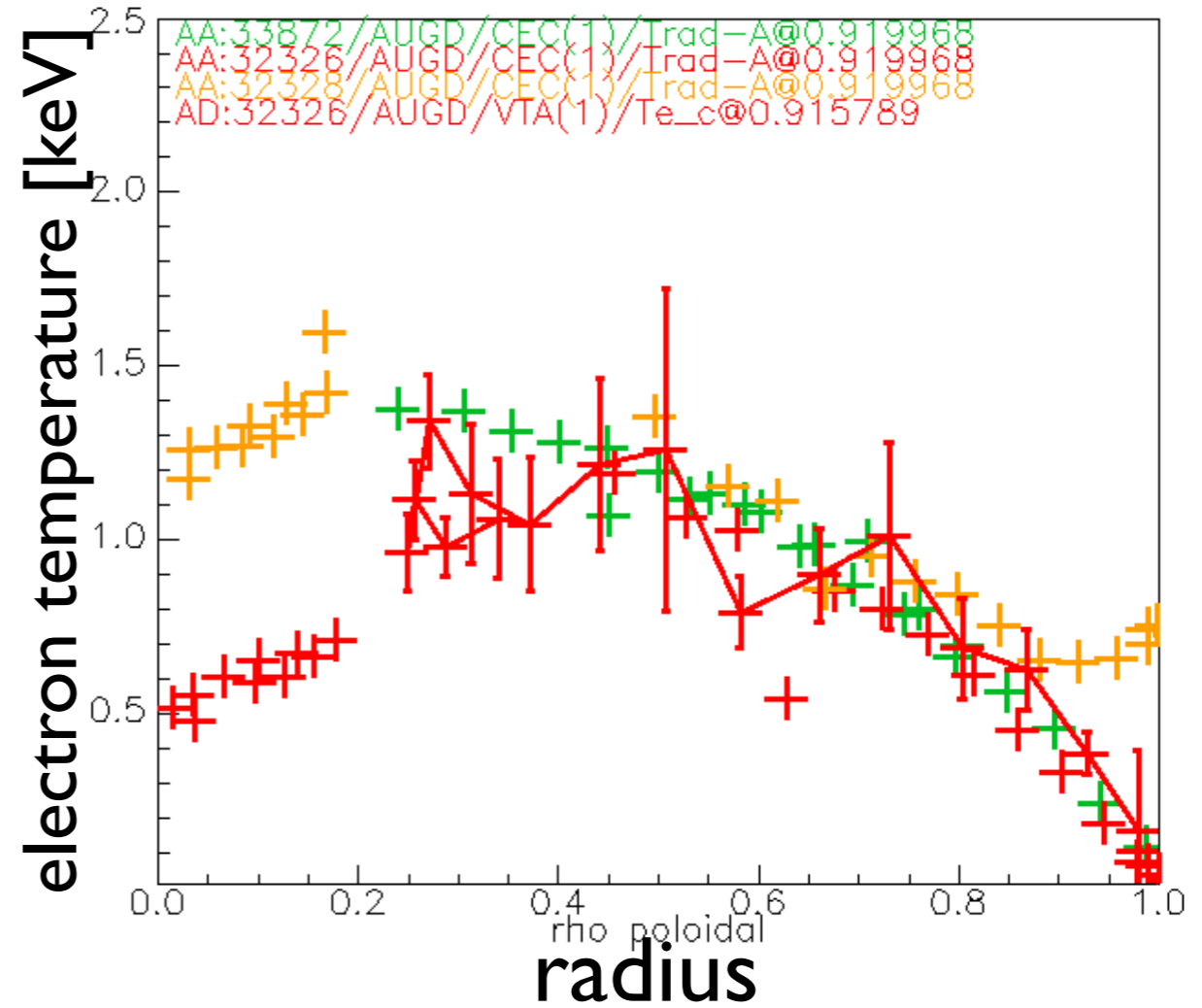
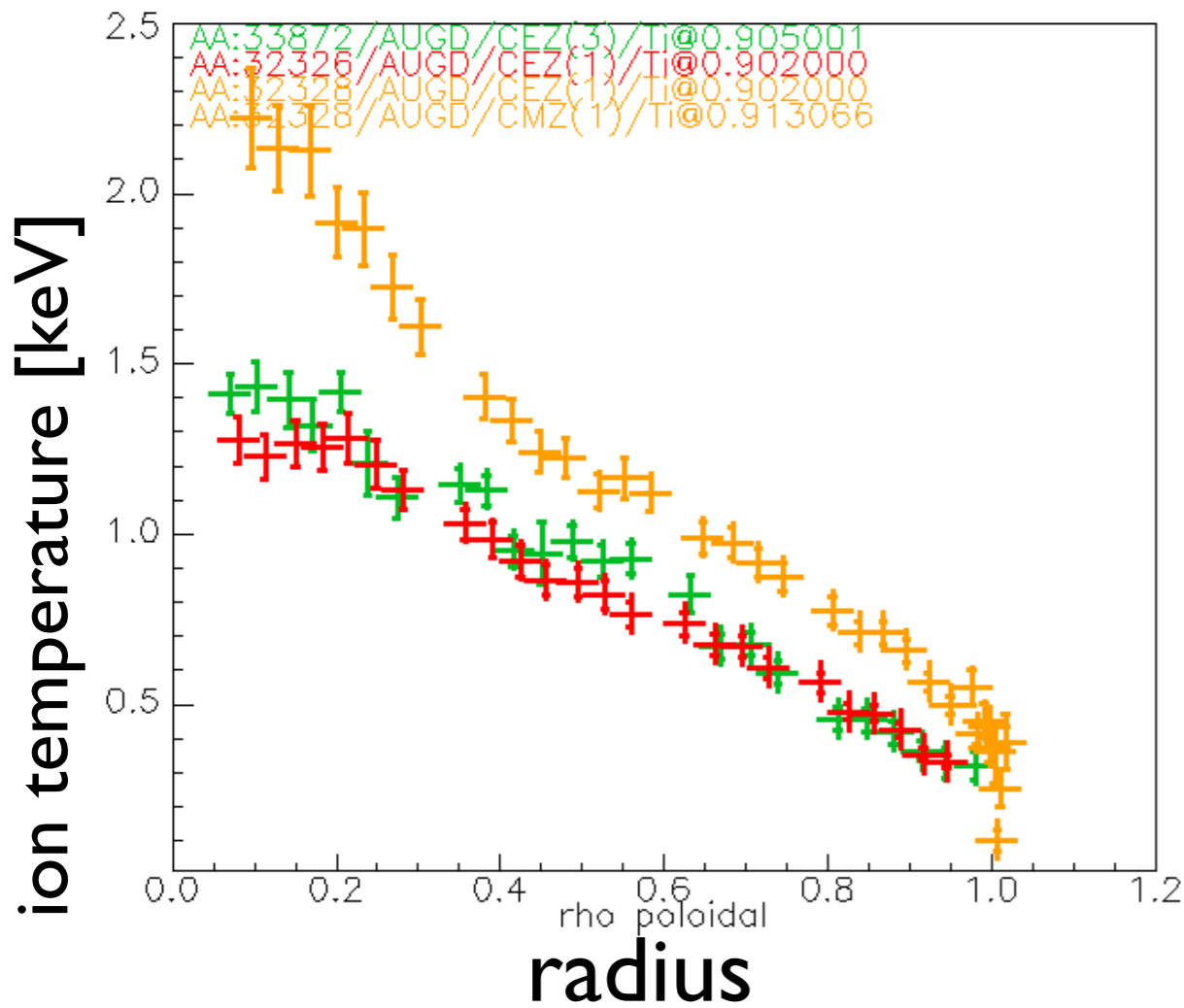


Toroidal mode numbers of AUGD 32388



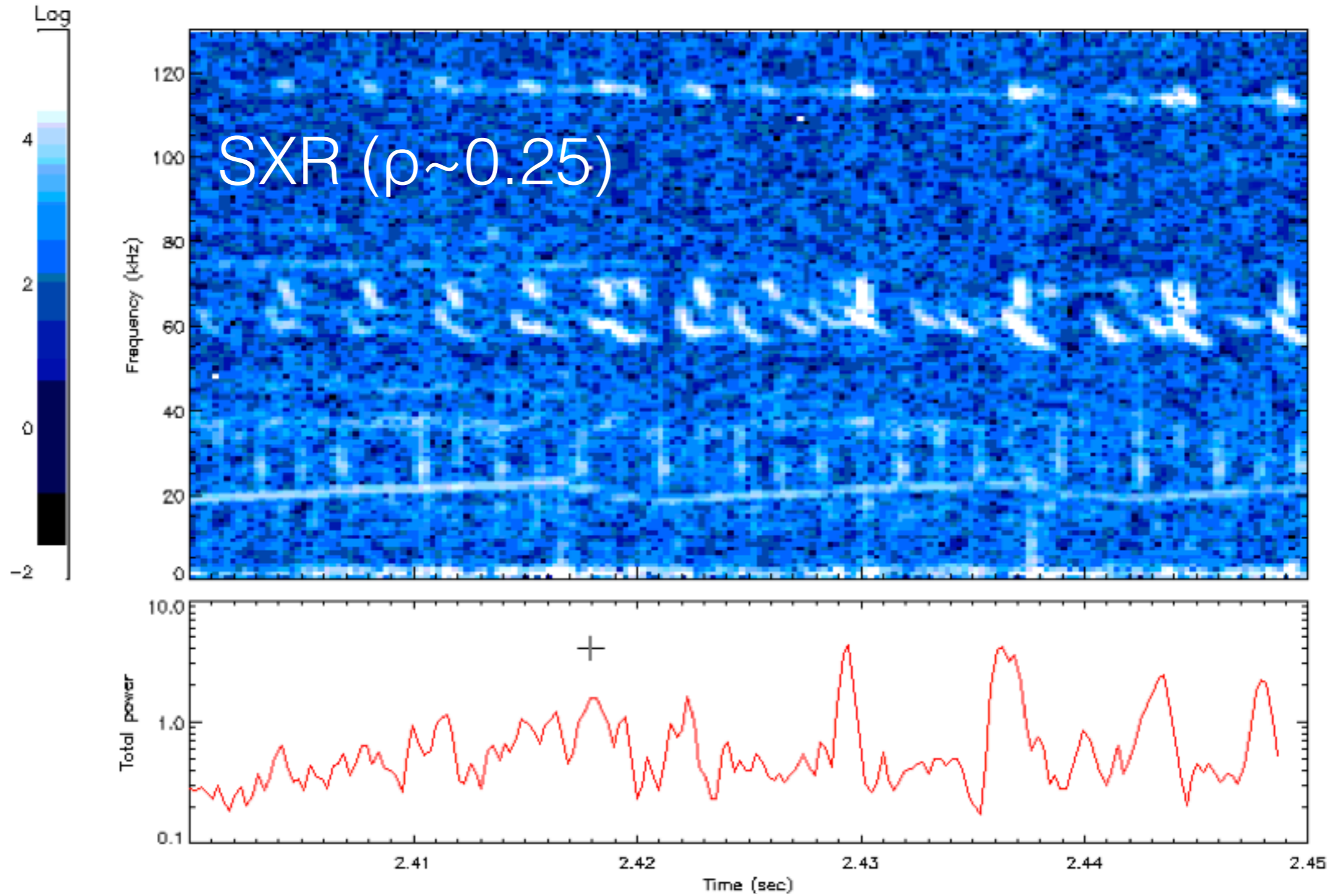
Time stamp: /afs/ipp
version: 1.8.0
shot: AUGD 32388
window: Gauss
winsize: 250
0.00050000127s
ires: 1000
step: 333
averages: 0
filter: Rel. pos.
mode steps: 1.000
Coherence limit: 0.0
Power limit: 0.0000
Q limit: 100 %
channel pairs: 15
MHA-B31-14-MHA
MHA-B31-14-MHA
MHA-B31-14-MHA
MHA-B31-14-MHA
MHA-B31-14-MHA
MHA-B31-03-MHA
MHA-B31-03-MHA
MHA-B31-03-MHA
MHA-B31-03-MHA
MHA-B31-01-MHA

discharge with EGAM
 discharge without EGAM
 discharge at marginal stability of EGAM



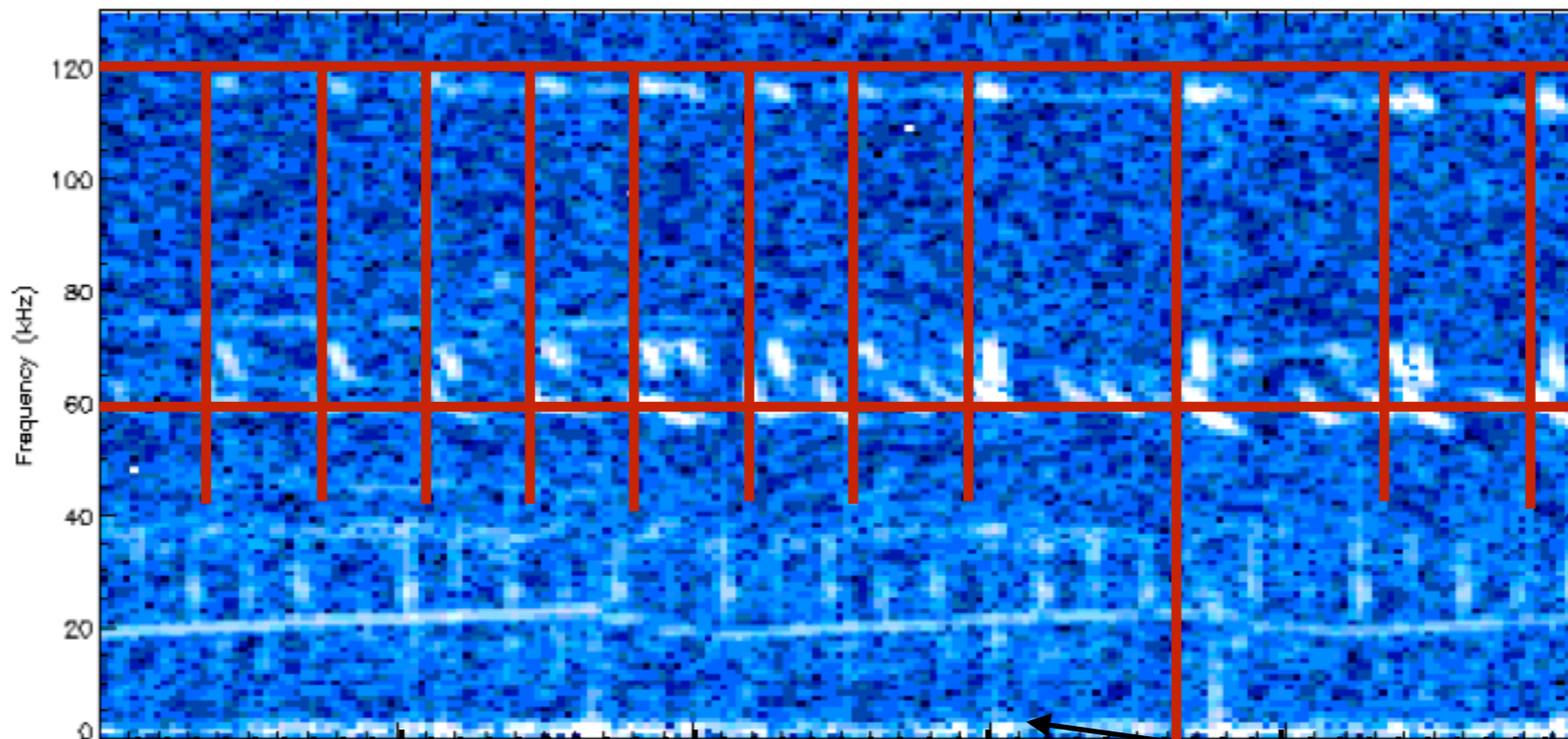
NLED/NAT base case profiles (step 1-4) are based on this...

new element observed: 'coupling' of TAEs, BAEs and EGAMs



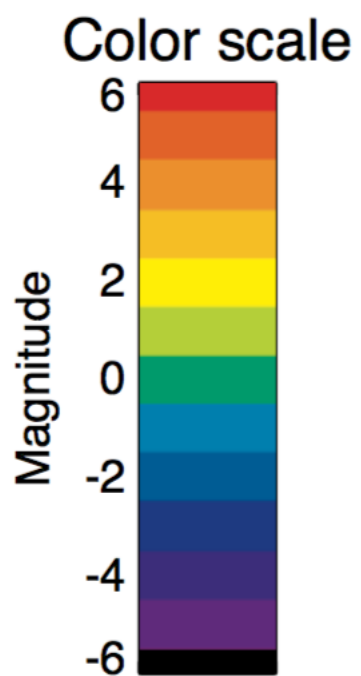


ASDEX Upgrade



$n=1$ TAE
not exactly
 $2 \cdot \omega_{BAE}$!

BAE/EGAM



120

100

80

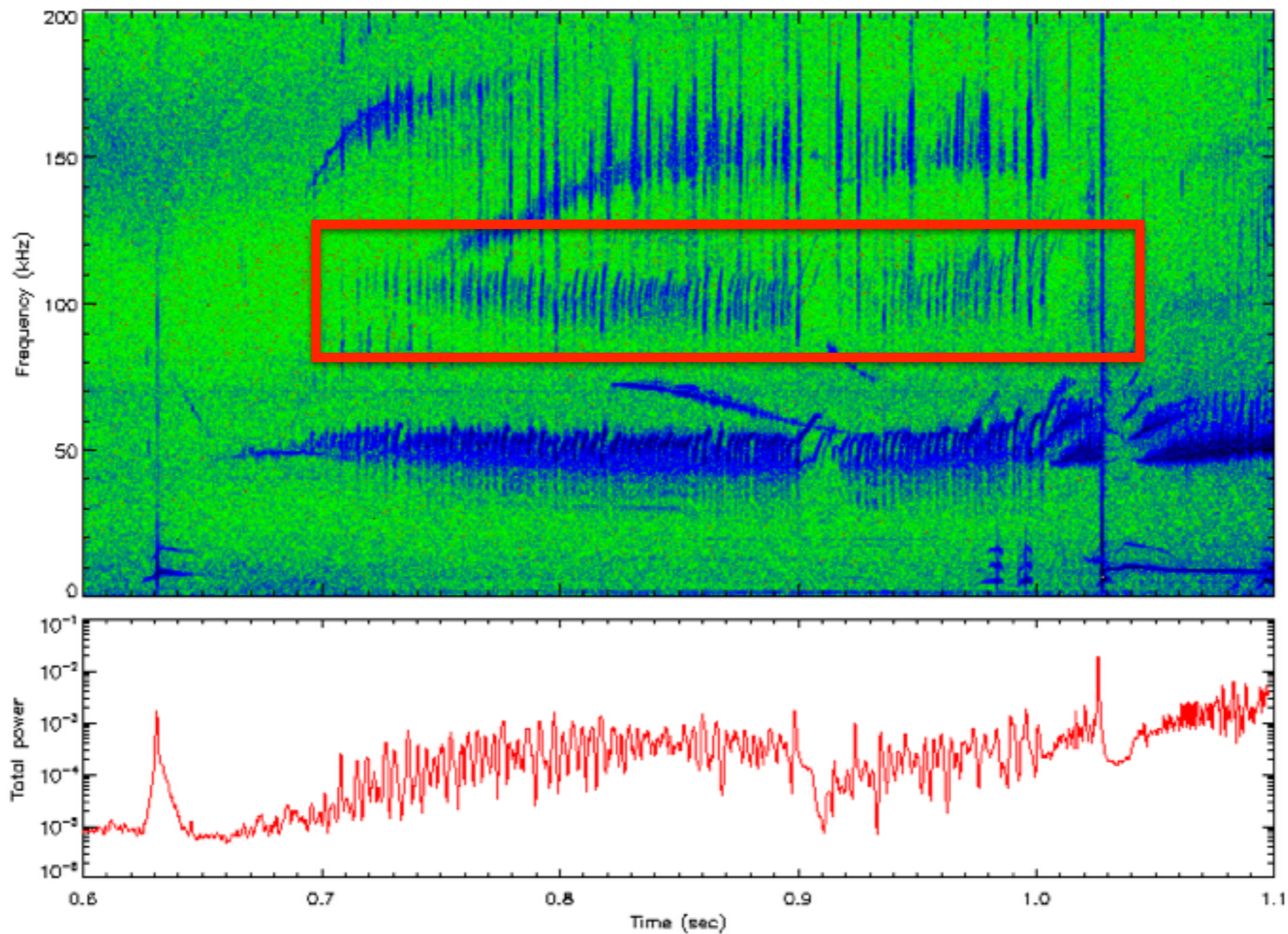
60

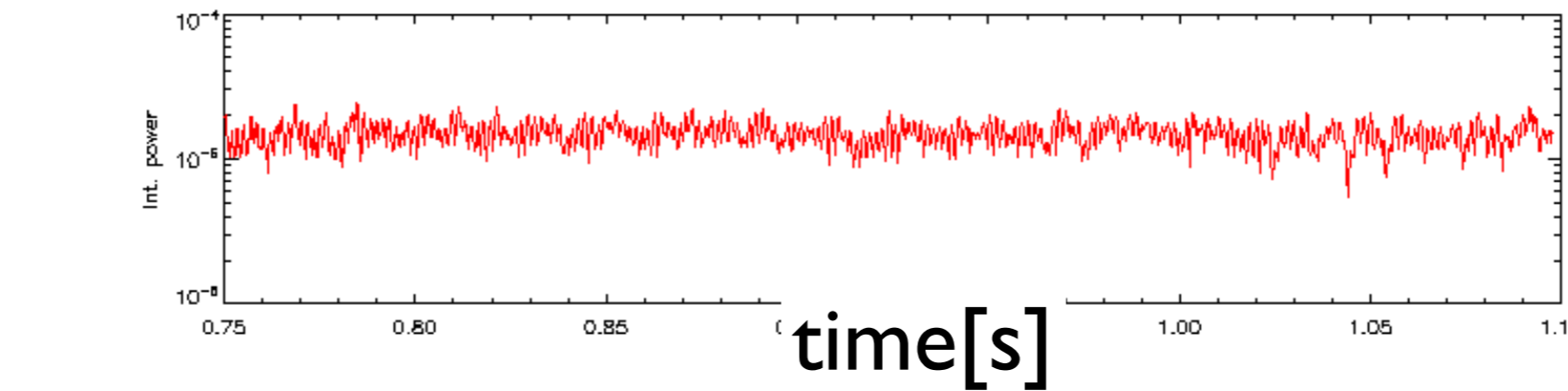
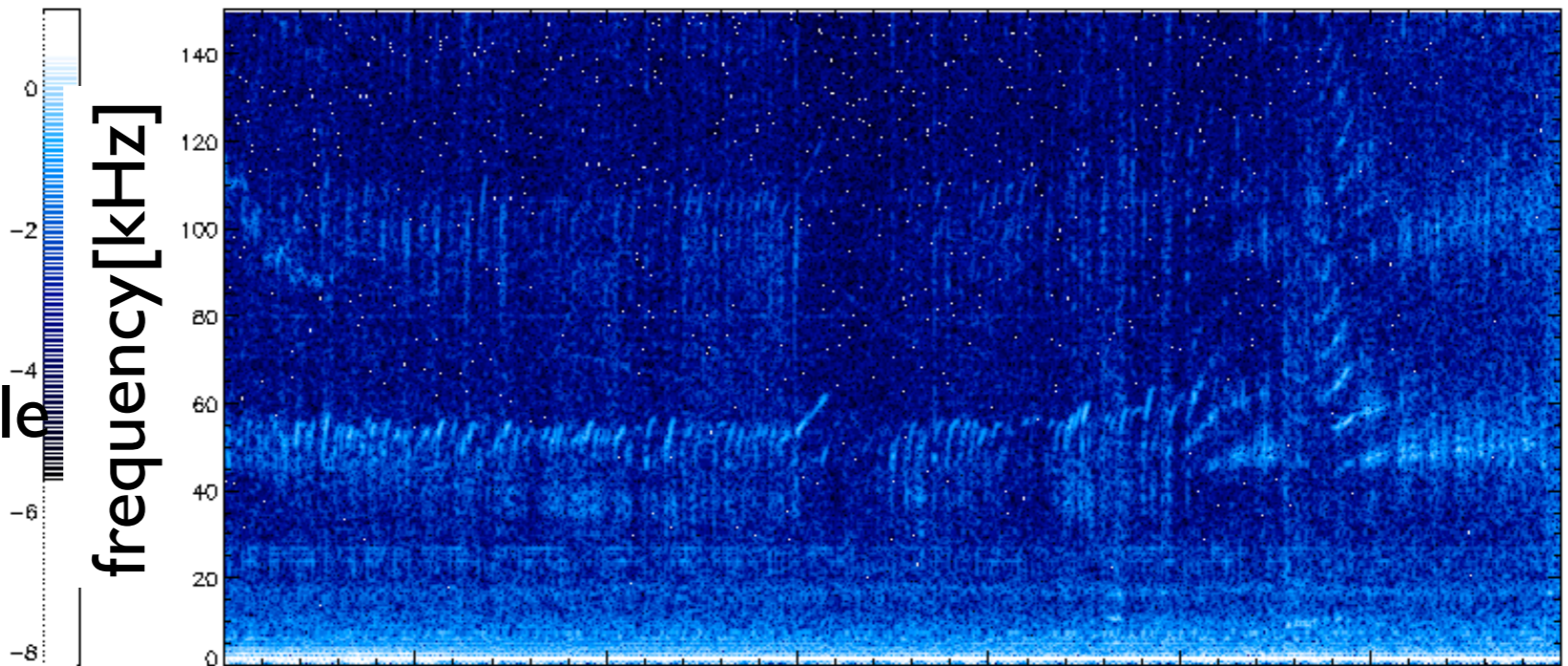
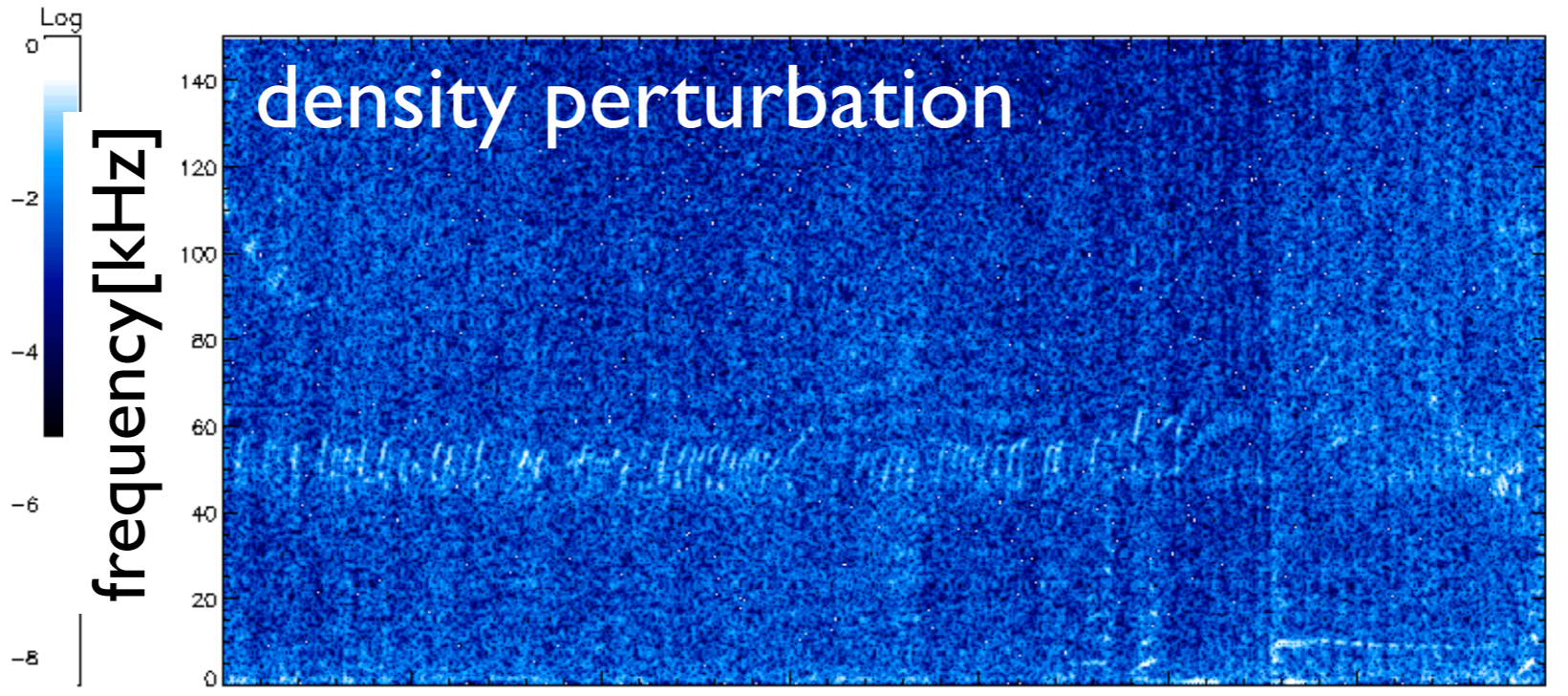
40

$\omega \sim 0$ mode?

EGAM onset
slightly
delayed

new experimental data on 2nd harmonic EGAM generation
in combination with recent improved measurements on the density
profile, quantitative assessment can be made
(compare, if possible to Qiu,Chavdarovski,Biancalani)





at
 AUG:
 first order
 EGAM
 harmonics
 dominates,
 2nd order
 perturbation visible
 on high field
 side

reflectometry:
 low field side

reflectometry
 high field side

factor ~ 15
 in \sim intensity
 between ω_{GAM}
 and $2 \omega_{GAM}$

Linear and non-linear characterization of transient waves and their interactions

Progress meeting for EnR project on Nonlinear interaction of Alfvénic and turbulent fluctuations in burning plasmas

Gergo Pokol^{1*}, Gergely Papp², G. Por¹, Peter Zs. Poloskei^{1,2}

collaborators: Ph. Lauber², L. Horvath³, ASDEX Upgrade team

*e-mail: pokol@reak.bme.hu

¹Institute of Nuclear Techniques, BME, Budapest, Hungary

²Max Planck Institute for Plasma Physics, Garching, Germany

³University of York, York, UK

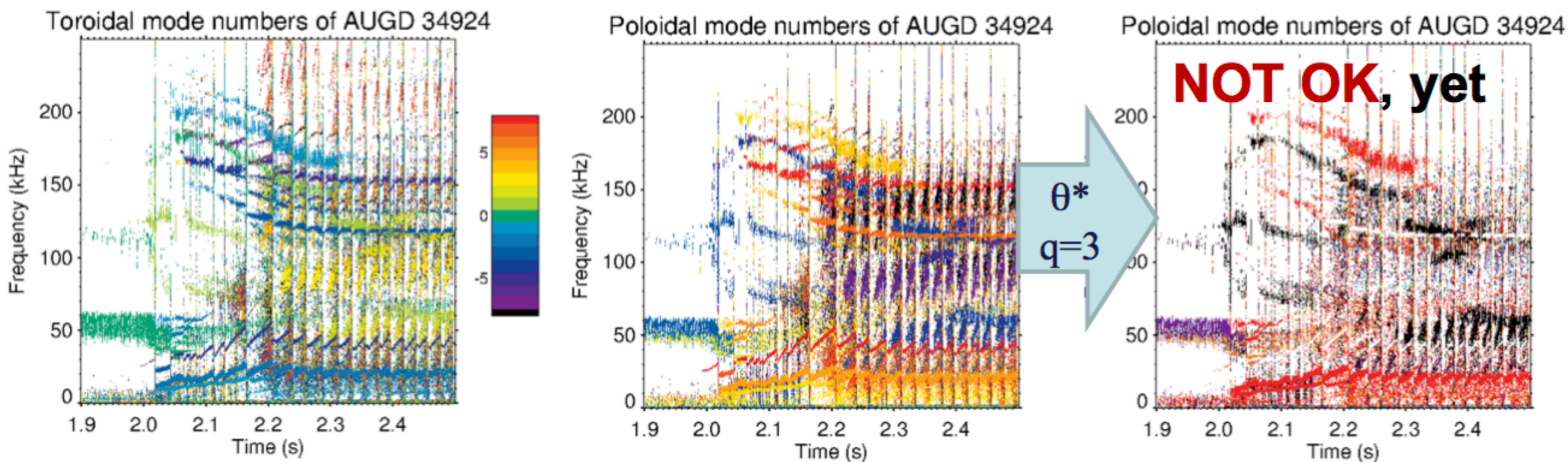


ASDEX Upgrade

27 February 2018

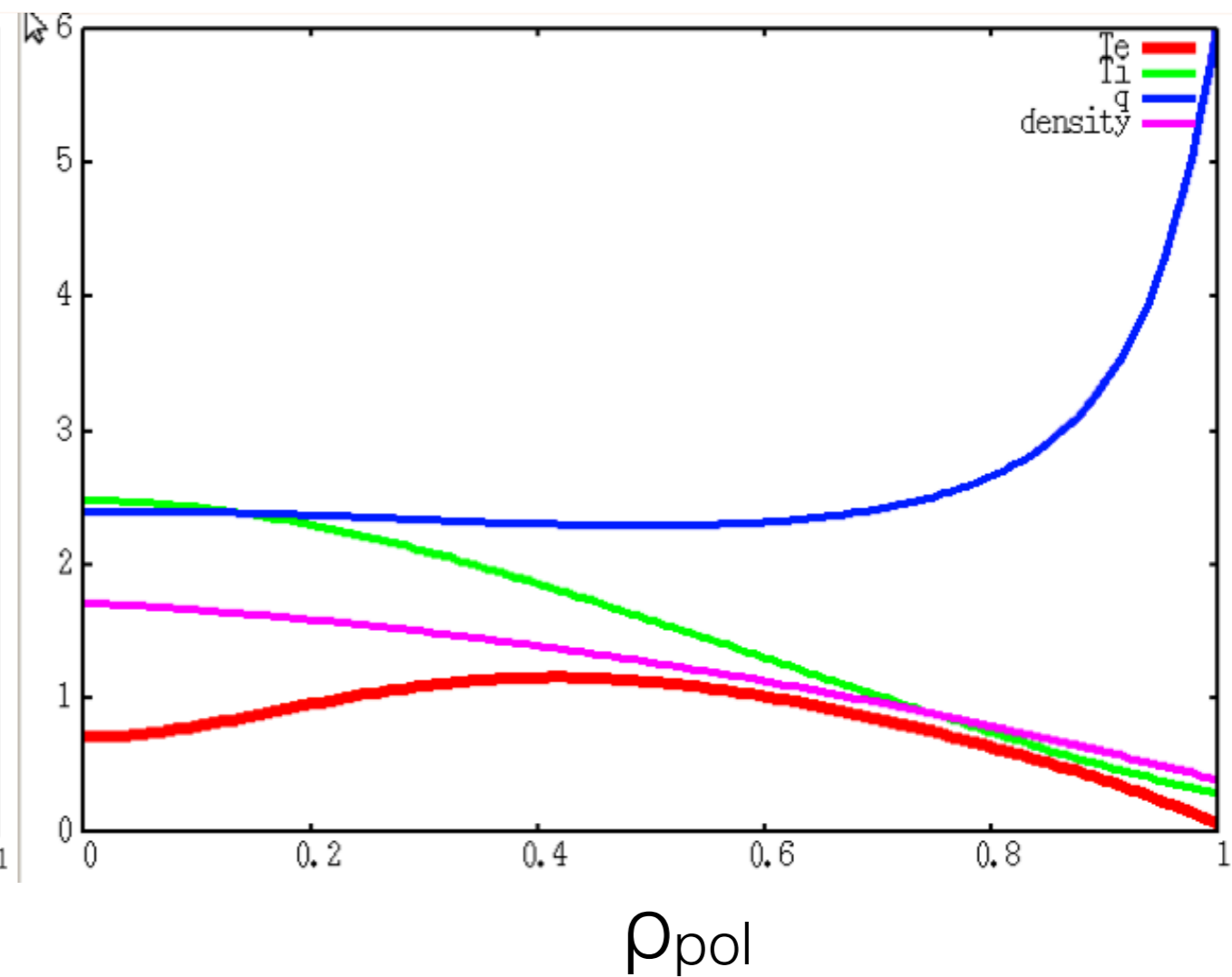
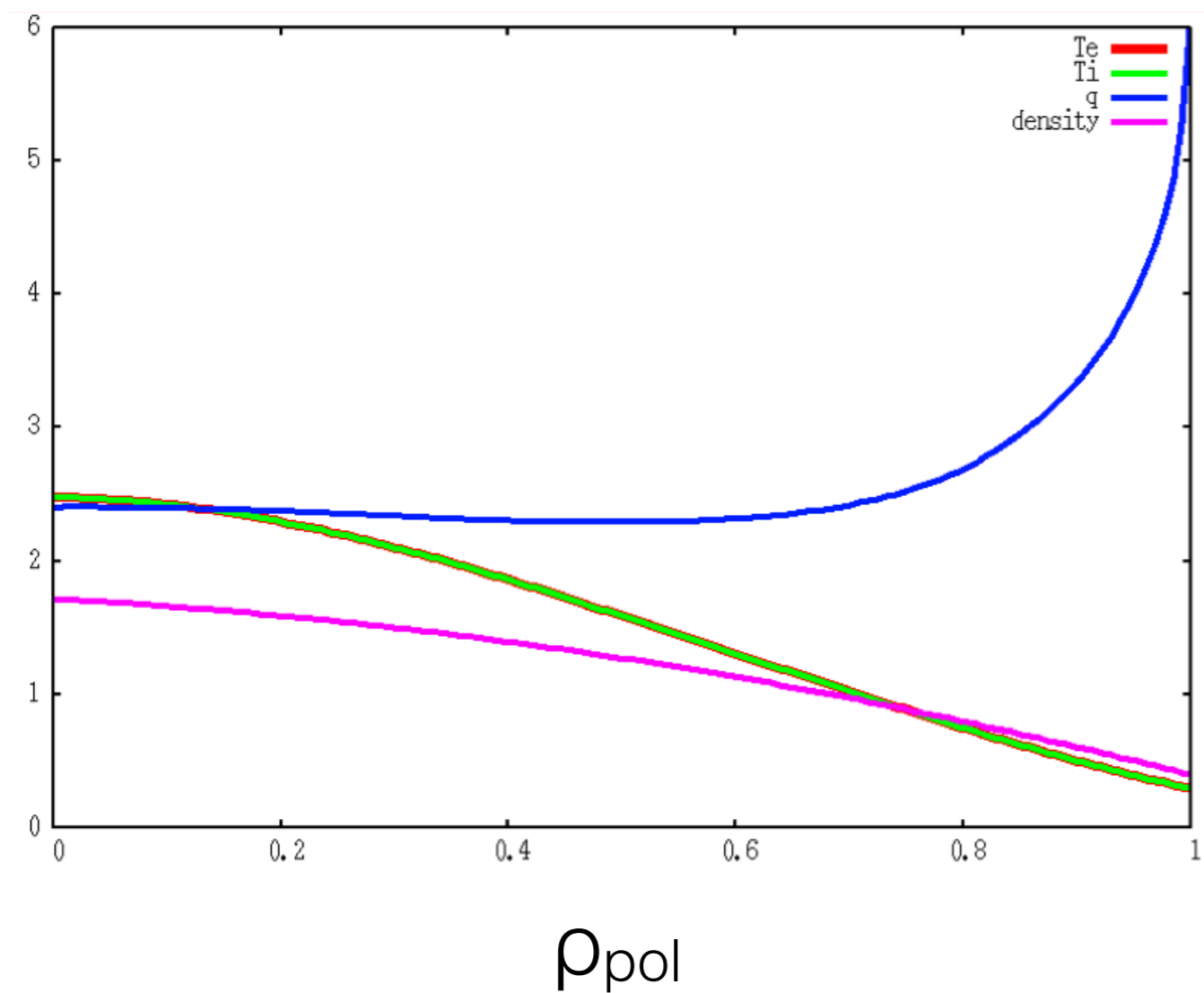
Theory-driven data processing

- **Released new version of NTI Wavelet Tools (1.8.1)**: Main fix was regarding the straight-field-line transform used in poloidal mode number estimation and compatibility with new signal types.
- **Analyzing shot 34924 with many modes**: Toroidal mode numbers ok, poloidal mode numbers require θ^* correction, bandpower-correlation and bicoherence analysis started recently
- **Discussion on turbulence and bicoherence**: Clarifying confidence levels, finishing paper

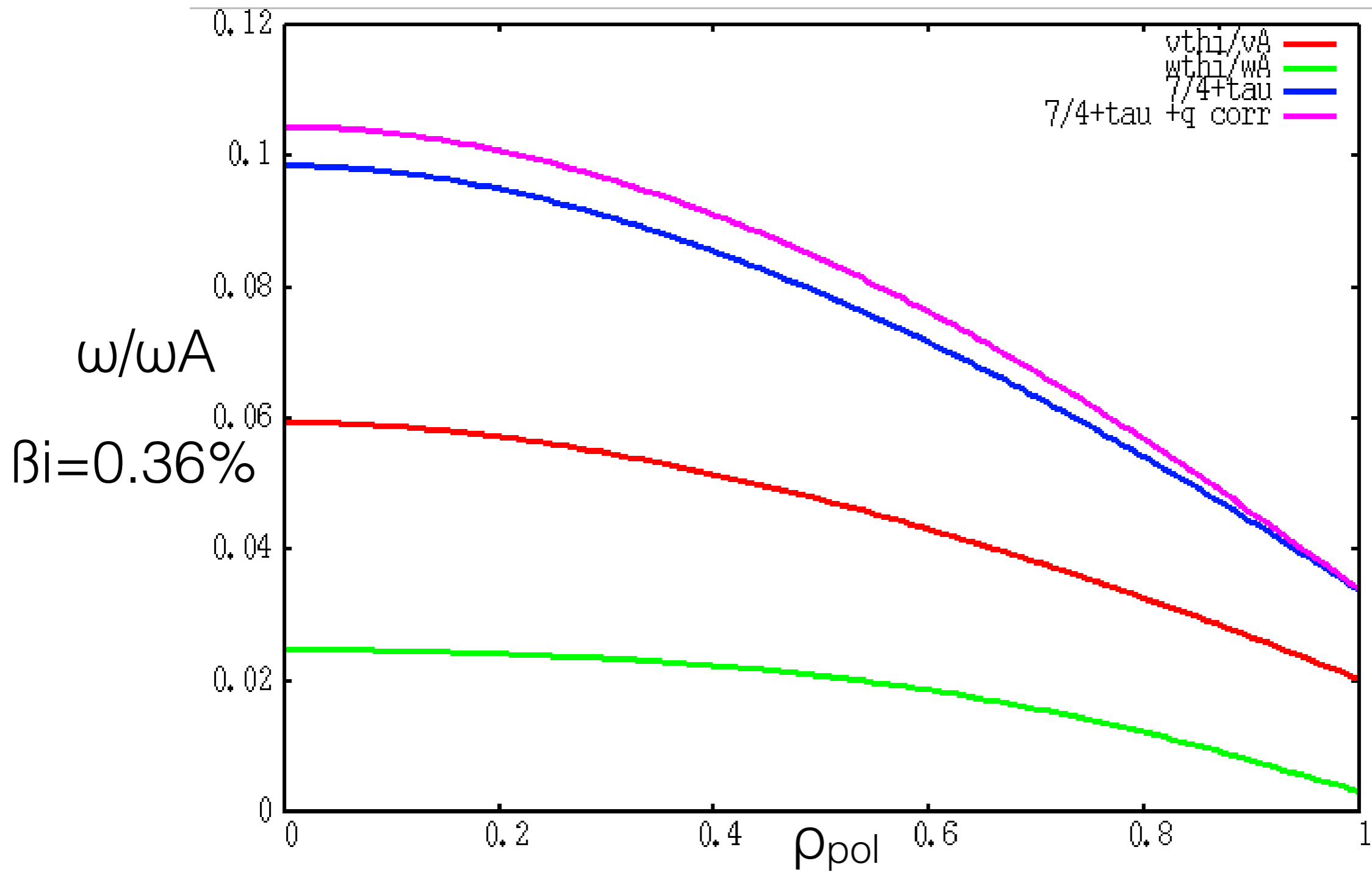


NLED base case: GAM continuum with LIGKA

1. circular boundary, $T_e = T_i$
2. circular boundary, $T_e \neq T_i$
3. experimental boundary, $T_e = T_i$
4. experimental boundary, $T_e \neq T_i$

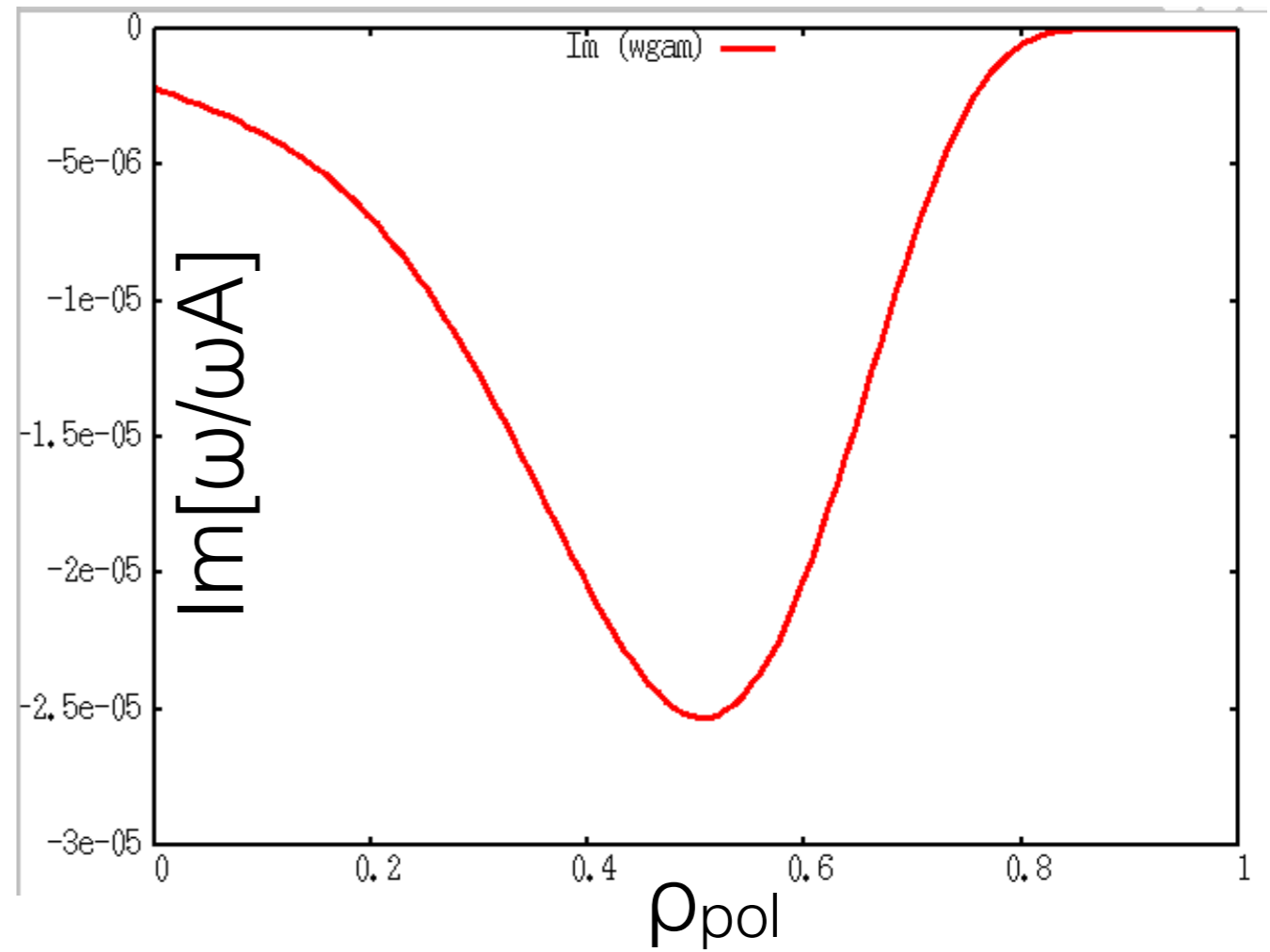
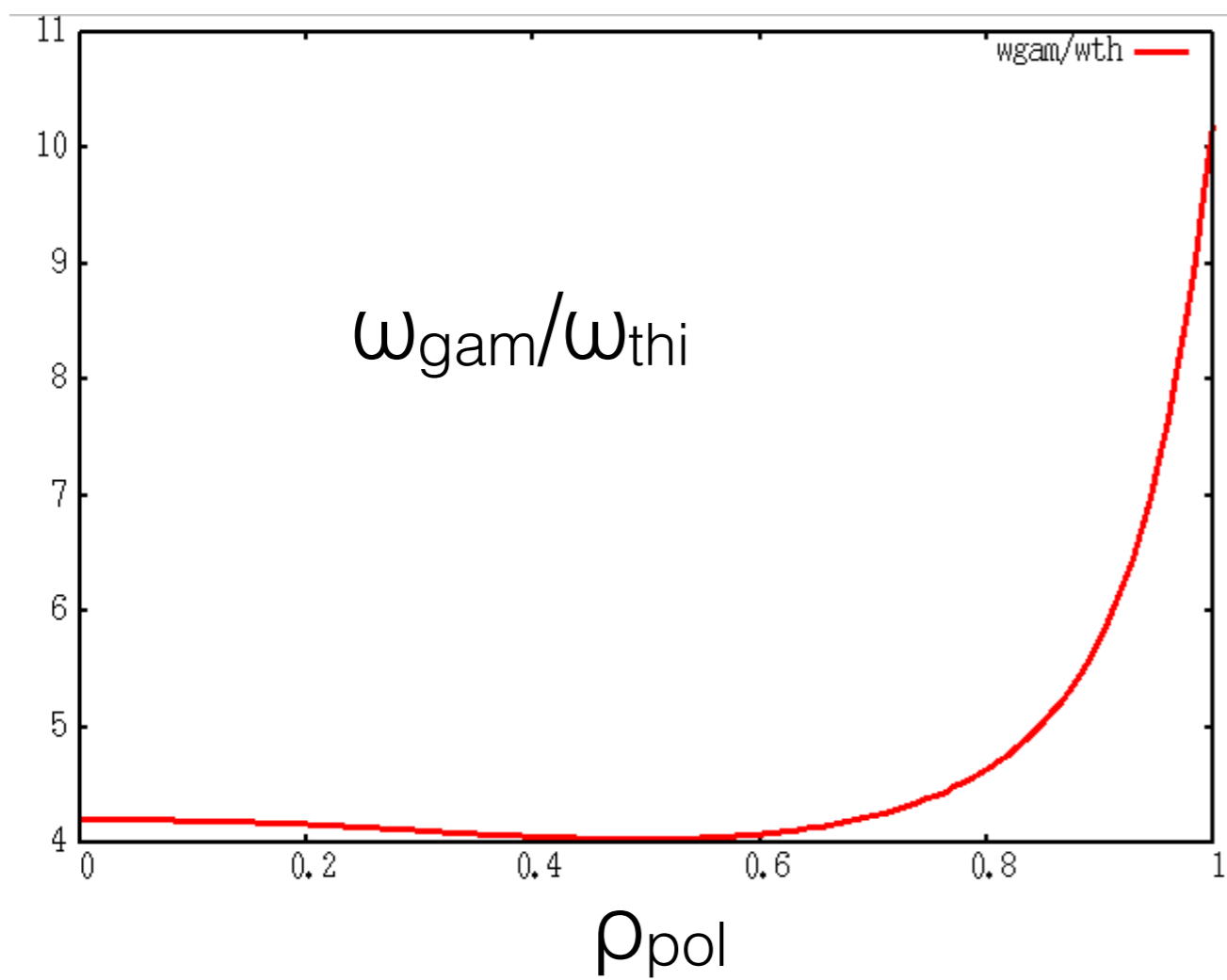


analytical GAM frequencies



$$\omega_G^2 = \frac{v_{thi}^2}{R_0^2} \left[\frac{7}{4} + \tau \right] \left[1 + \frac{2(23 + 16\tau + 4\tau^2)}{q^2(7 + 4\tau)^2} \right]$$

analytical ion Landau damping rate:

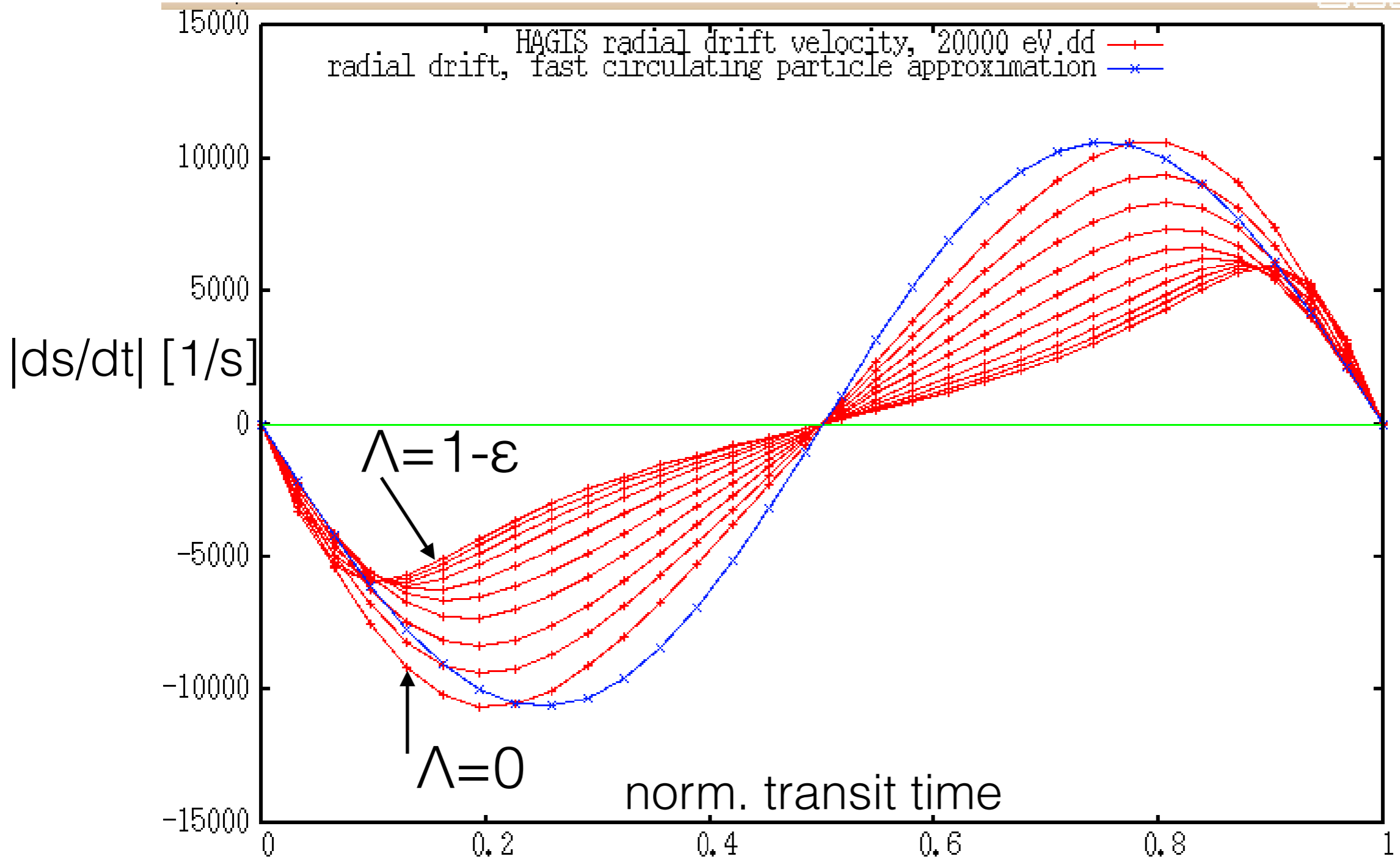


[Sugama, no FLR/FOW]

local GAM damping with LIGKA:

- check radial geodesic curvature drifts: HAGIS vs eq
- check moments of geodesic curvature drifts
- check resonances
- check dispersion relation
- role of electrons

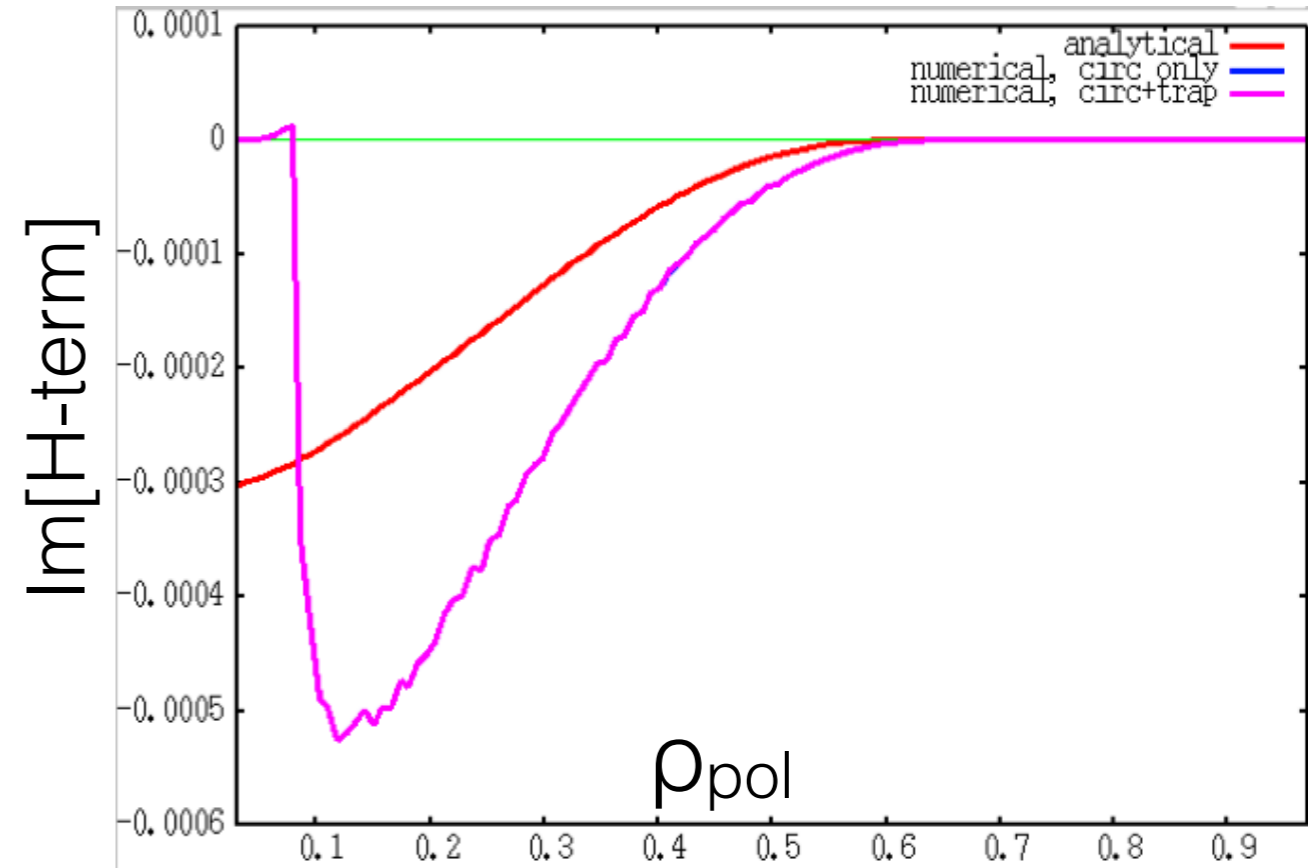
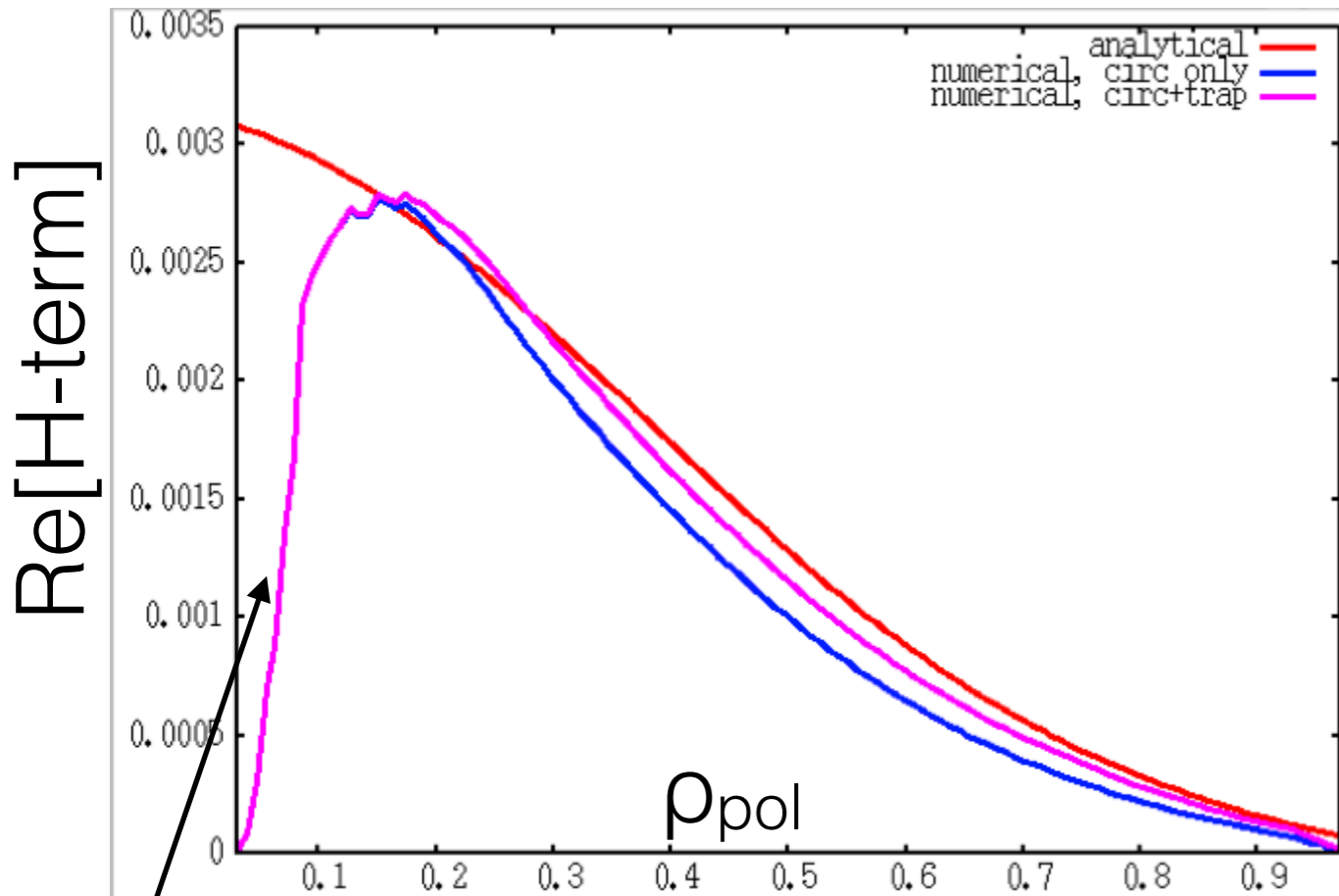
radial drifts: HAGIS orbits compared to fast circulating particle approximation



$$\mathbf{v}_d \cdot \nabla r = \frac{v_{th,i}^2}{\Omega_i} \mathbf{b} \times \kappa \cdot \nabla r \approx -\frac{v_{th,i}^2}{\Omega_i} \sin(\theta) / R_0$$

$$\omega_t \hat{t} \approx \theta \text{ and } \omega_t \approx |v_{||}| / qR_0$$

compare v-space integrals for v_{dr} moments:



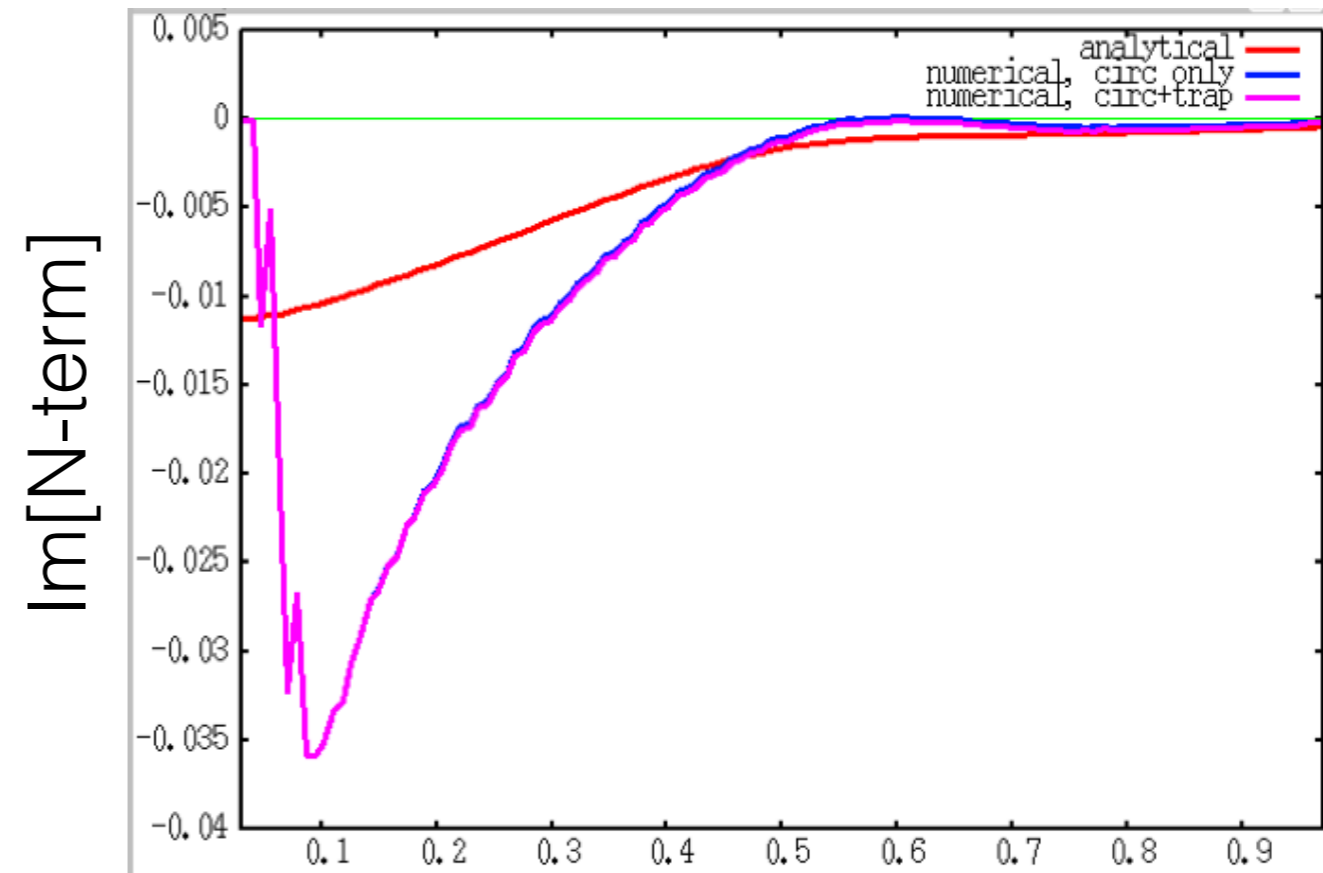
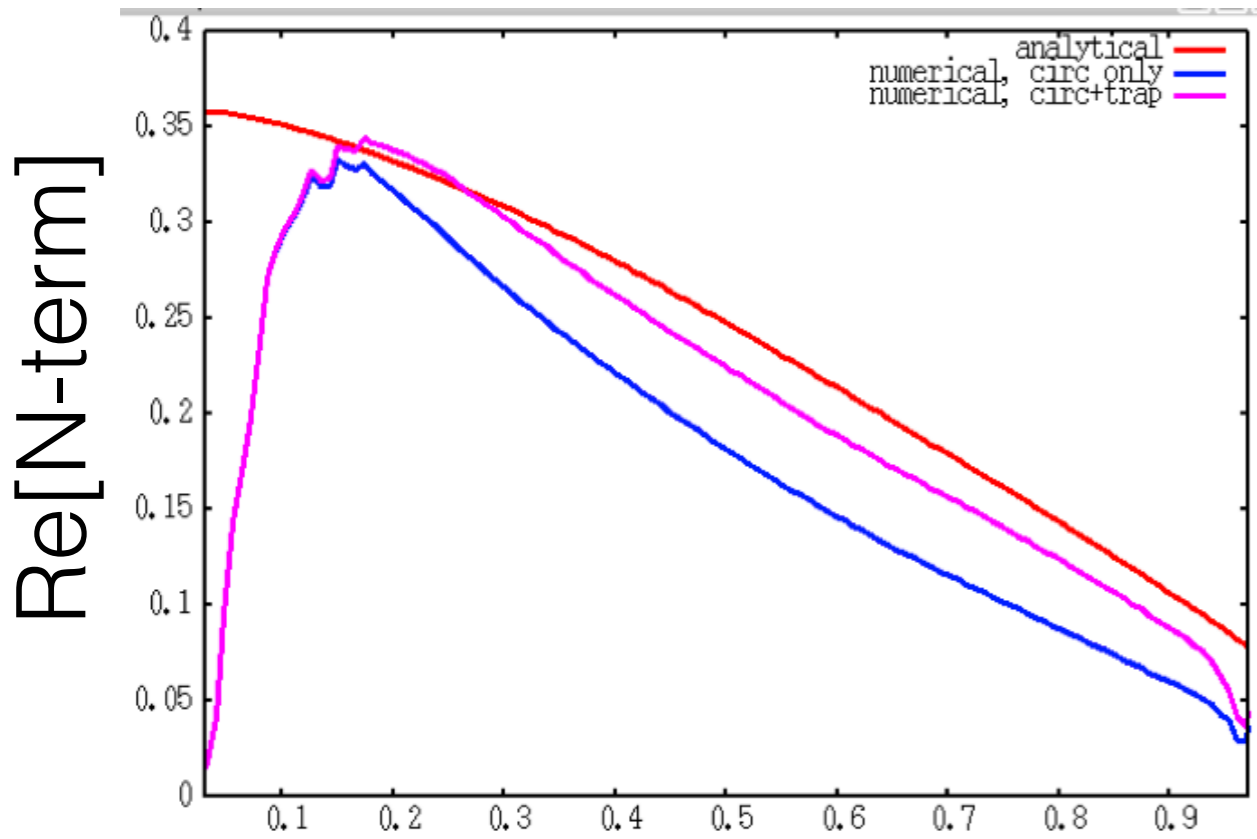
non-standard orbits
excluded so far (large q₀)

$$(v_{dr} \cdot \nabla r)^2 \rightarrow 7/4$$

$$\omega^2 \left(1 - \frac{\omega_* (1 + \eta)}{\omega} \right) - k_{\parallel}^2 \omega_A^2 R_0^2 = 2 \frac{v_{thi}^2}{R_0^2} \left(- \left[H(x_{m-1}) + H(x_{m+1}) \right] + \tau \left[\frac{N^m(x_{m-1}) N^{m-1}(x_{m-1})}{D(x_{m-1})} + \frac{N^m(x_{m+1}) N^{m+1}(x_{m+1})}{D(x_{m+1})} \right] \right)$$

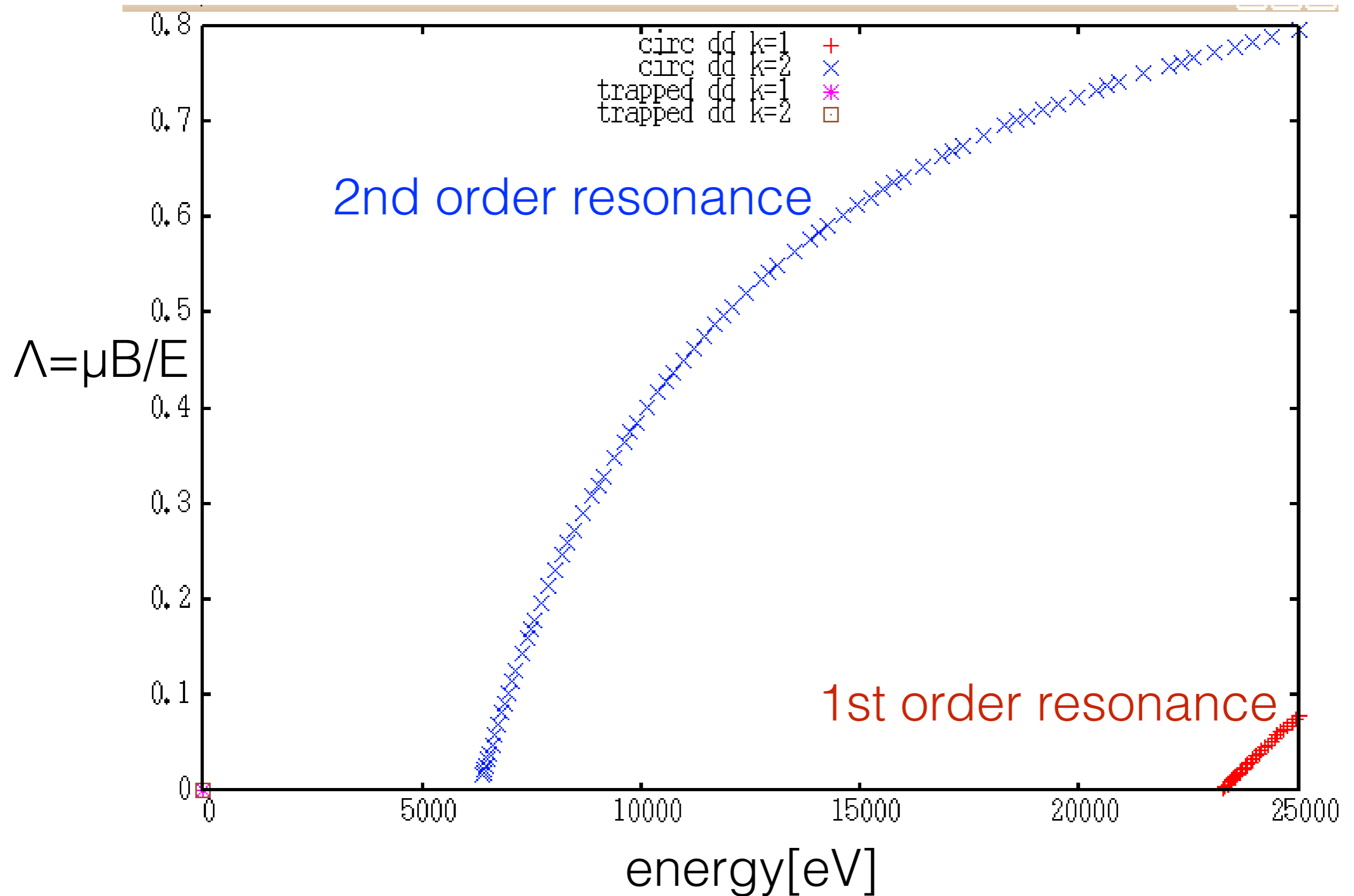
same for N, D terms...

compare v-space integrals for v_{dr} moments - sidebands

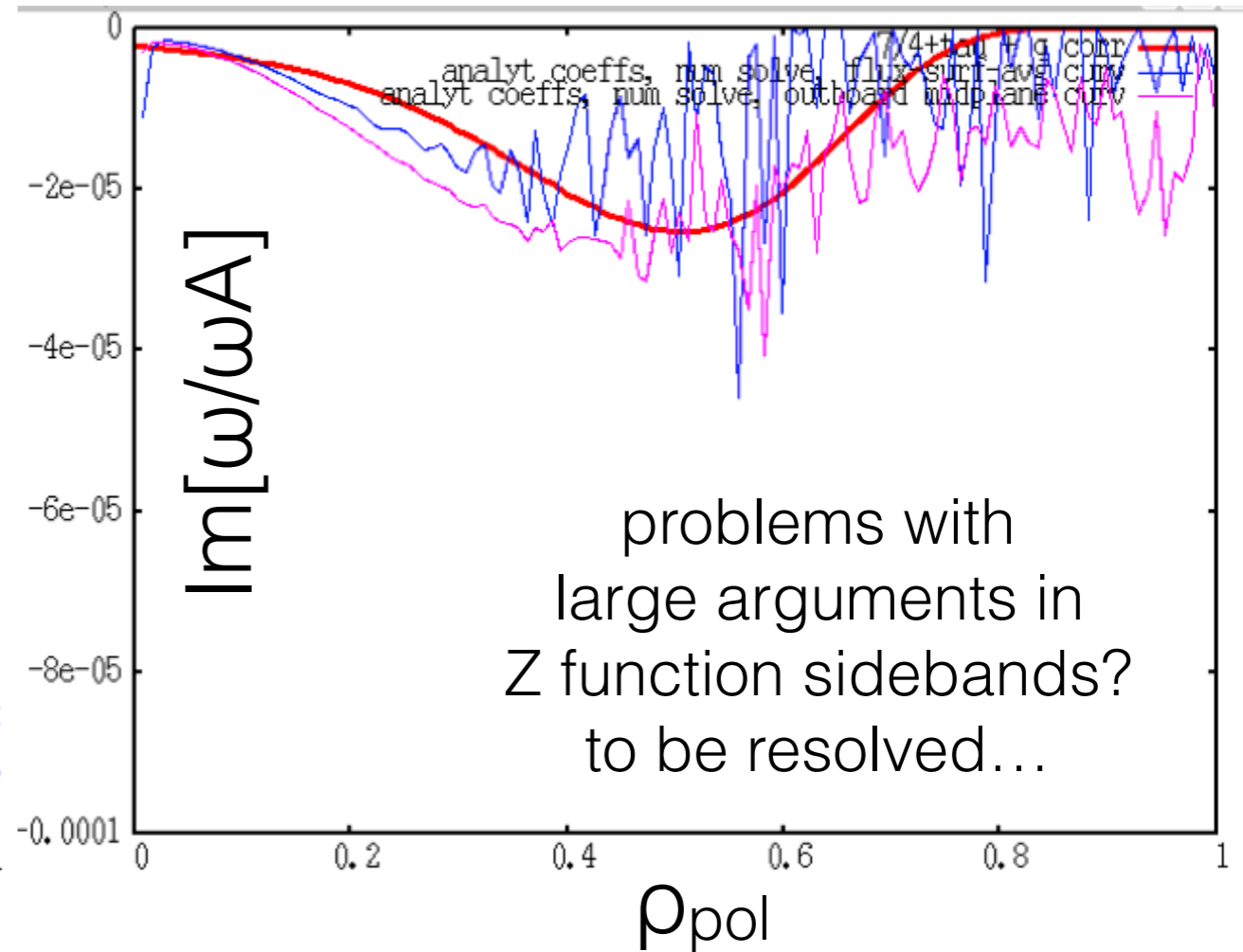
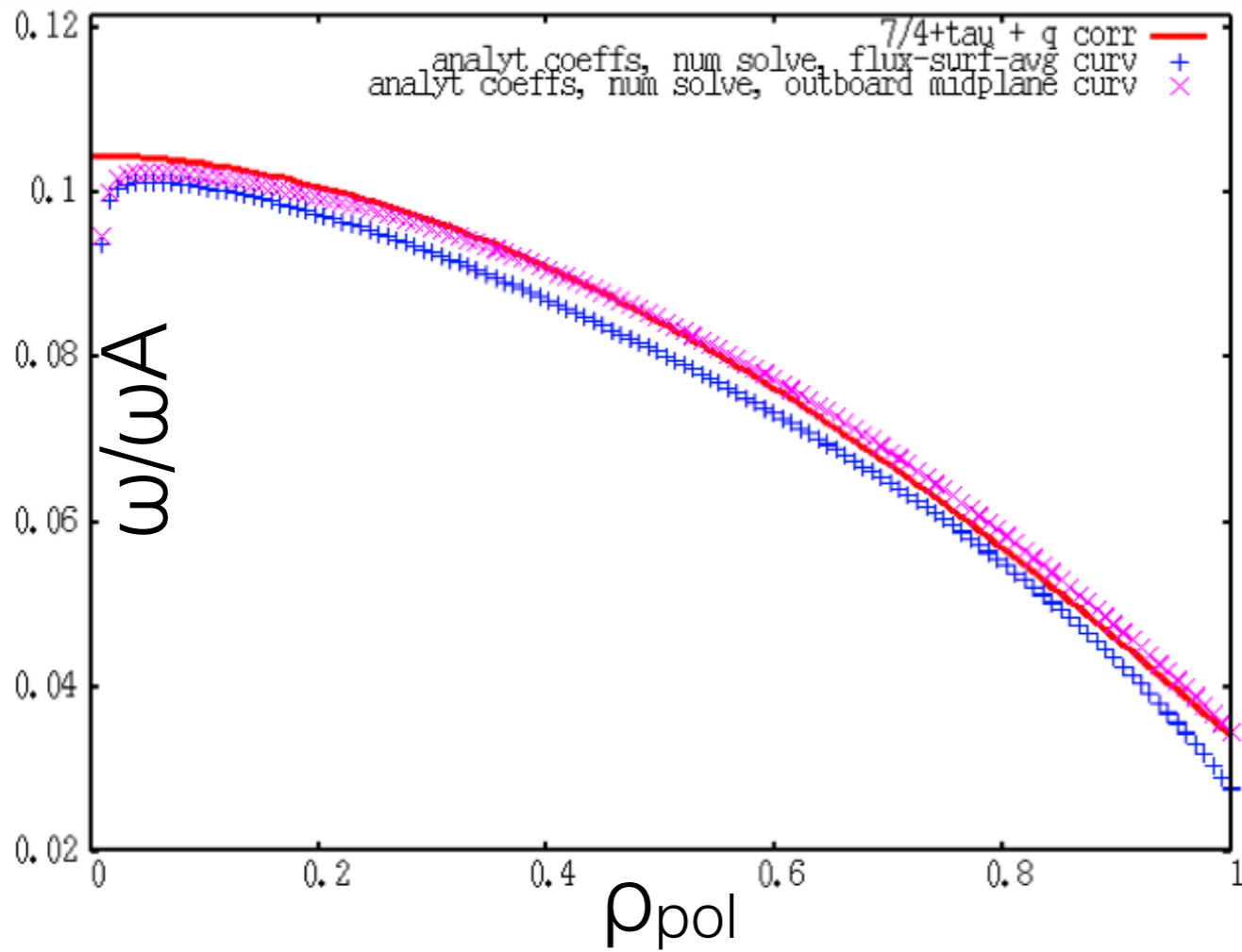


$$\omega^2 \left(1 - \frac{\omega_*(1 + \eta)}{\omega} \right) - k_{\parallel}^2 \omega_A^2 R_0^2 = 2 \frac{v_{thi}^2}{R_0^2} \left(- [H(x_{m-1}) + H(x_{m+1})] + \tau \left[\frac{N^m(x_{m-1}) N^{m-1}(x_{m-1})}{D(x_{m-1})} + \frac{N^m(x_{m+1}) N^{m+1}(x_{m+1})}{D(x_{m+1})} \right] \right)$$

resonances: deuterium ions, $r=0.25$, $\omega=0.089 \omega_A$

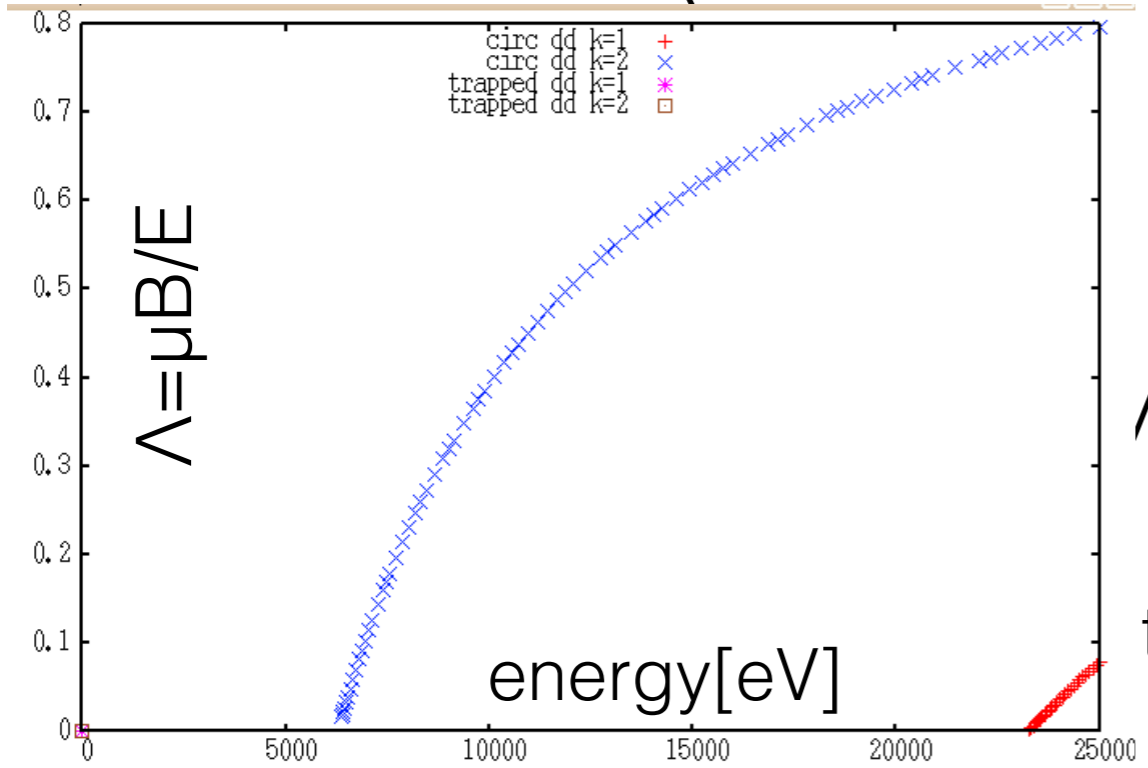
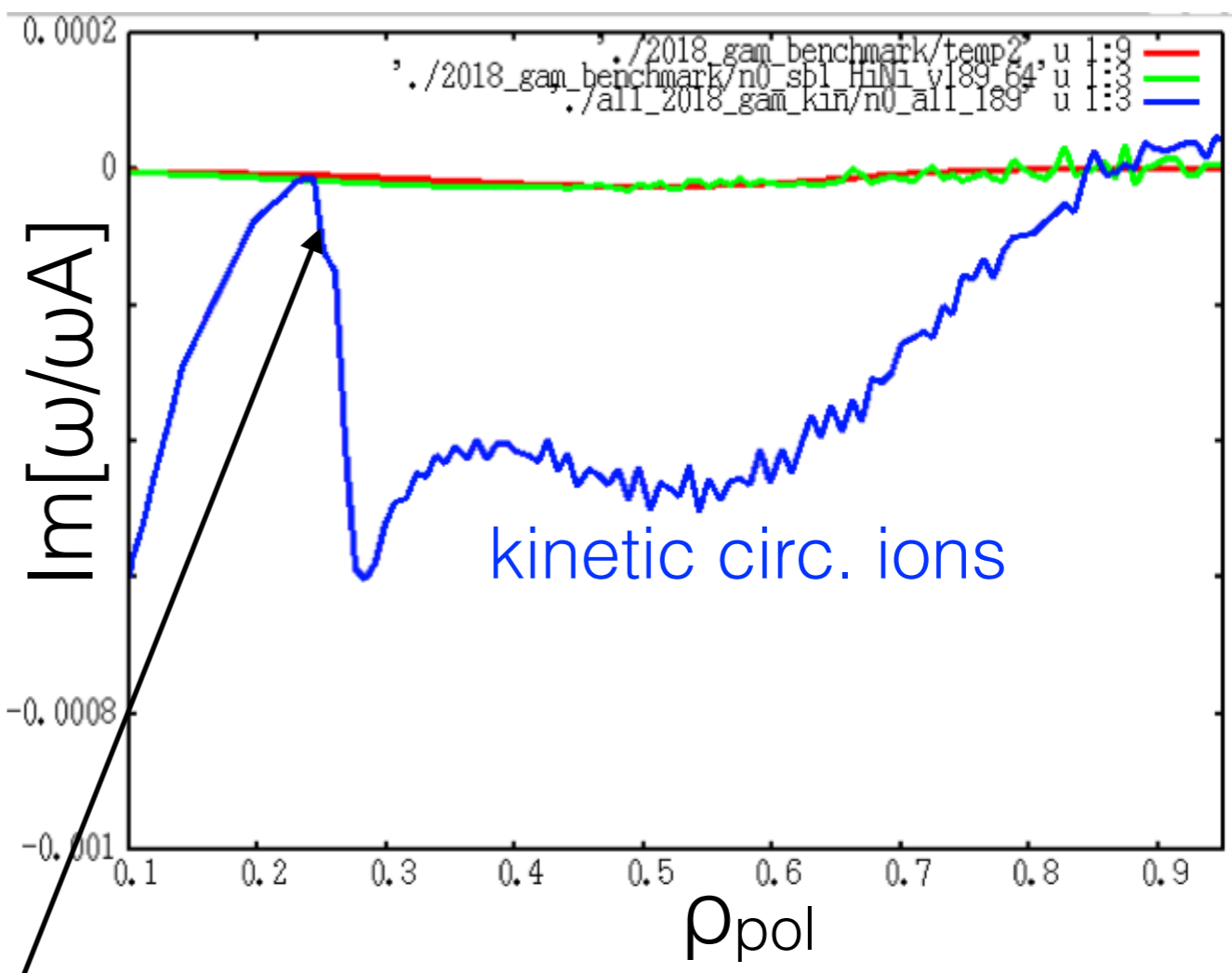
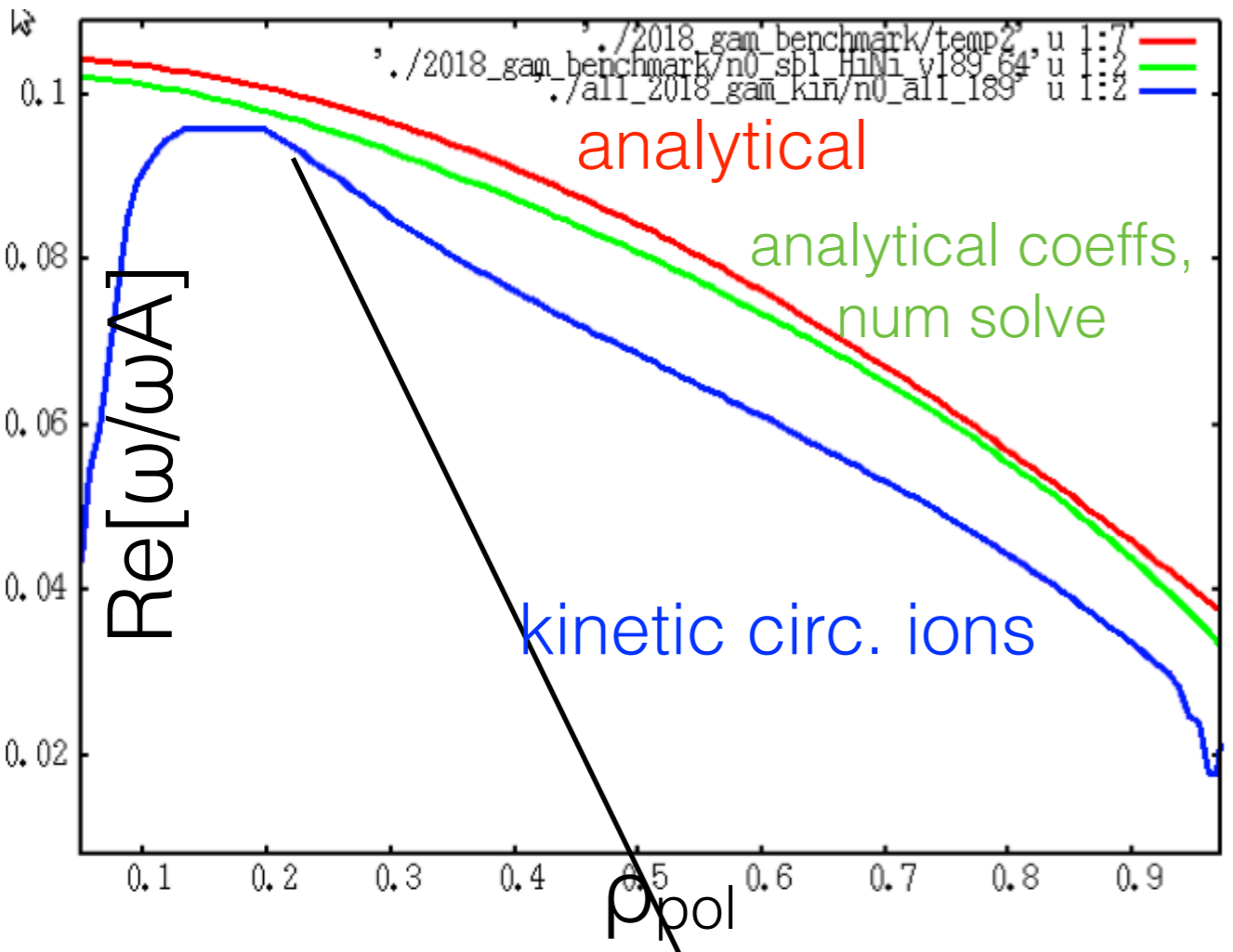


analytical coefficients, numerical solve
 (=contours in complex plane)



CERNLIB Z(x) routine uses different num. methods for different quadrants...

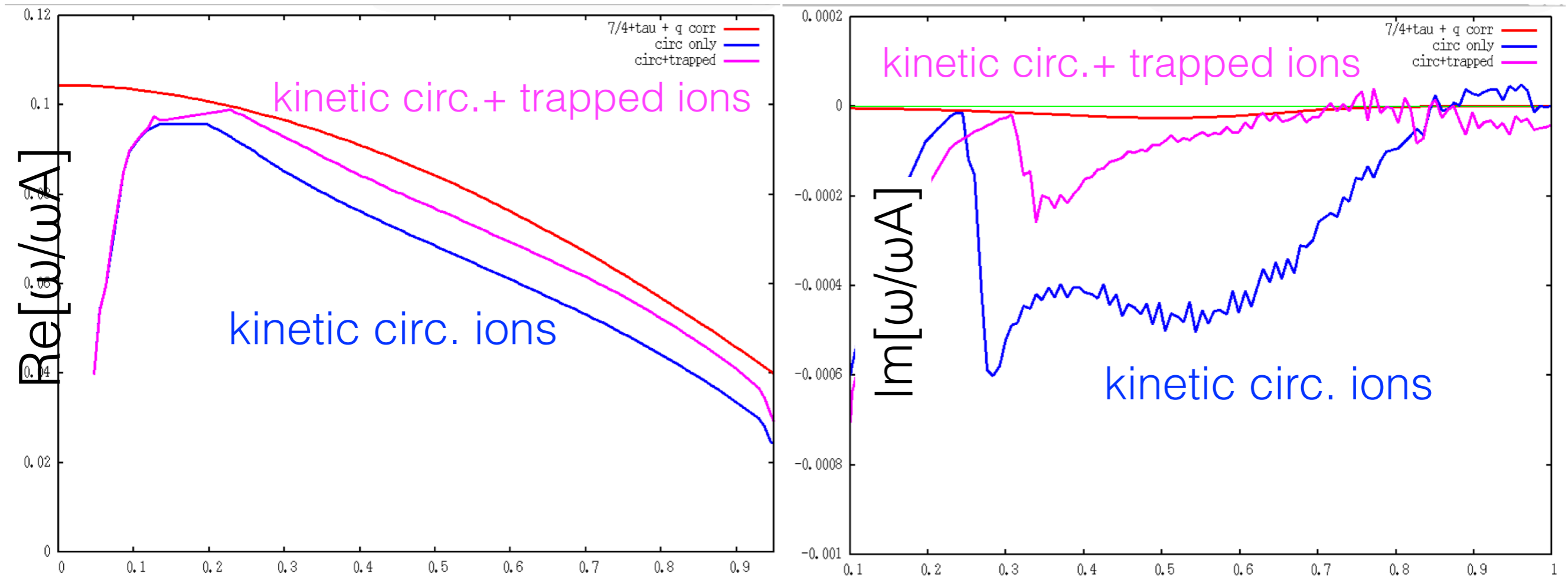
kinetic ions: only circulating ions, one sideband



kinetic ions: higher damping rate due to lower ω GAM!

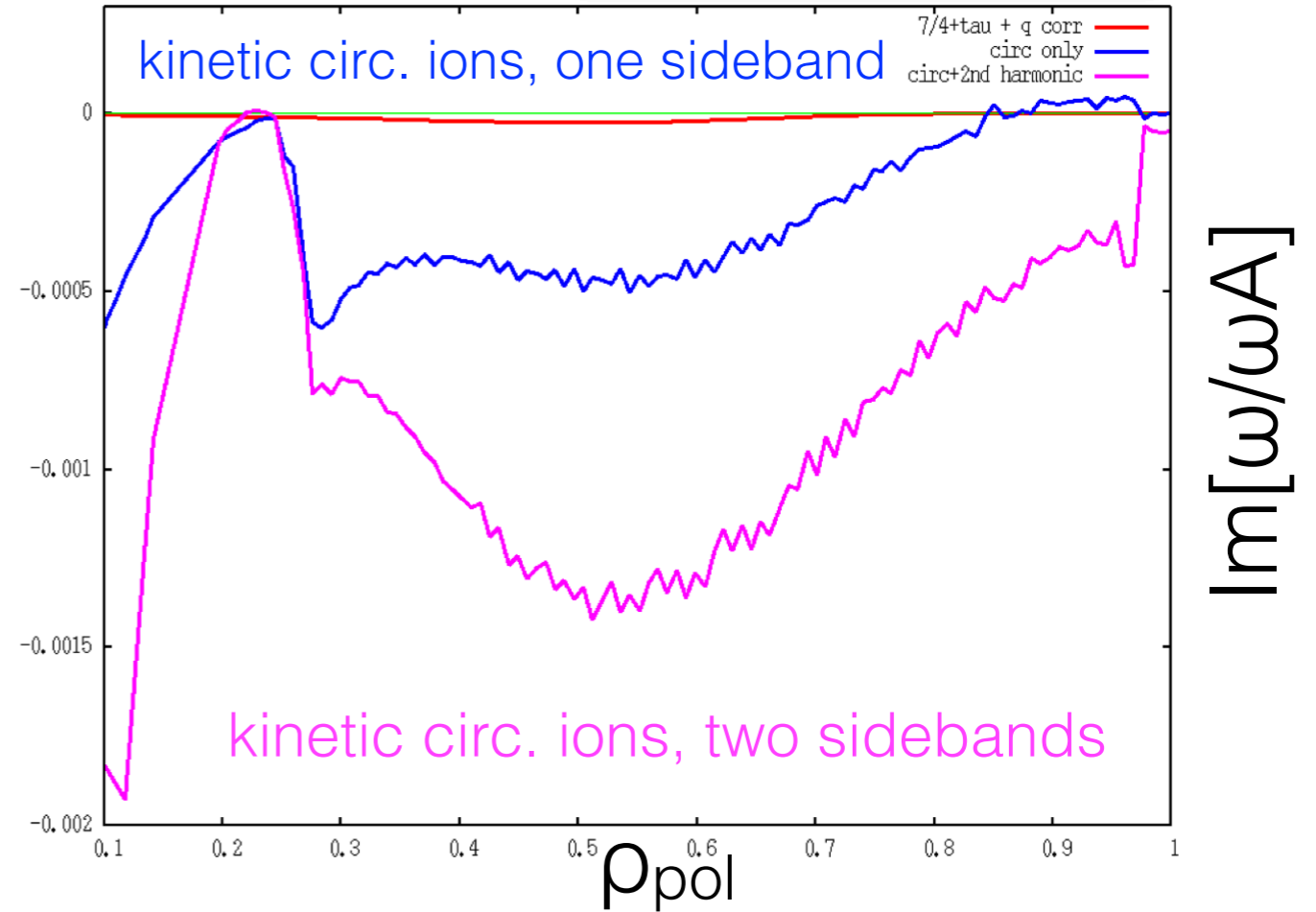
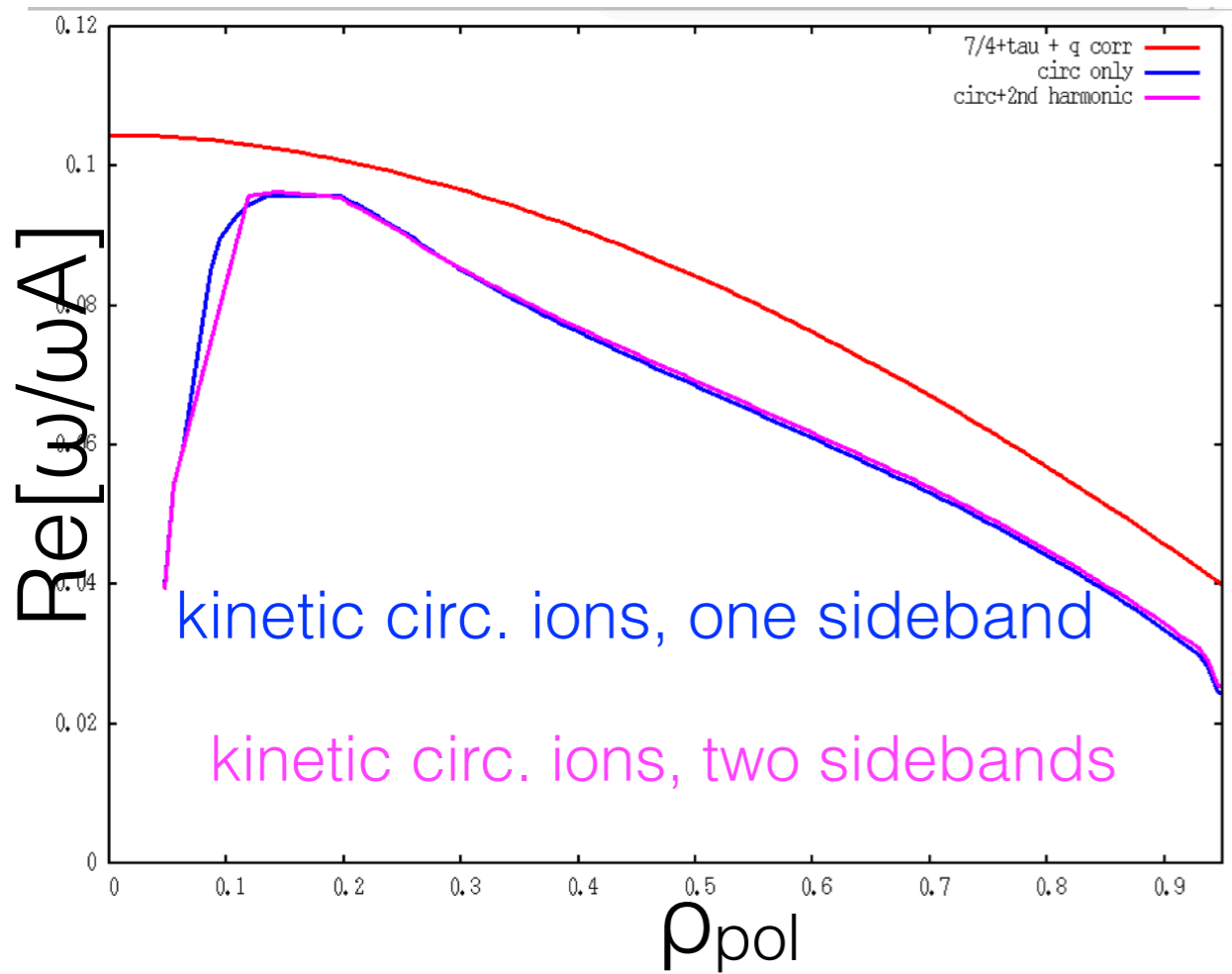
transition will become smoother for wider E-grid

fully kinetic ions: circulation and trapped ions, one sideband

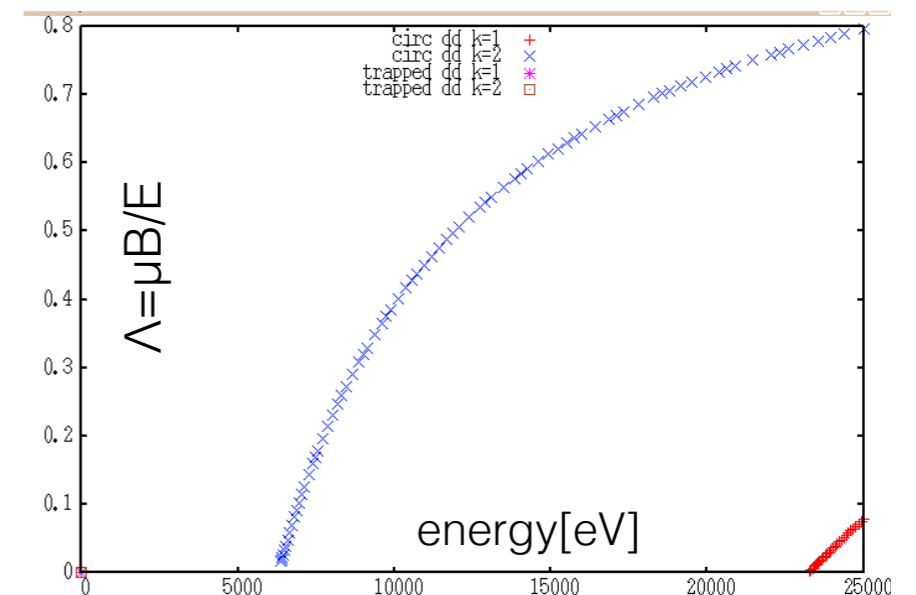


indeed: trapped response increases ω_{GAM} , decreases damping

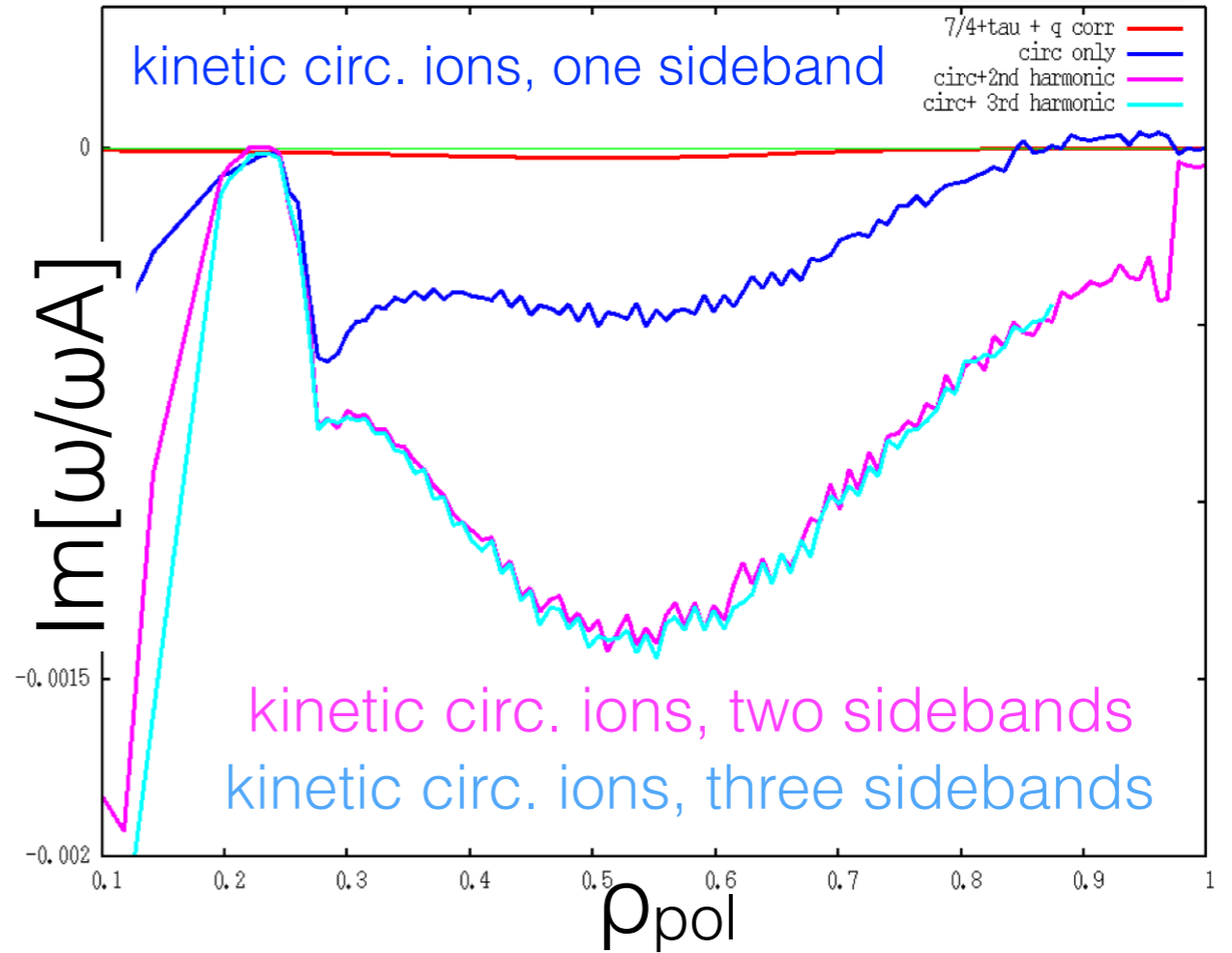
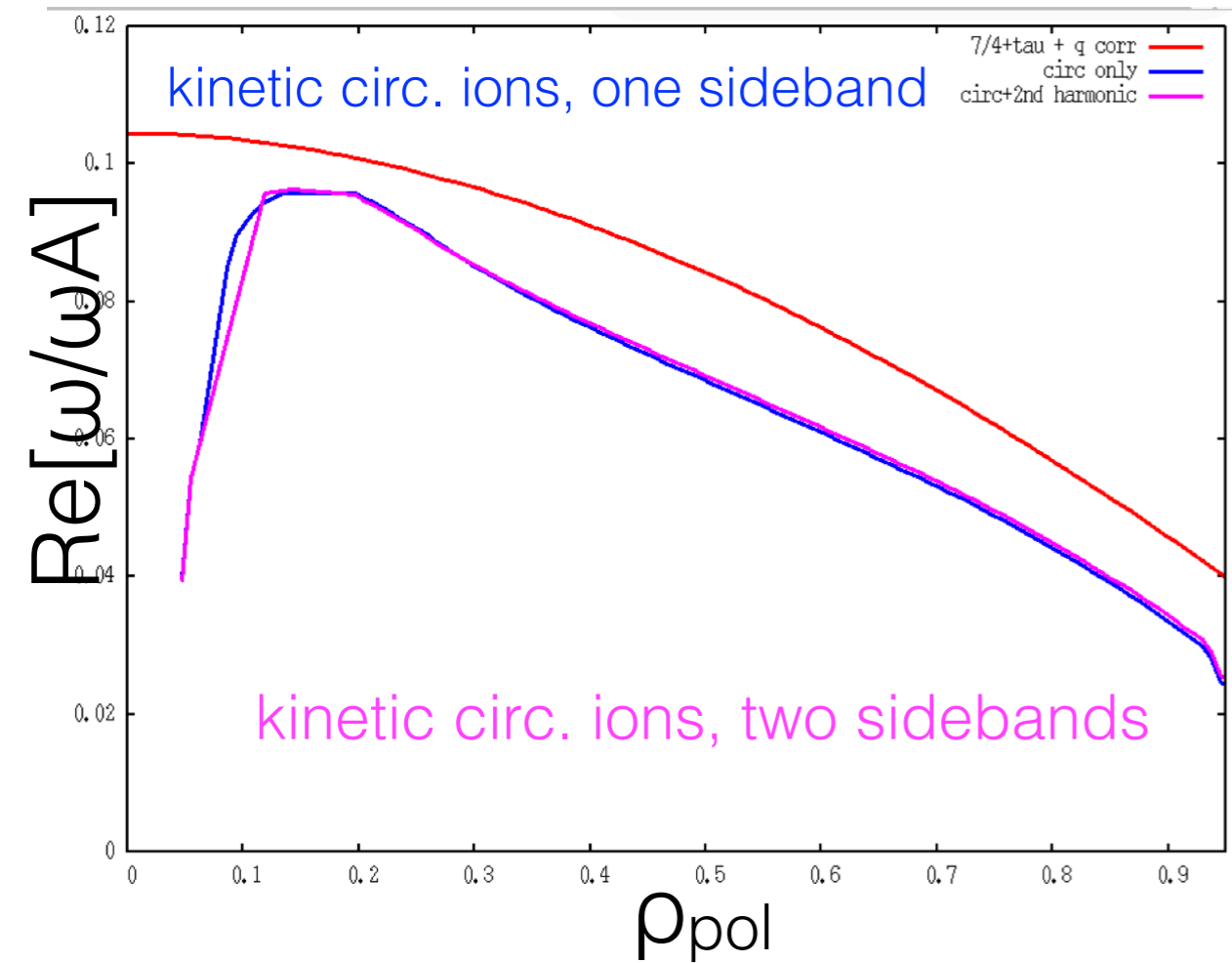
fully kinetic ions: only circulating ions, two sidebands



2nd order resonances significantly increase damping rate!
[Sugama,Zhang,...]

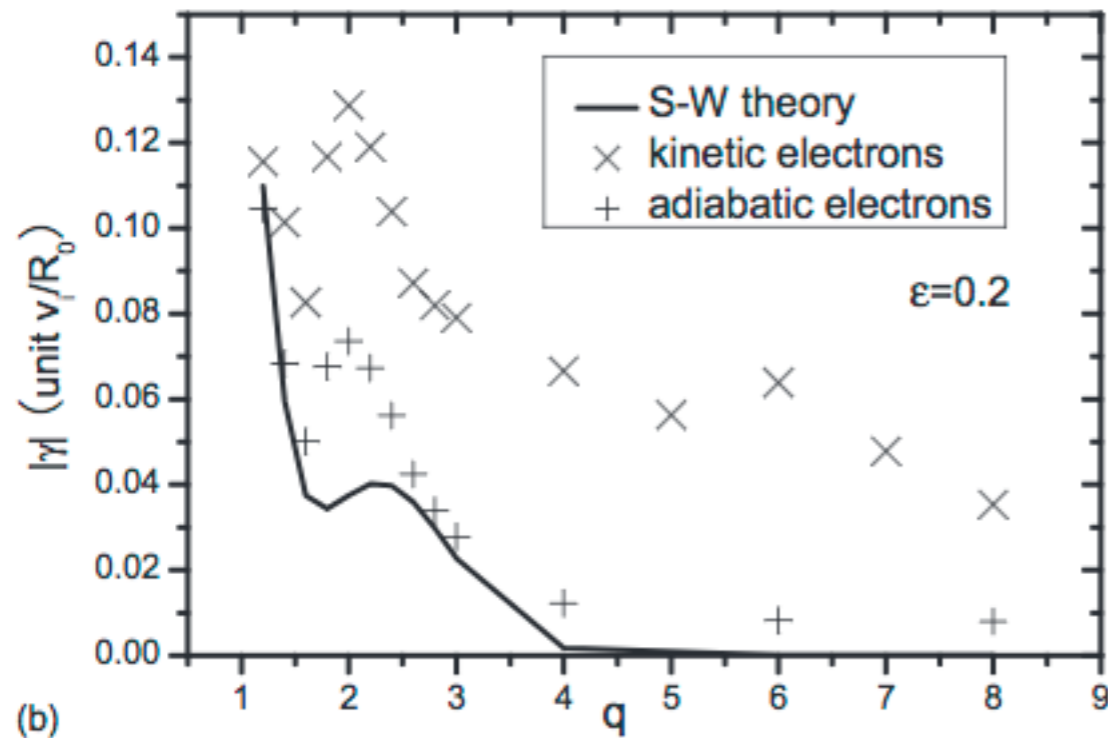


fully kinetic ions: only circulating ions, three sidebands



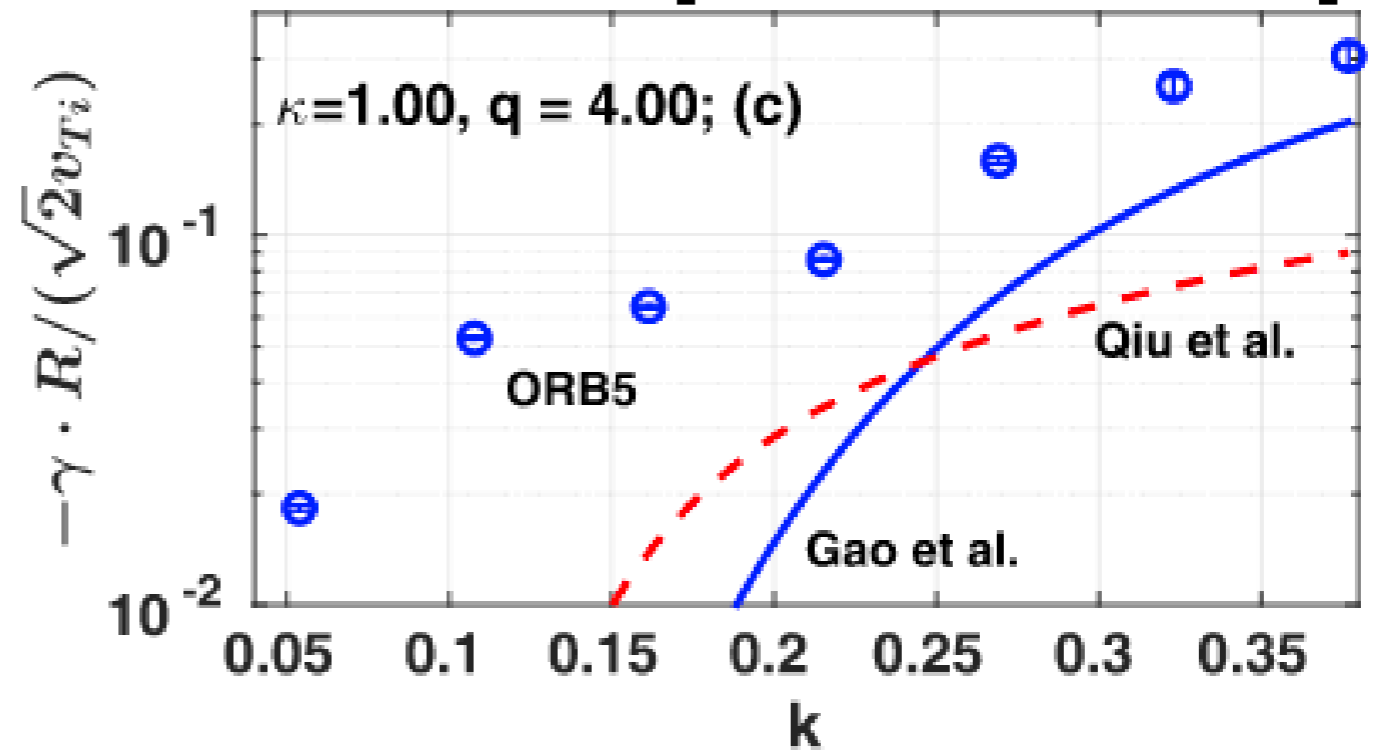
3rd order resonances not important

role of kinetic, non-adiabatic electrons

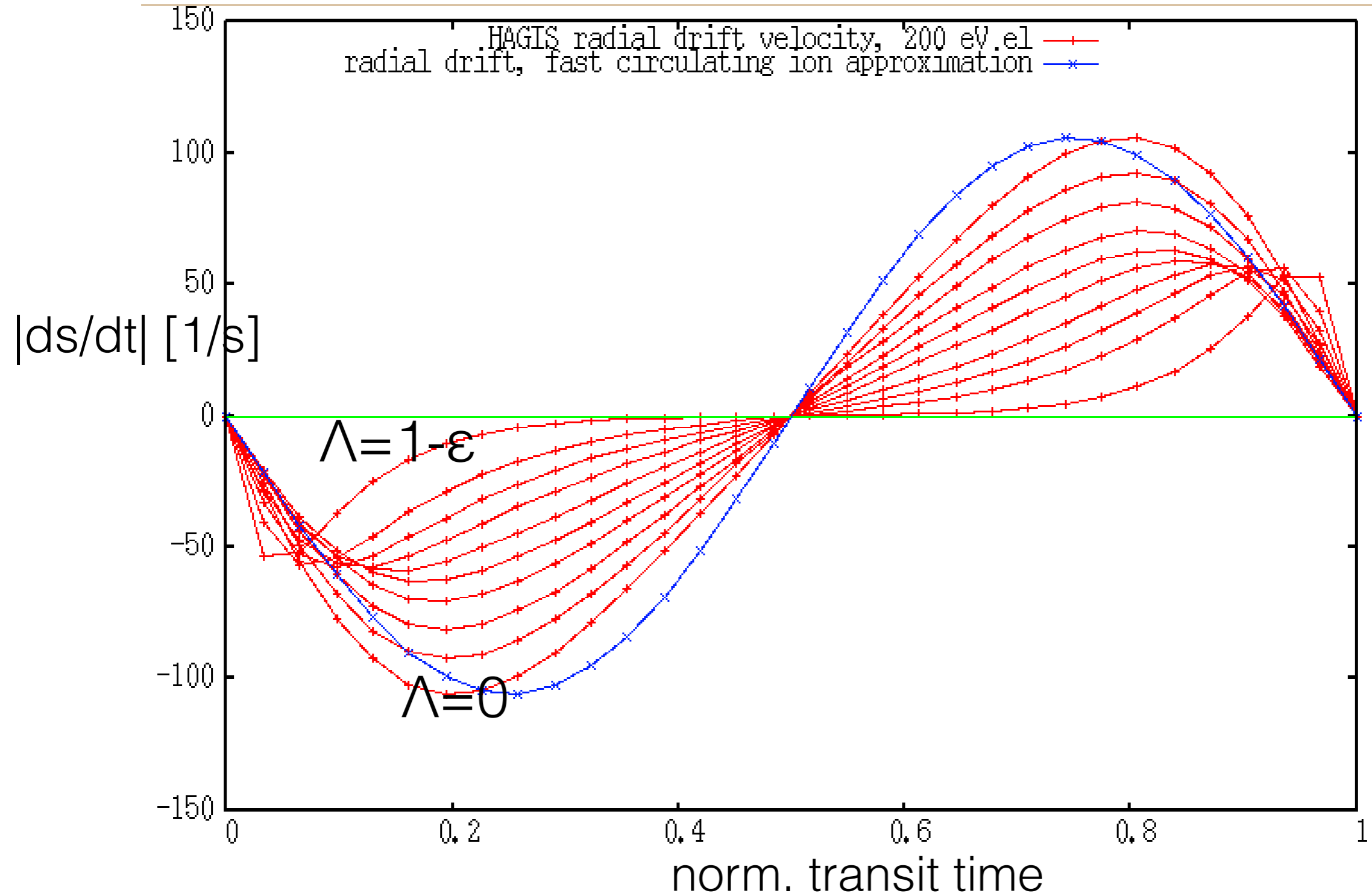


[Zhang 2010]

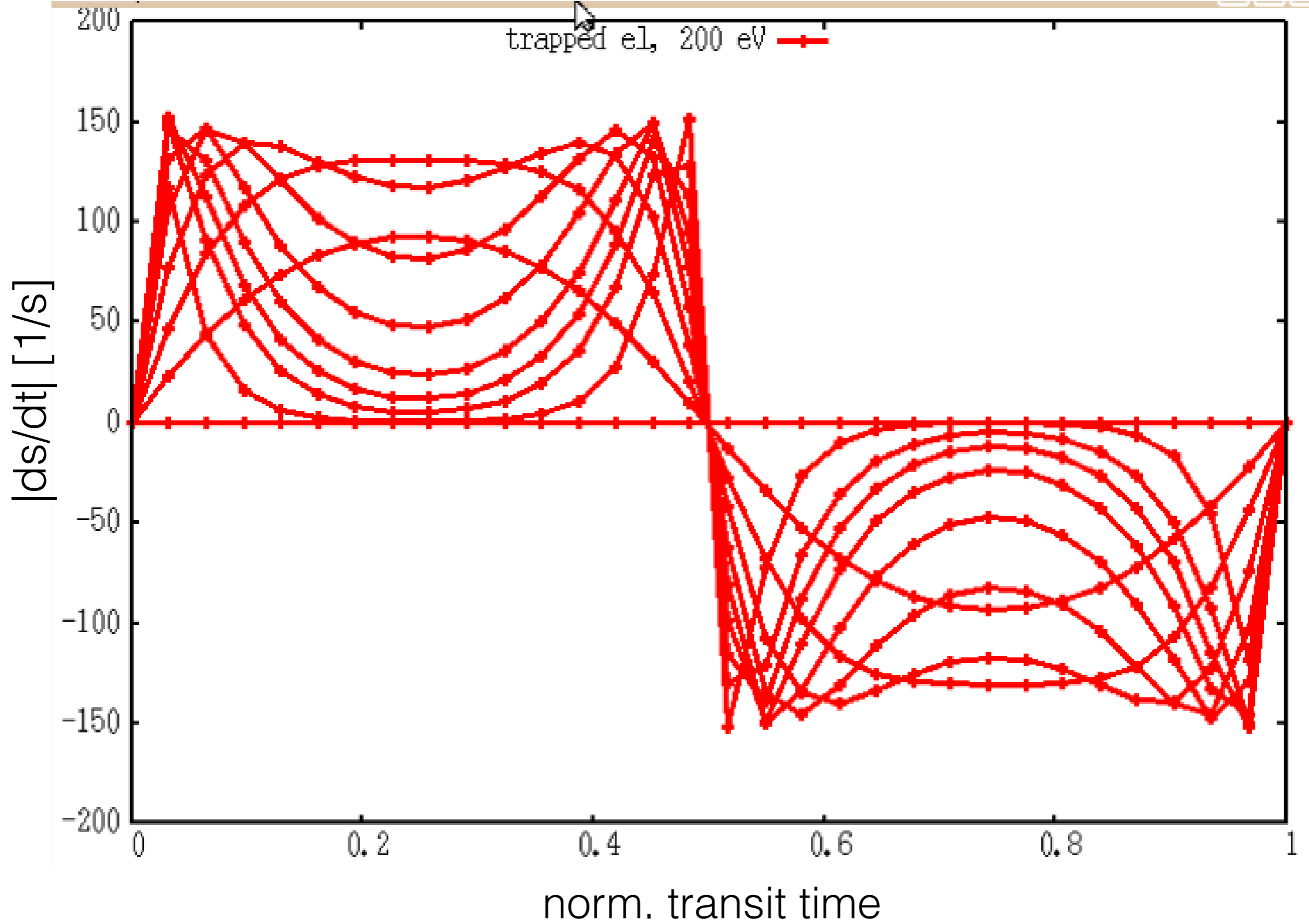
[Novikau, 2017]



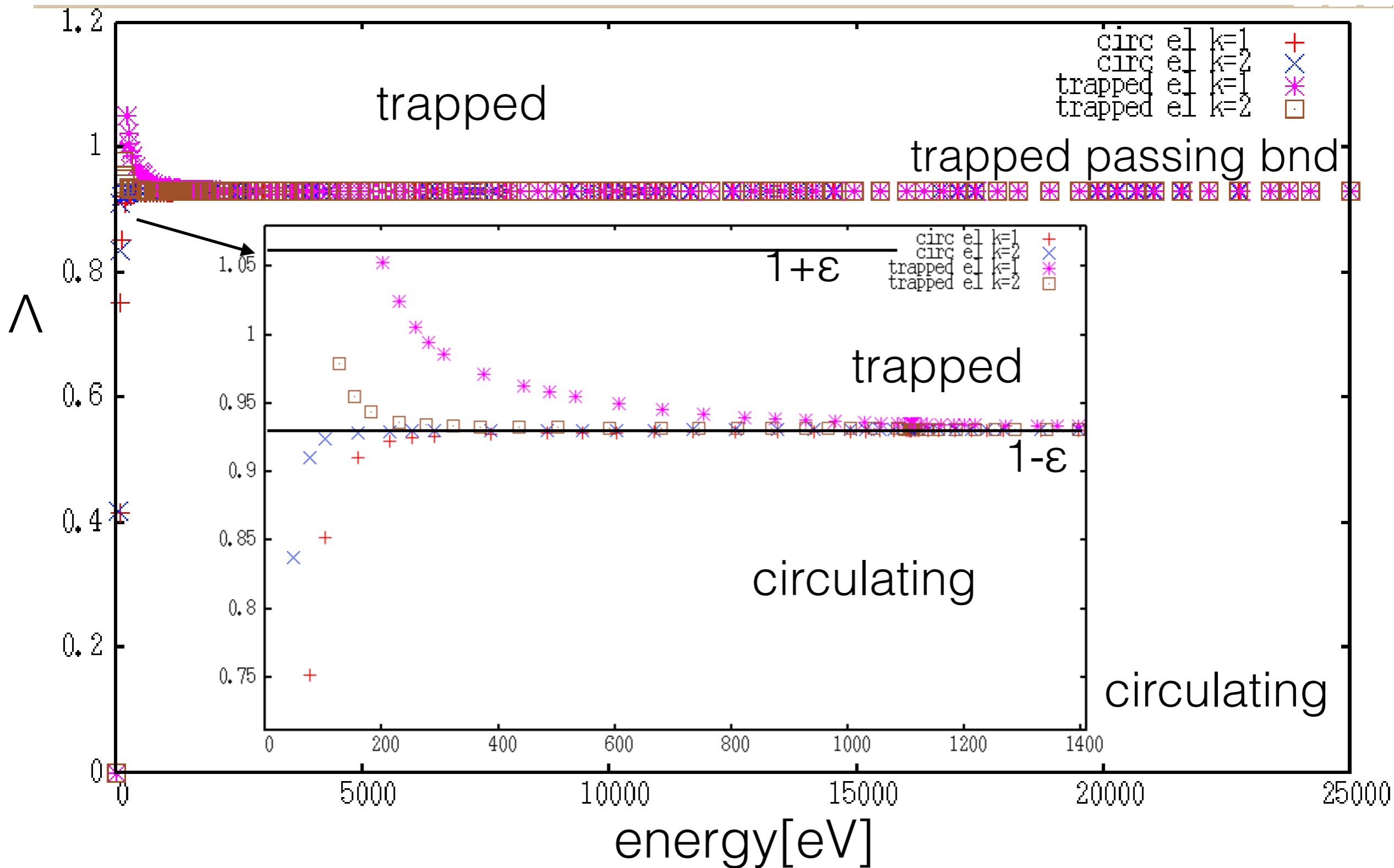
circulating electrons



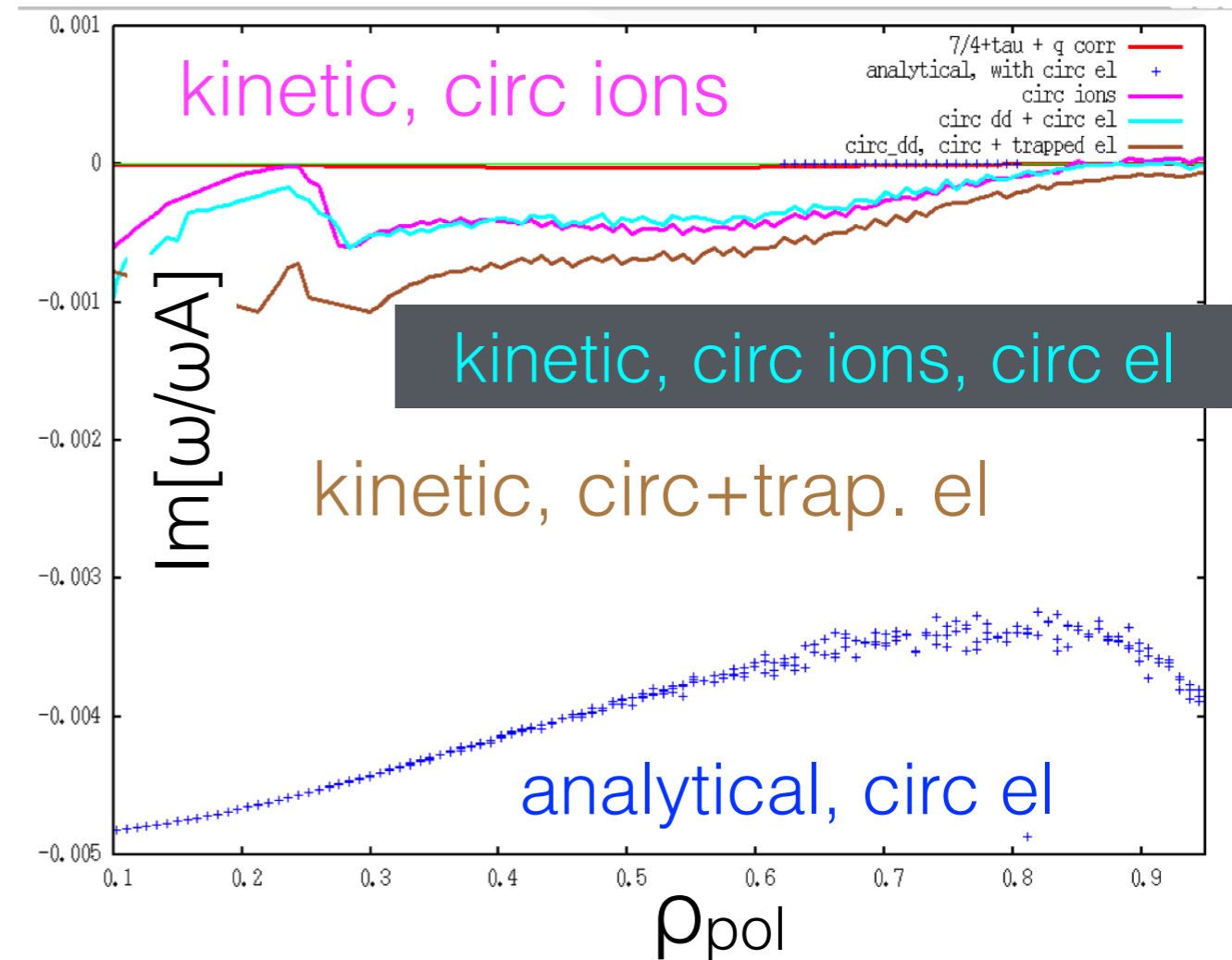
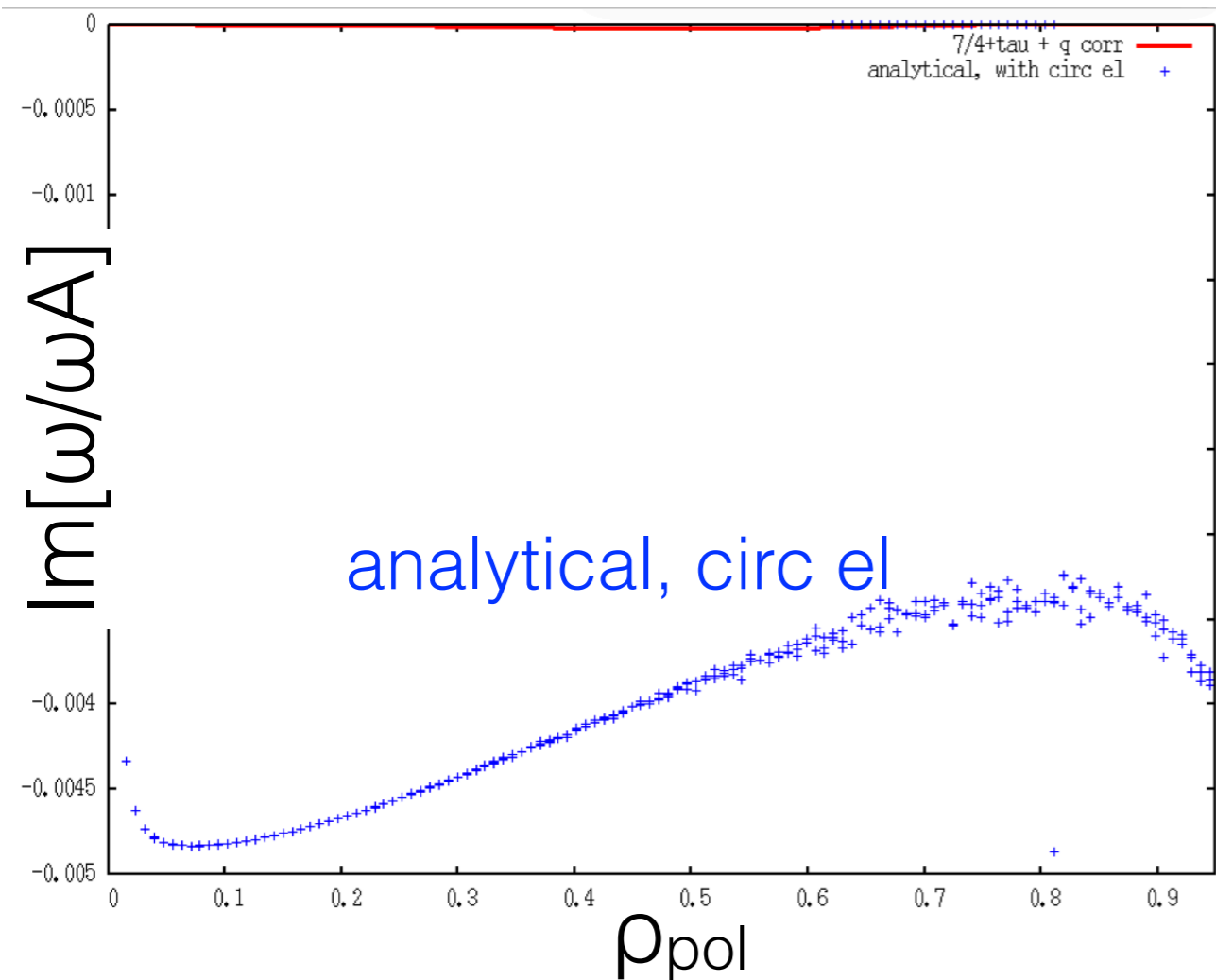
trapped electrons



resonances: electrons $r=0.25$, $w=0.089$ wA



analytical coefficients, numerical solve vs kinetic solve



as expected, analytical model for electrons (fast circulating el approximation) over-predicts damping significantly

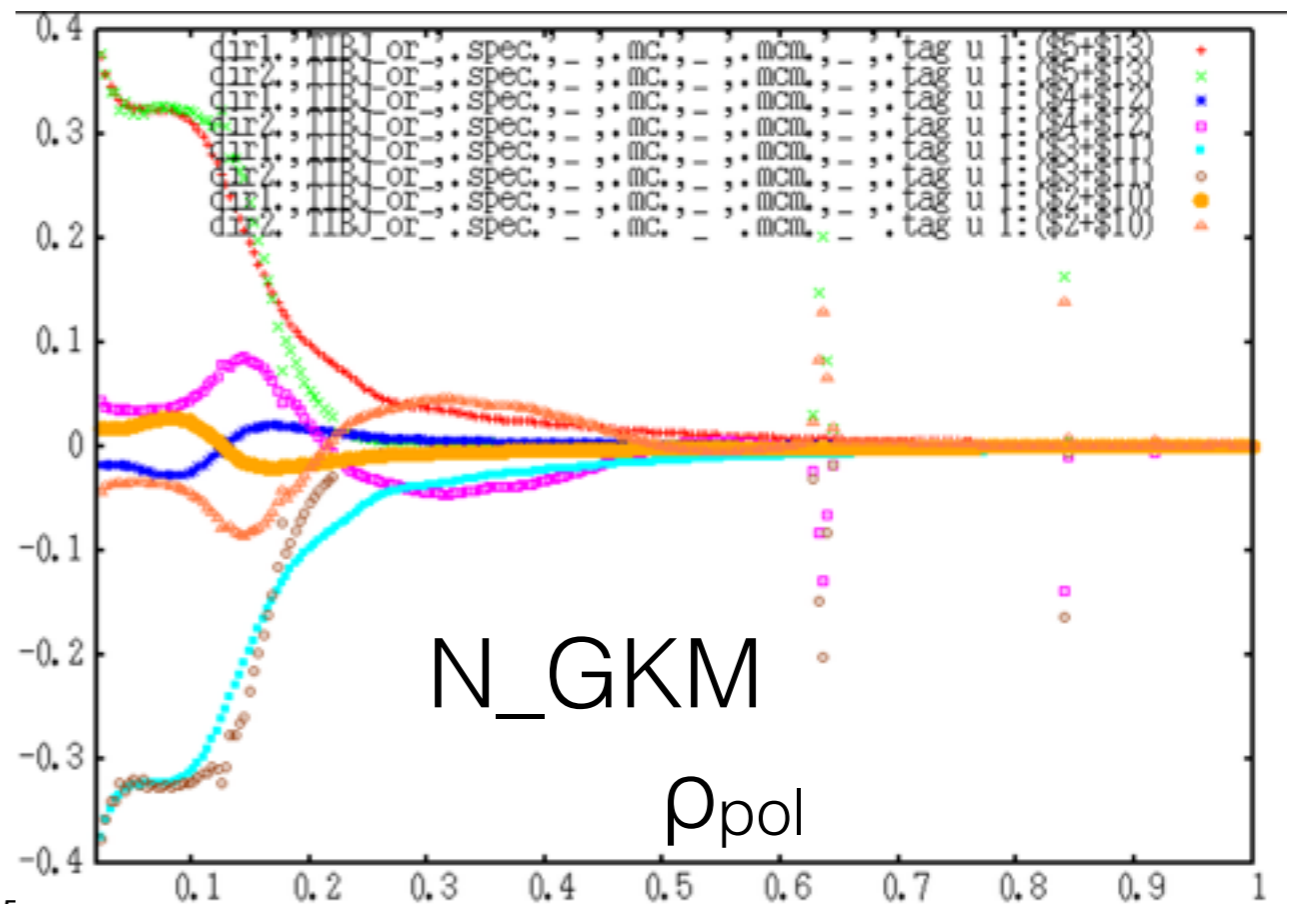
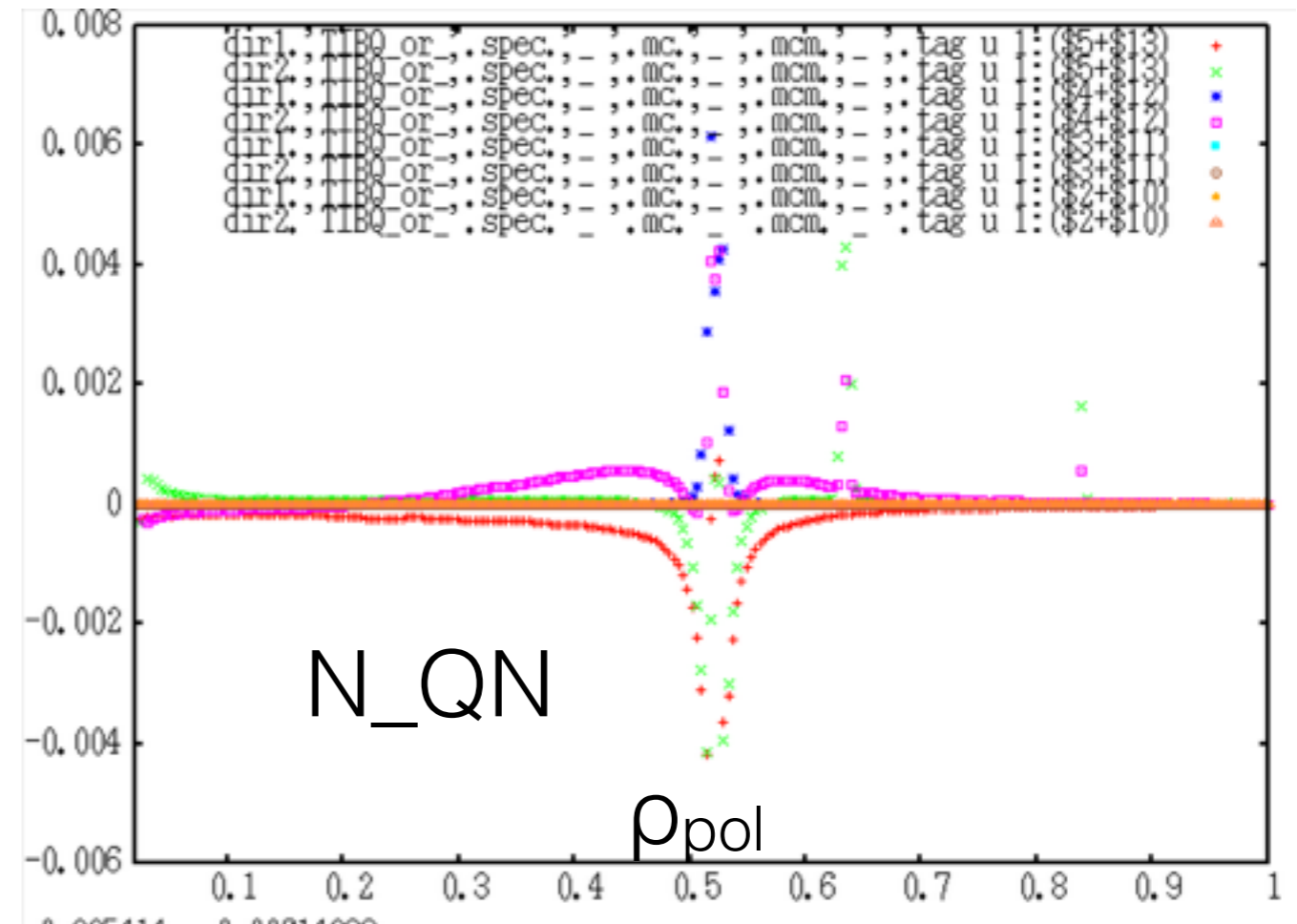
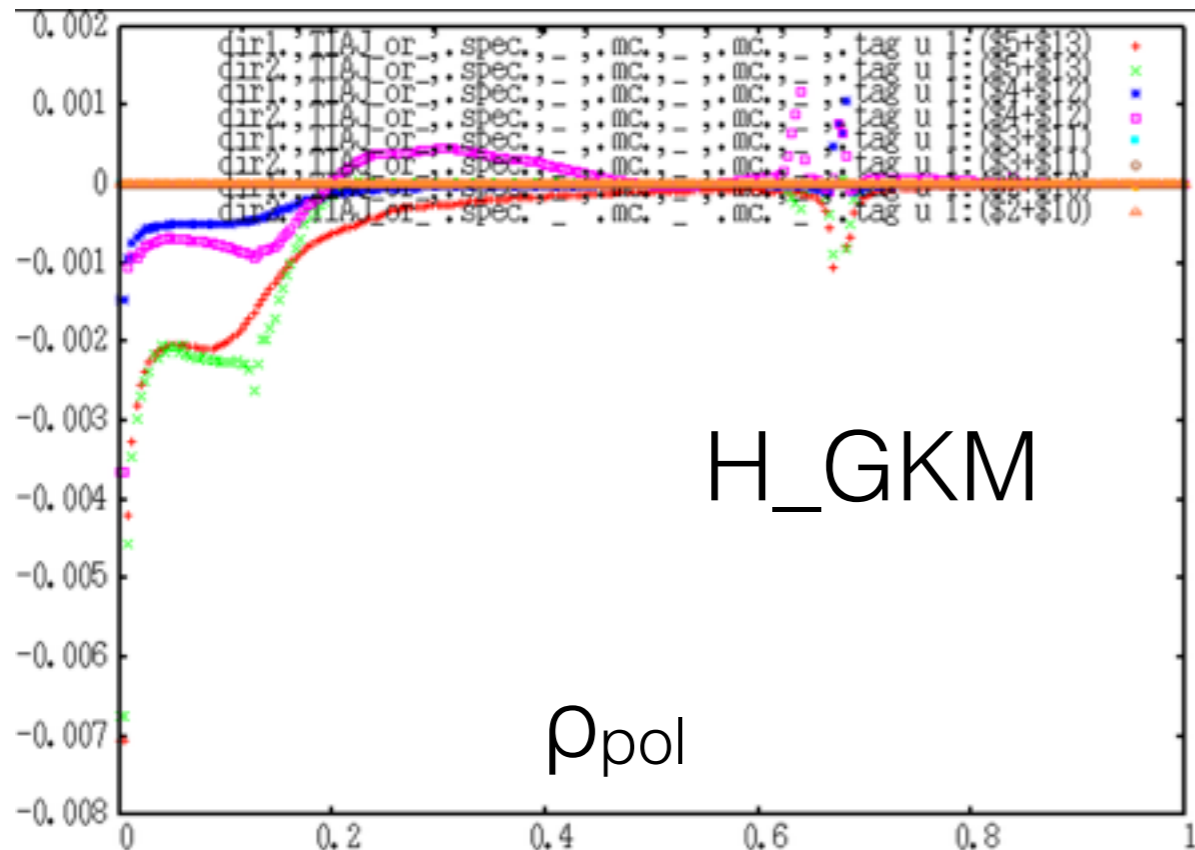
mainly trapped electrons contribute to damping

note: for large ω and finite n ,
 analytical formula for electrons leads
 typically to reasonable results (TAEs)

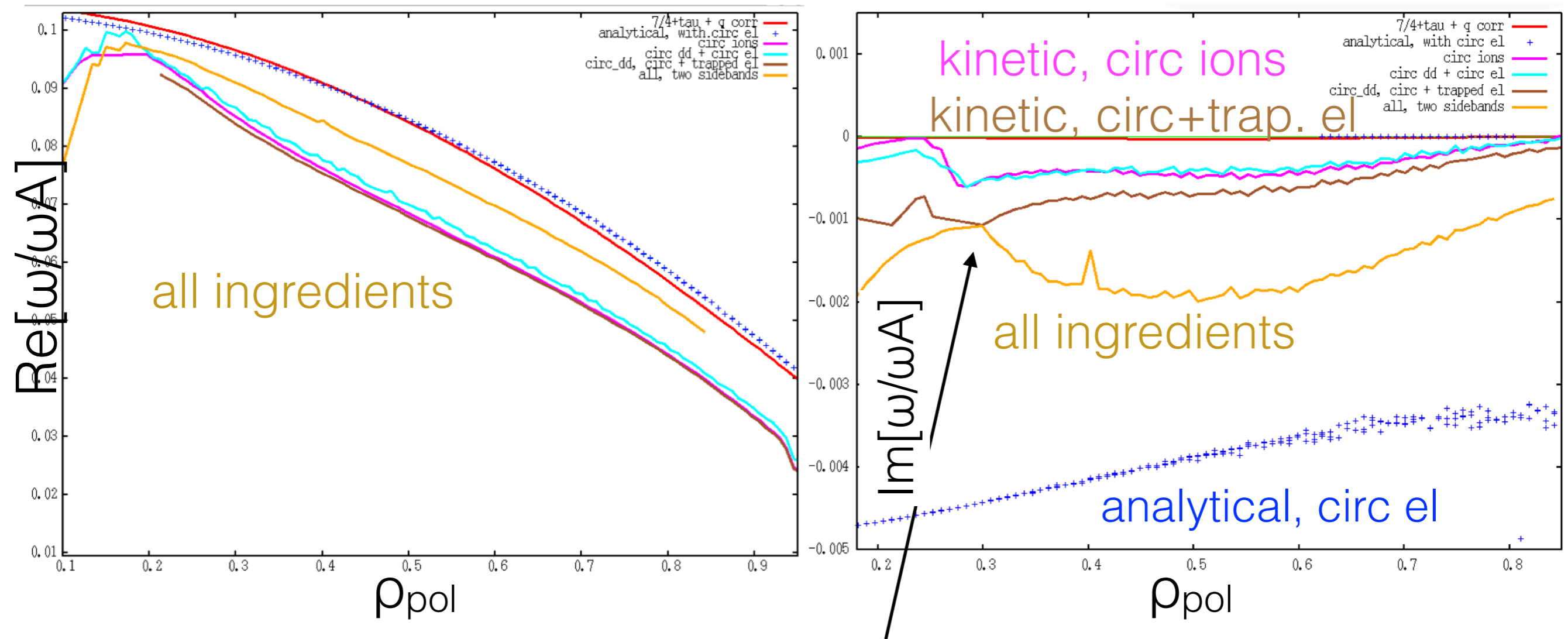
JT60U Eq, electrons
 $n=3$

ψ $\omega=(0.25-0.025i) \omega_A$
 $\omega_{th}/\omega_A=0.07$

■ analytical Re ■ analytical Im
■ numerical Re ■ numerical Im



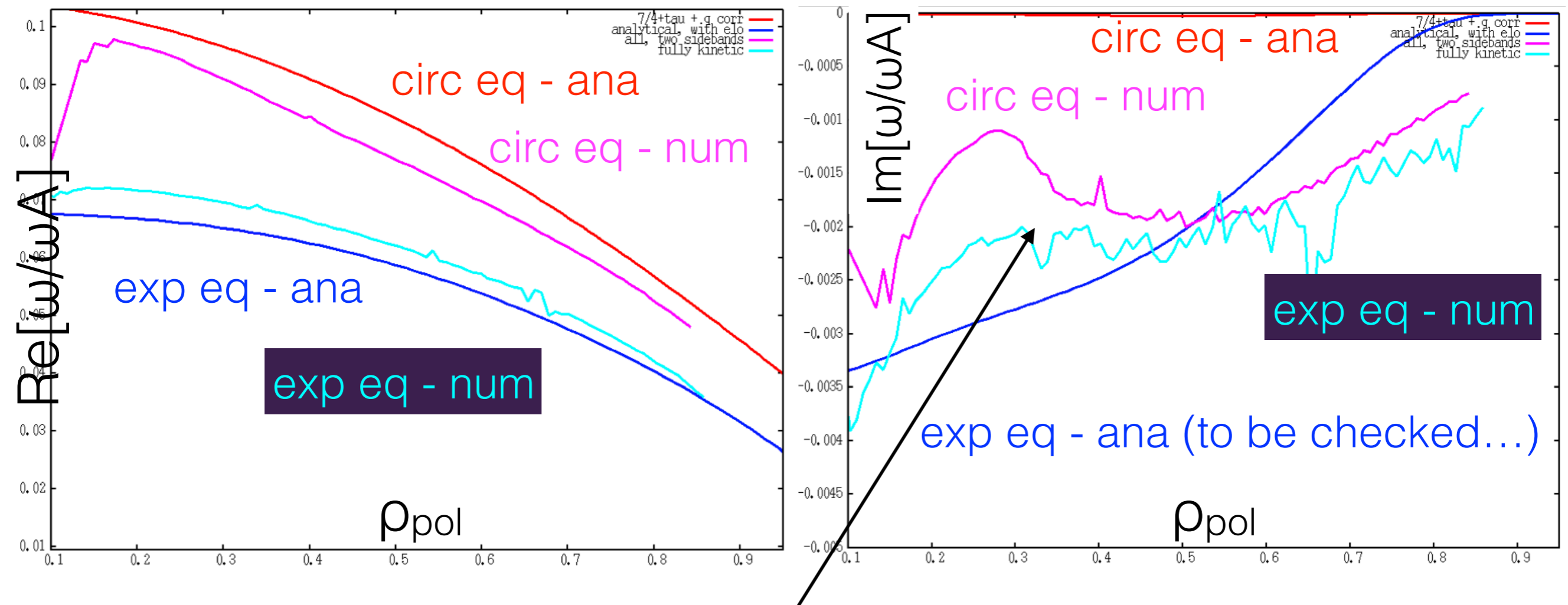
final result: 2 sidebands, with electrons



all together: complex combination of $q, T_e, T_i, \text{local } \epsilon$
 leads to minimum in damping close to observed EGAM location

so far: circular equilibrium with $T_e = T_i$

now: add elongation and inverted T_e

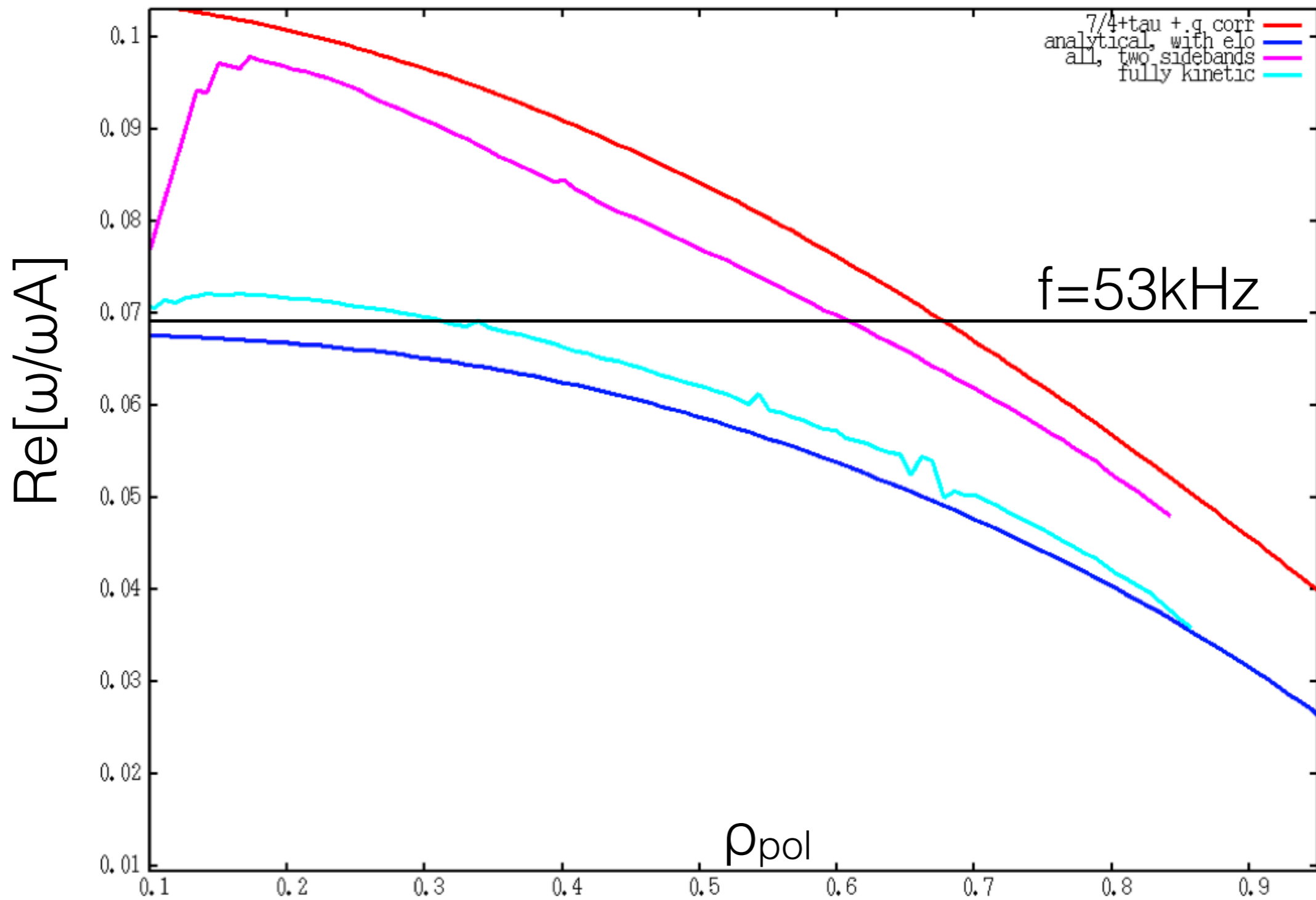


again: (shallow) minimum in damping close to core

note: same q -profile in both cases

but it is likely that the inverted T_e case leads to a more strongly inverted q -profile \rightarrow more pronounced minimum in damping

exp. eq - analytical expression: [Gao, 2008] $\omega = \omega \sqrt{(2/1 + \kappa^2)}$

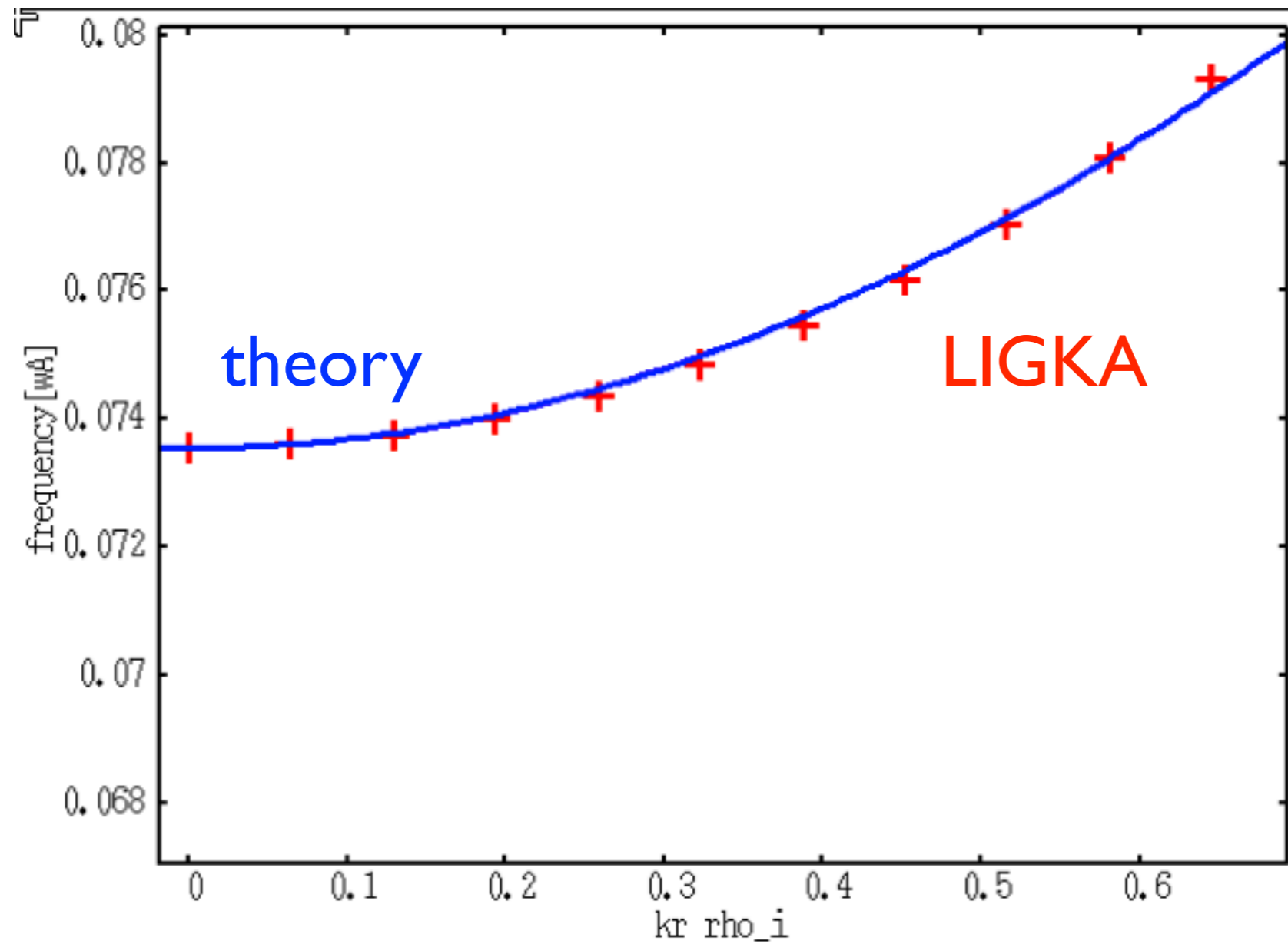


very close to observed onset of EGAM activity at AUG

adding FLR and FOW effects: KGAM benchmark: analytical theory vs LIGKA

$q=3.25$
 $\tau=0.05$

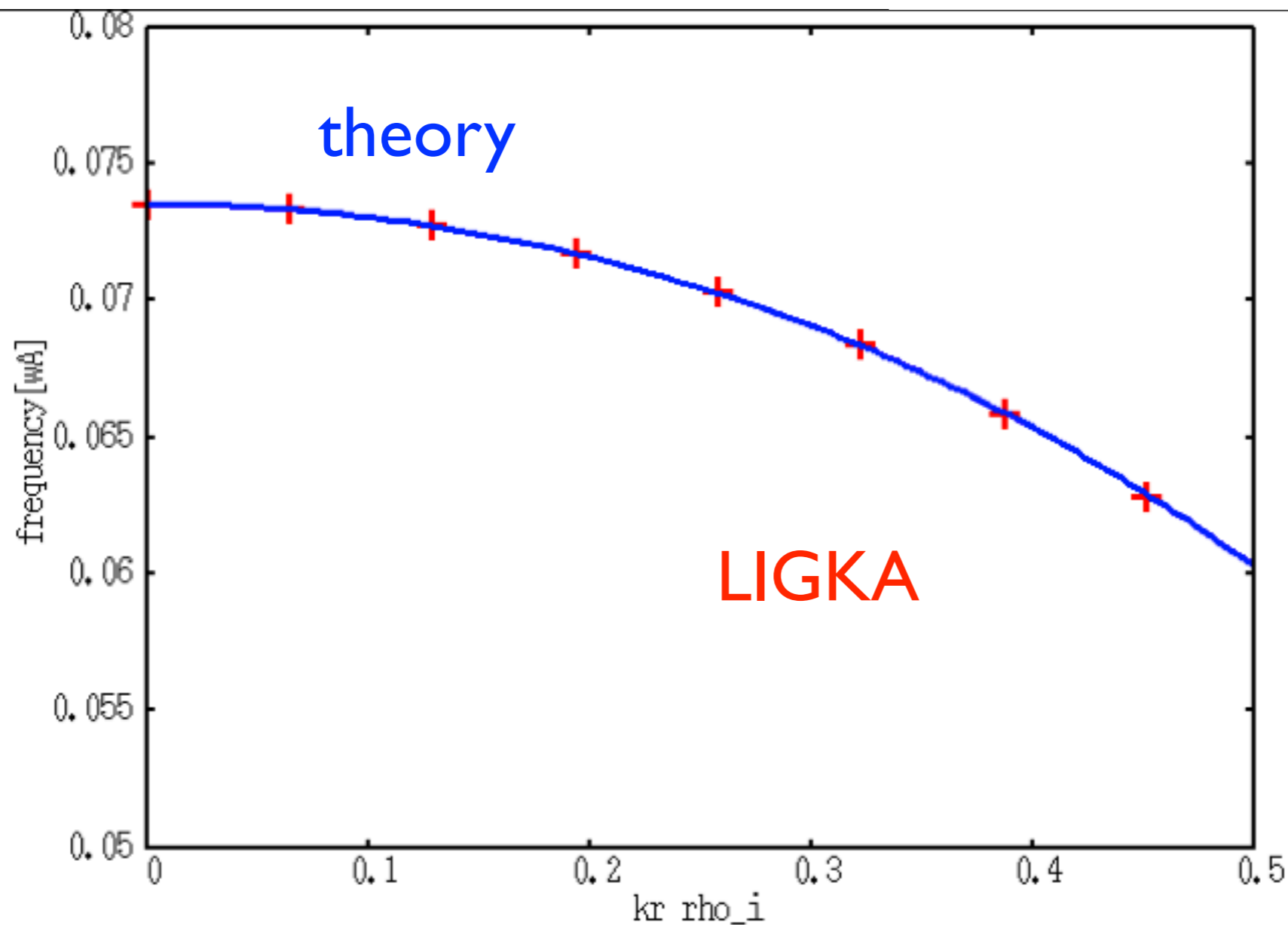
$$\begin{aligned} \frac{3}{4} + \frac{q^2}{\Omega} S_0(\Omega) &\approx \frac{3}{4} - \frac{q^2}{\Omega^2} \left(\frac{13}{4} + 3 \frac{T_e}{T_i} + \frac{T_e^2}{T_i^2} \right) \\ &+ \frac{q^4}{\Omega^4} \left(\frac{747}{32} + \frac{481}{32} \frac{T_e}{T_i} + \frac{35}{8} \frac{T_e^2}{T_i^2} + \frac{1}{2} \frac{T_e^3}{T_i^3} \right) \\ &- i\pi^{1/2} q^4 e^{-\Omega^2/4} \left[\Omega^5/256 + (1 + T_e/T_i)\Omega^3/32 \right] \end{aligned}$$



KGAM benchmark: analytical theory vs LIGKA

$q=3.25$
 $\tau=0.05$

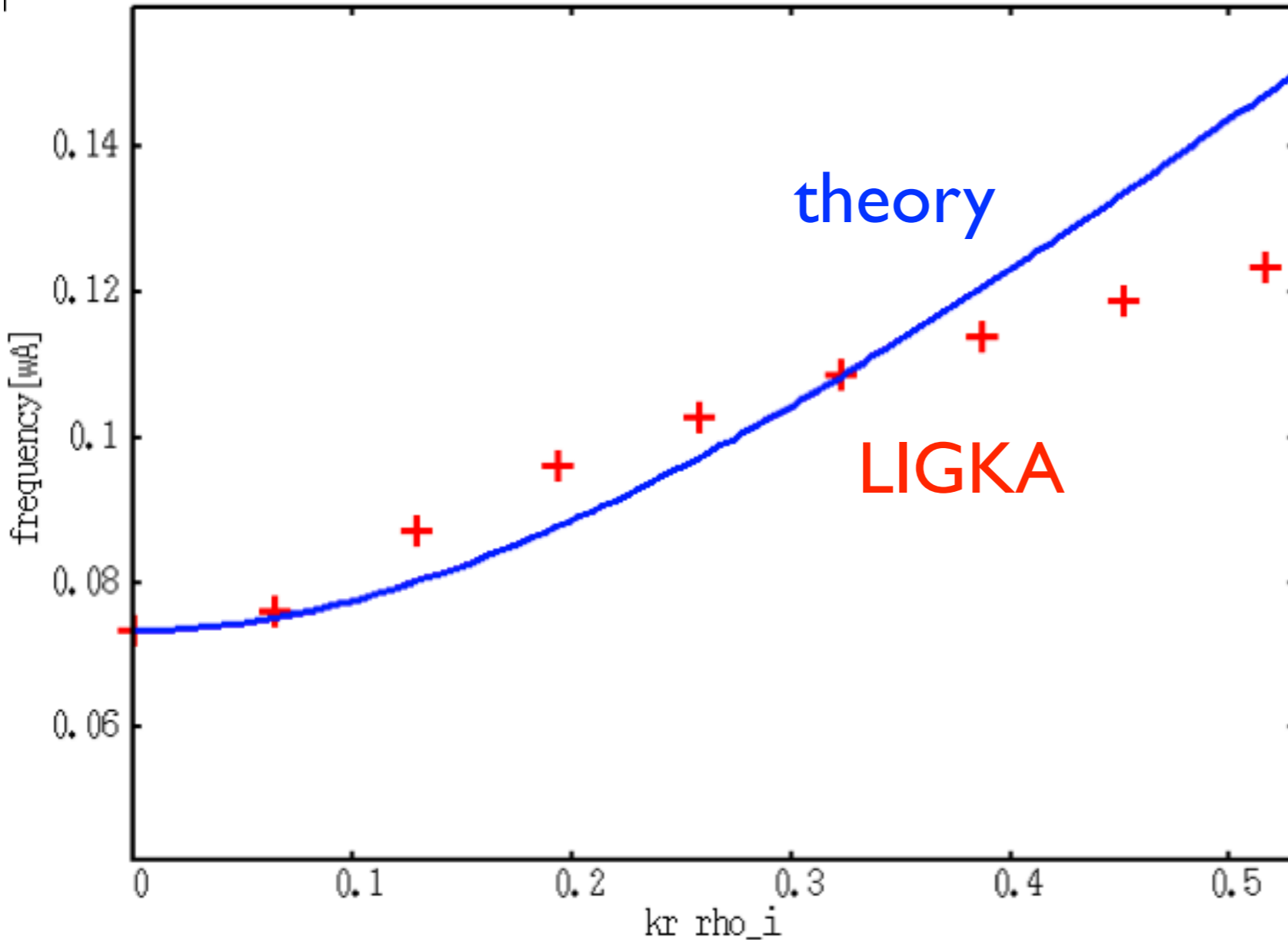
$$\frac{3}{4} + \frac{q^2}{\Omega} S_0(\Omega) \approx \frac{3}{4} - \frac{q^2}{\Omega^2} \left(\frac{13}{4} + 3 \frac{T_e}{T_i} + \frac{T_e^2}{T_i^2} \right) + \frac{q^4}{\Omega^4} \left(\frac{747}{32} + \frac{481}{32} \frac{T_e}{T_i} + \frac{35}{8} \frac{T_e^2}{T_i^2} + \frac{1}{2} \frac{T_e^3}{T_i^3} \right) - i\pi^{1/2} q^4 e^{-\Omega^2/4} \left[\Omega^5/256 + (1 + T_e/T_i)\Omega^3/32 \right]$$



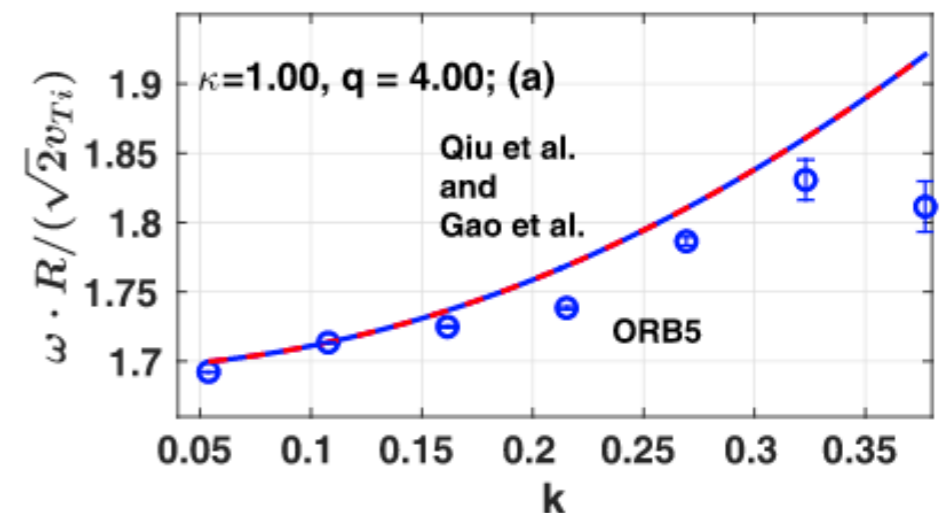
KGAM benchmark: analytical theory vs LIGKA

$q=3.25$
 $\tau=0.05$

$$\frac{3}{4} + \frac{q^2}{\Omega} S_0(\Omega) \approx \frac{3}{4} - \frac{q^2}{\Omega^2} \left(\frac{13}{4} + 3 \frac{T_e}{T_i} + \frac{T_e^2}{T_i^2} \right) + \frac{q^4}{\Omega^4} \left(\frac{747}{32} + \frac{481}{32} \frac{T_e}{T_i} + \frac{35}{8} \frac{T_e^2}{T_i^2} + \frac{1}{2} \frac{T_e^3}{T_i^3} \right) - i\pi^{1/2} q^4 e^{-\Omega^2/4} \left[\Omega^5/256 + (1 + T_e/T_i)\Omega^3/32 \right]$$



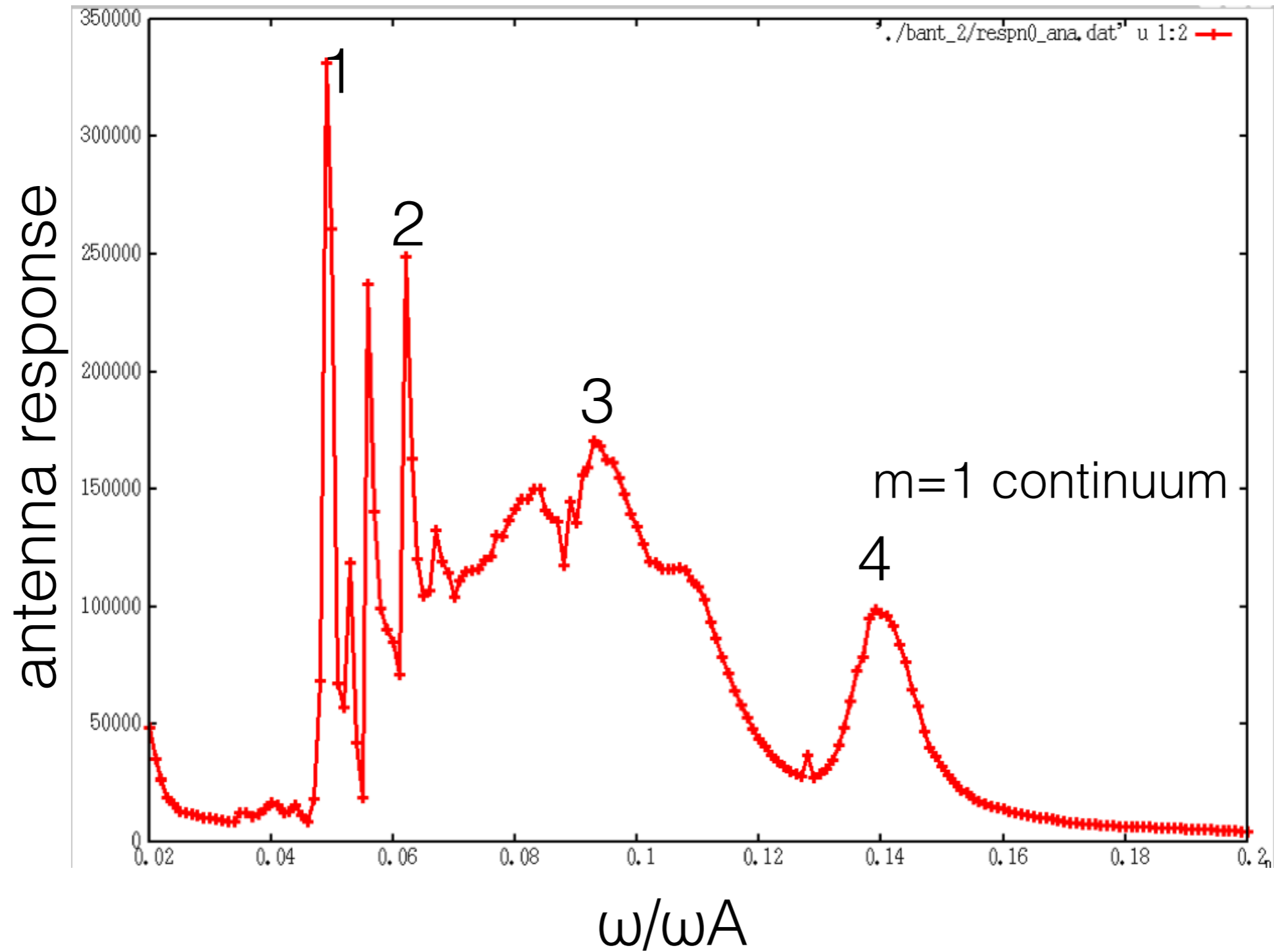
deviations from simple formula if equation is solved non-perturbatively



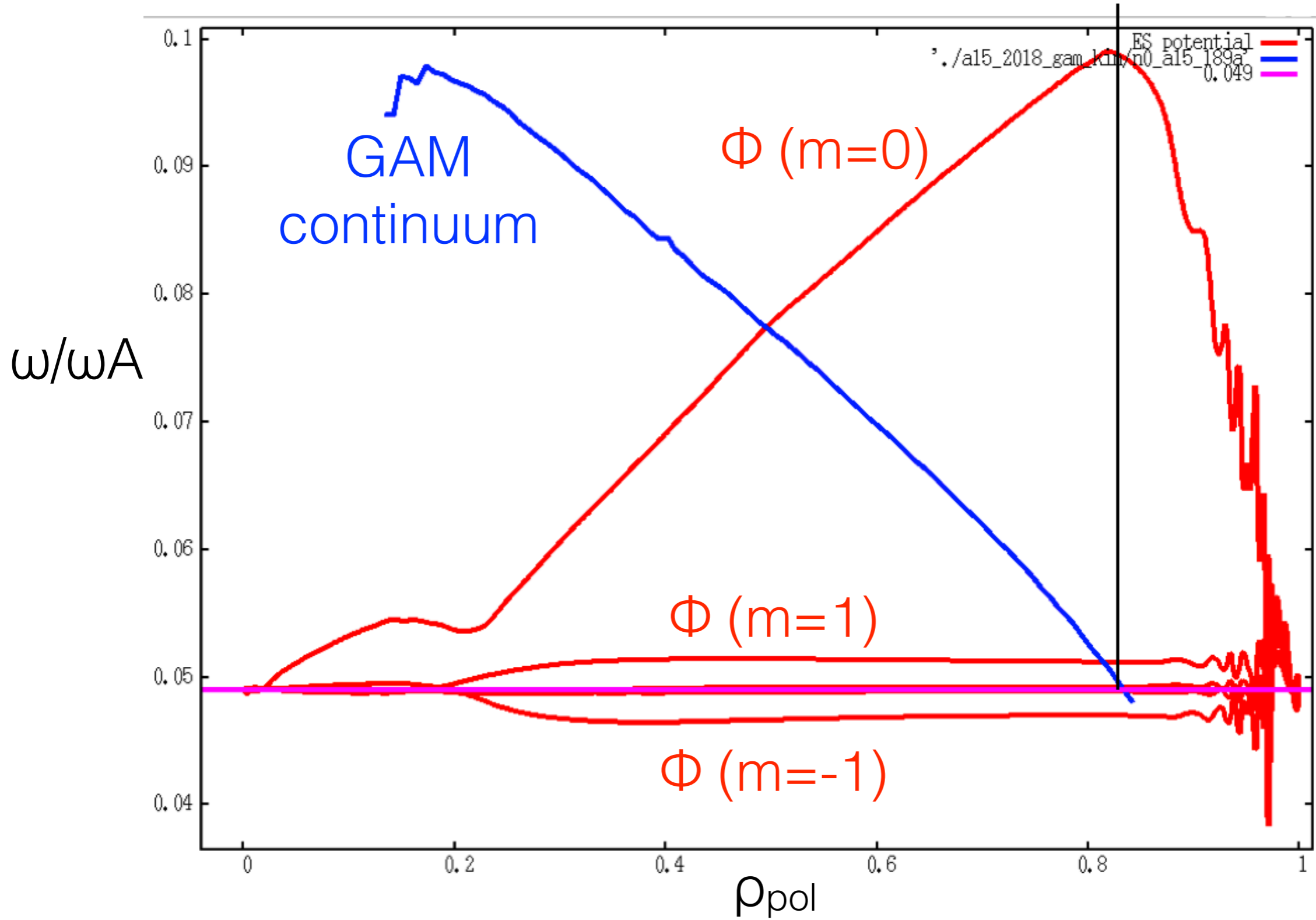
similar to [Novikau, 2017]

global solutions: fully kinetic, non-adiabatic, 2 sidebands

use antenna version to localise modes: drive $m=1$ sideband at mid radius

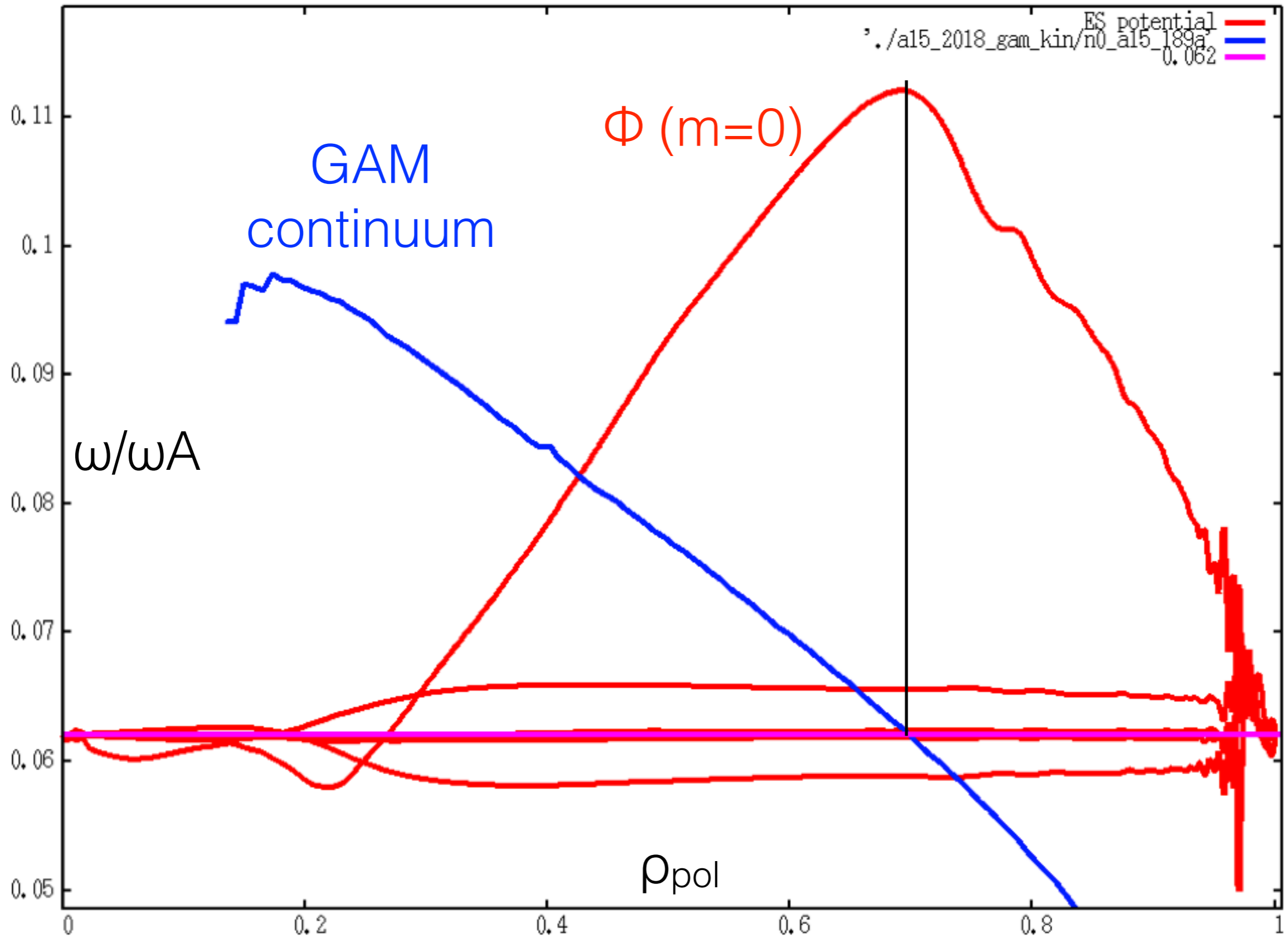


peak 1

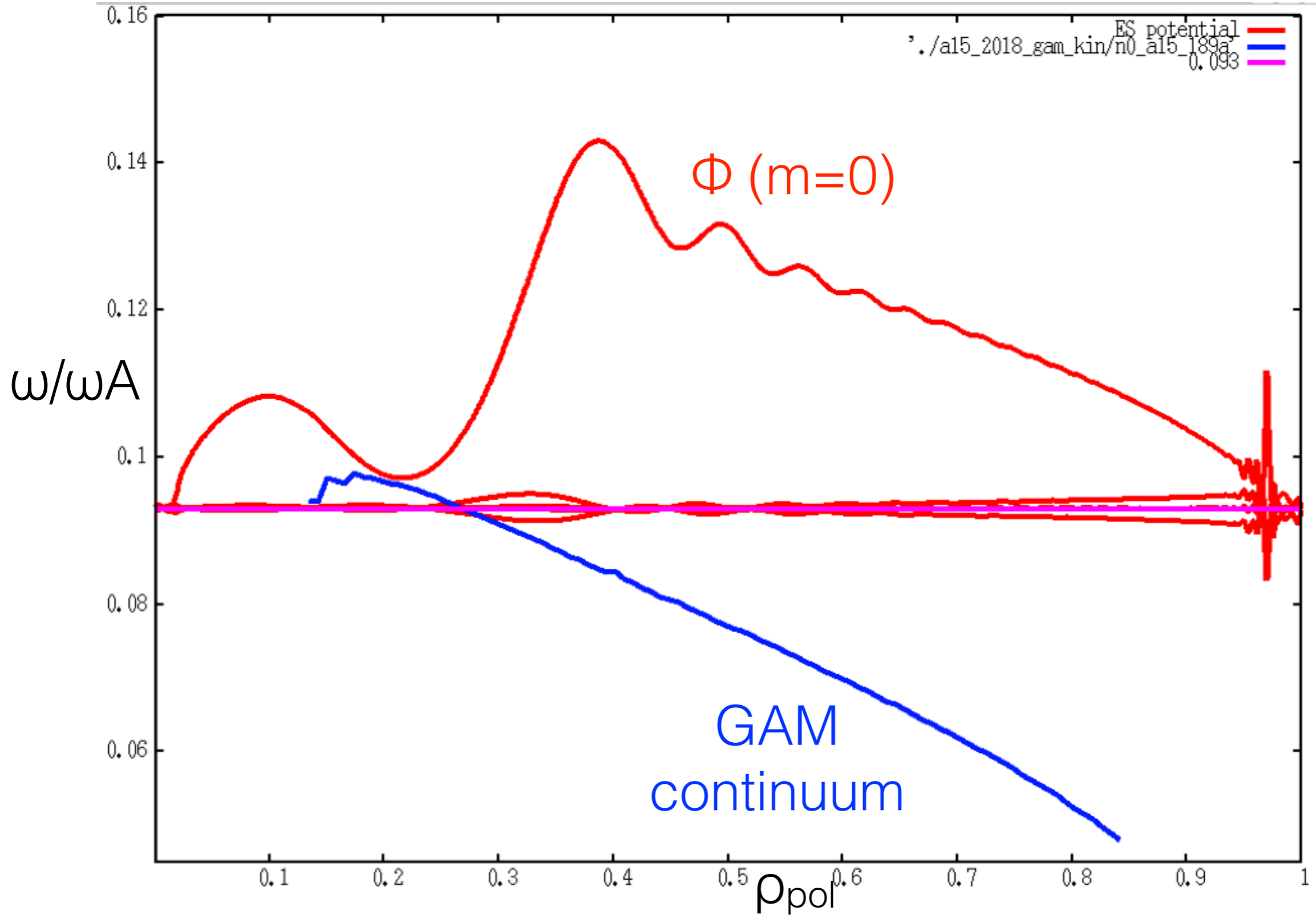


mode's maximum at continuum intersection point

peak 2

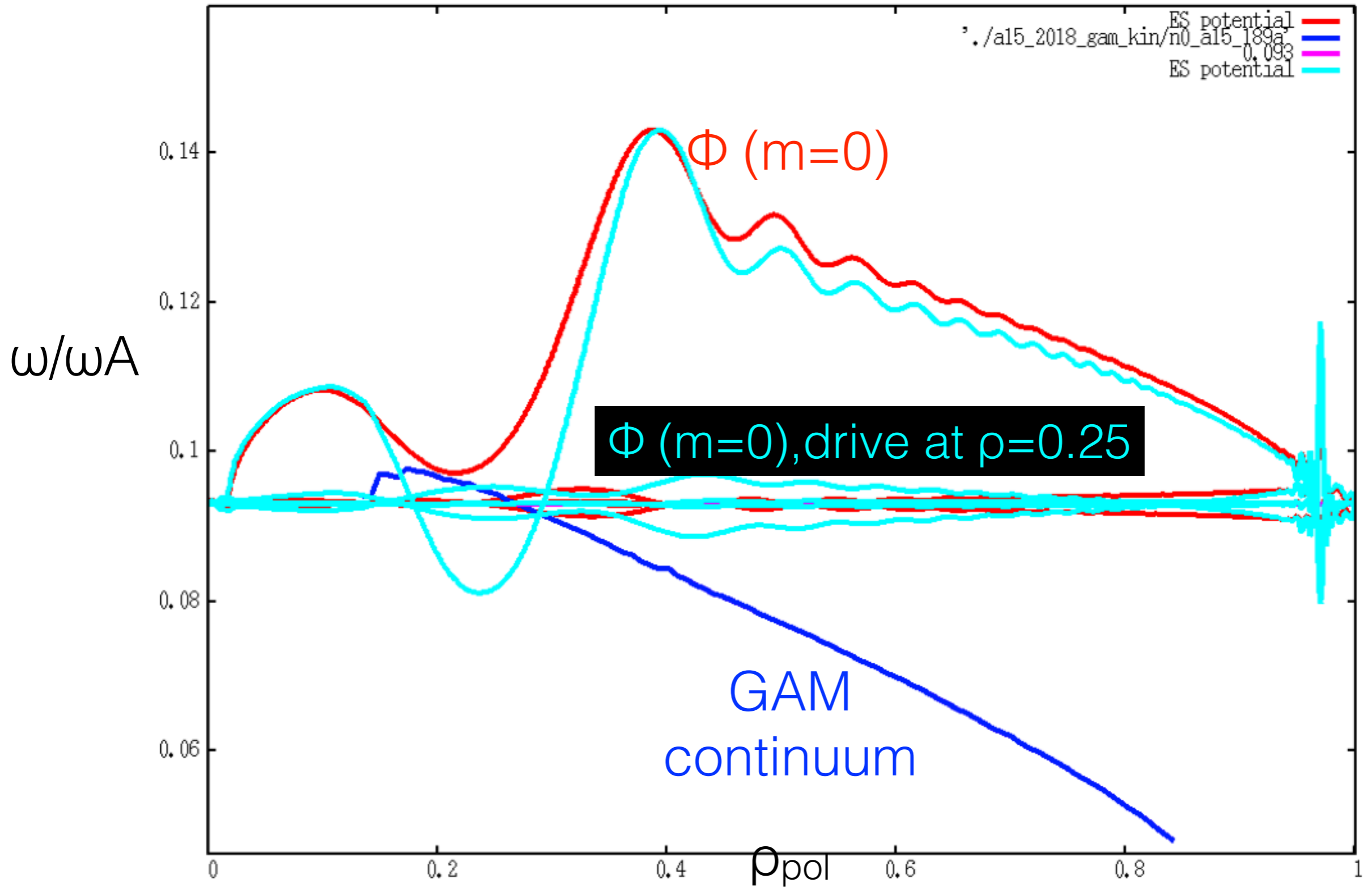


peak 3



inner boundary conditions seems to influence solution slightly;
outward propagation observed

peak 3



change of antenna drive ($\rho=0.25$) does not change results significantly

summary:

- GAM and kGAM damping is a complex problem
- many different physics elements play together:
 - shape of q
 - shape of T_i , T_e
 - local aspect ratio
 - plasma shape
- kinetic ions with second harmonics, kinetic electrons are found to be important for correct scaling of kGAM damping
- global EGAMs excited by EPs expected to be similar to antenna solution
- previously found resonance condition for EPs verified

open ends:

- treatment of core orbits
- plasma dispersion function evaluation
- add anisotropic EPs (TRANSP data available)
- compare to ORB5

ZF model for HAGIS

- 3-wave interaction equations have been derived (forced excitation), to be re-written in HAGIS formulation
- implementation has not been started (later in December)
- milestone slightly delayed

forced oscillation: $n=0$ 'eigenmode' structure: $(kr \text{ ps} \rightarrow 0)$

$$\frac{\phi(t)}{\phi_0} = A + (1 - A) \cos(\omega_{GAM} t) e^{-\gamma t} \quad A = \frac{1}{1 + 1.6q_0^2/\sqrt{\epsilon}} \quad \gamma = \omega_{GAM} e^{-q_0^2}$$

or [Xiao, Catto]...

assume (for now) fixed spatial of Φ_0 : radial envelope of pump AEs

spatial structure of $v = E \times B$:

$$v_z = \frac{-\nabla\phi(r, t)}{B} (0, 1, -2q \cos(\theta))$$

ZF model for HAGIS

$$\mathcal{L}_w = \underbrace{\sum_j \left\{ \frac{1}{2} m v_j^2 + e (\mathbf{A}_j \cdot \mathbf{v}_j - \Phi_j) \right\}}_{\mathcal{L}_{bulk}} + \underbrace{\frac{1}{2\mu_0} \int_V \left\{ \frac{1}{c^2} E^2 - B^2 \right\} d^3x}_{\mathcal{L}_{em}}$$

$$\mathcal{L}_w = \sum_{\substack{\text{bulk} \\ \text{plasma}}} \left[\frac{1}{2} m \left\{ \mathbf{v}_0 + \sum_k \frac{\tilde{\mathbf{E}}_k \wedge \mathbf{B}_0}{B_0^2} + \sum_{k,k'} \frac{\tilde{\mathbf{E}}_k \wedge \tilde{\mathbf{B}}_{k'}}{B_0^2} \right\} \right. \\ \left. + e \left\{ \left(\mathbf{A}_0 + \sum_k \tilde{\mathbf{A}}_k \right) \cdot \left\{ \mathbf{v}_0 + \sum_k \frac{\tilde{\mathbf{E}}_k \wedge \mathbf{B}_0}{B_0^2} + \sum_{k,k'} \frac{\tilde{\mathbf{E}}_k \wedge \tilde{\mathbf{B}}_{k'}}{B_0^2} \right\} - \sum_k \tilde{\Phi}_k \right\} \right] \\ + \frac{1}{2\mu_0} \int_V \left\{ \frac{1}{c^2} \sum_k \tilde{E}_k^2 - B_0^2 - \sum_k (2\mathbf{B}_0 \cdot \tilde{\mathbf{B}}_k + \tilde{B}_k^2) \right\} d^3x,$$

use $\mathbf{v} = \mathbf{v}_0 + \mathbf{v}_z \rightarrow$ 3rd order terms, Lagrangian \rightarrow vary

$$L_3 = -m_i n_i \sum_{k,k',k''} = \frac{(\mathbf{E}_k \times \mathbf{B}_0) \cdot (\mathbf{E}'_k \times \mathbf{B}''_k)}{B_0^4} = \frac{(\mathbf{B}_0 \cdot \mathbf{E}'_k)(\mathbf{E}_k \cdot \mathbf{B}''_k)}{B_0^4}$$

$$L_{int} = \sum_{j=1}^{N_p} \sum_{k=1}^{N_w} \frac{1}{\omega_k} \sum_m (k_{\parallel} v_{\parallel j} - \omega_k) \cdot \left[\Xi_k C_{jkm} + Y_k S_{jkm} \right] + \sum_{k=1}^{N_w} \sum_{k'=1}^{N_w} i \rho_z B_{k'} \omega_k C_{k,z,k'} \epsilon_{k,z,k'}$$

small coding effort: additional term for std wave-particle interaction equation;
extension to EGAM case

additional equation for ZF evolution equation (trivial)

for spontaneous excitation: different coupling coeffs: Hasegawa-Mima-type ,
modulational instability [Chen,Zonca] 49

ZF model for HAGIS

- code has been extended, all except scattering cross sections has been implemented (thx to T Hayward)
- start with MHD 3-wave problem: two Alfvén, one sound wave (trivial cross sections given in literature): forced excitation problem (compare to ORB5, XHMGC,...)
- TAE ITPA $n=6, -6$ case, $n=0$ perturbations (mode structures already prepared)
- ready for first tests...

Progress on zonal structure generated by Alfvén wave with XHMGC (NAT WP3)

Results of 2017:

- GAM

XHMGC (both reduced equations¹ and full set of equations) has been successfully applied to the simulations of GAM. The real frequency, damping rate and residual level agree well between simulations and theory. Those results show the importance of accounting for the kinetic thermal ion effects on the GAM/zonal flow simulations with hybrid codes.

- Zonal flow

Preliminary results of XHMGC show that the zonal flow is forced driven by an EP-driven Alfvén mode², and the Alfvén mode saturation level is modified.

- Mode-mode coupling

A multi-mode simulation has been performed by XHMGC. As a first step, the zonal structure generation has not been taken into account. Two type of simulations have been performed: coupling through particle phase space vs. coupling through both phase space and MHD mode-mode couplings. The results show different mode dynamics, including of growth-rate, saturation level etc.

Plans for 2018:

- EGAM

Linear and nonlinear simulations of EGAM driven by a single-pitch-angle anisotropic slowing down EP are planned.

- Zonal flow

Both saturation levels of the forced-driven zonal flow and the modified Alfvén mode are needed to compare with the analytical results and/or the simulations by other codes.

- Mode-mode coupling

Test-particle analysis will be used to study the particle dynamics in the multi-mode simulations.

1. The reduced equations mean that only the evolution of electrostatic potential has been kept in the MHD equations.

2. Both BAE and TAE simulations have been performed.

General discussion

- other WP updates
- planned travel for 2018
- conferences: EPS/IAEA/Varenna/APS
- any other business?

additional material

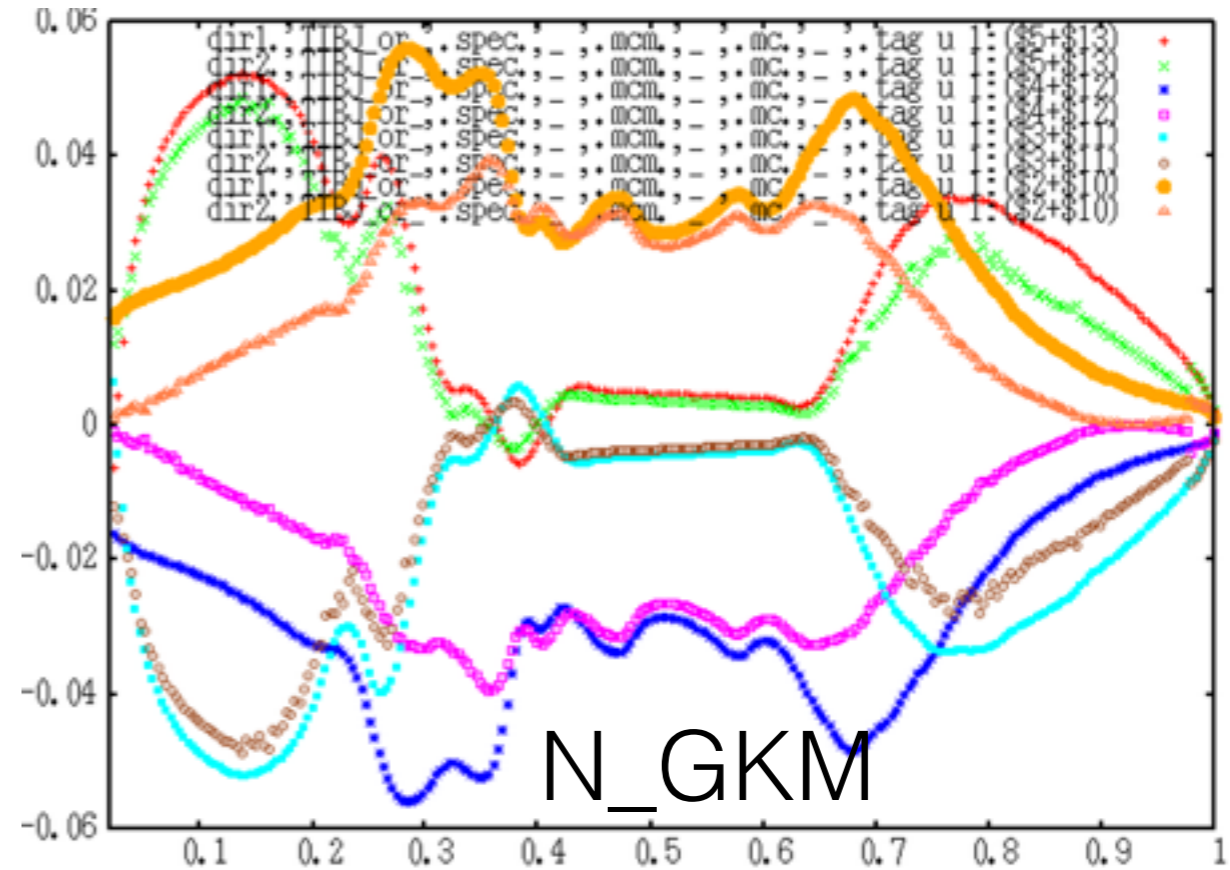
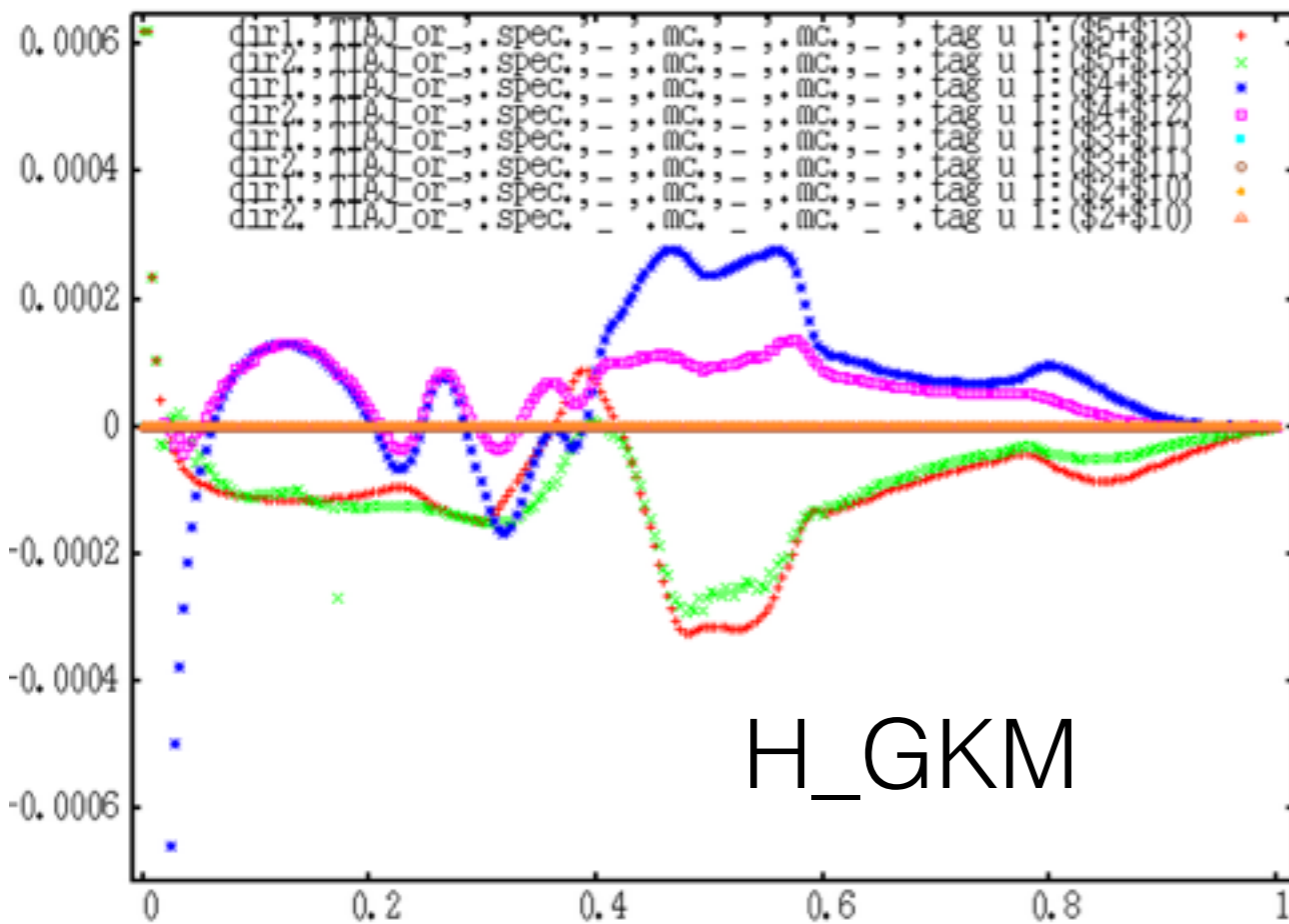
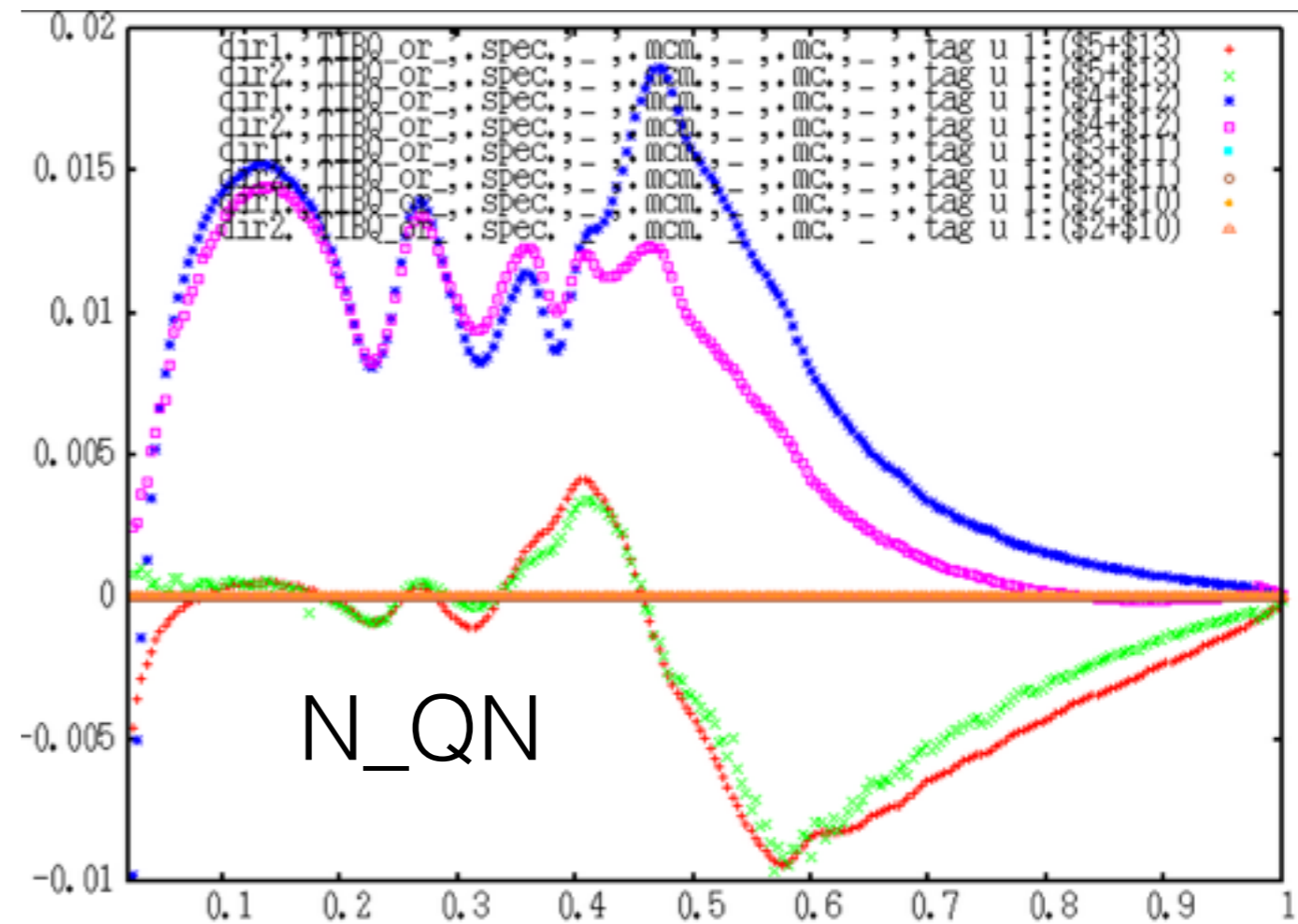
$$\omega = (0.05 - 0.005i) \omega_A$$

$$\omega_{th}/\omega_A = 0.07$$

JT60U Eq, deuterium

ψ $n=3$

- analytical Re
- analytical Im
- numerical Re
- numerical Im



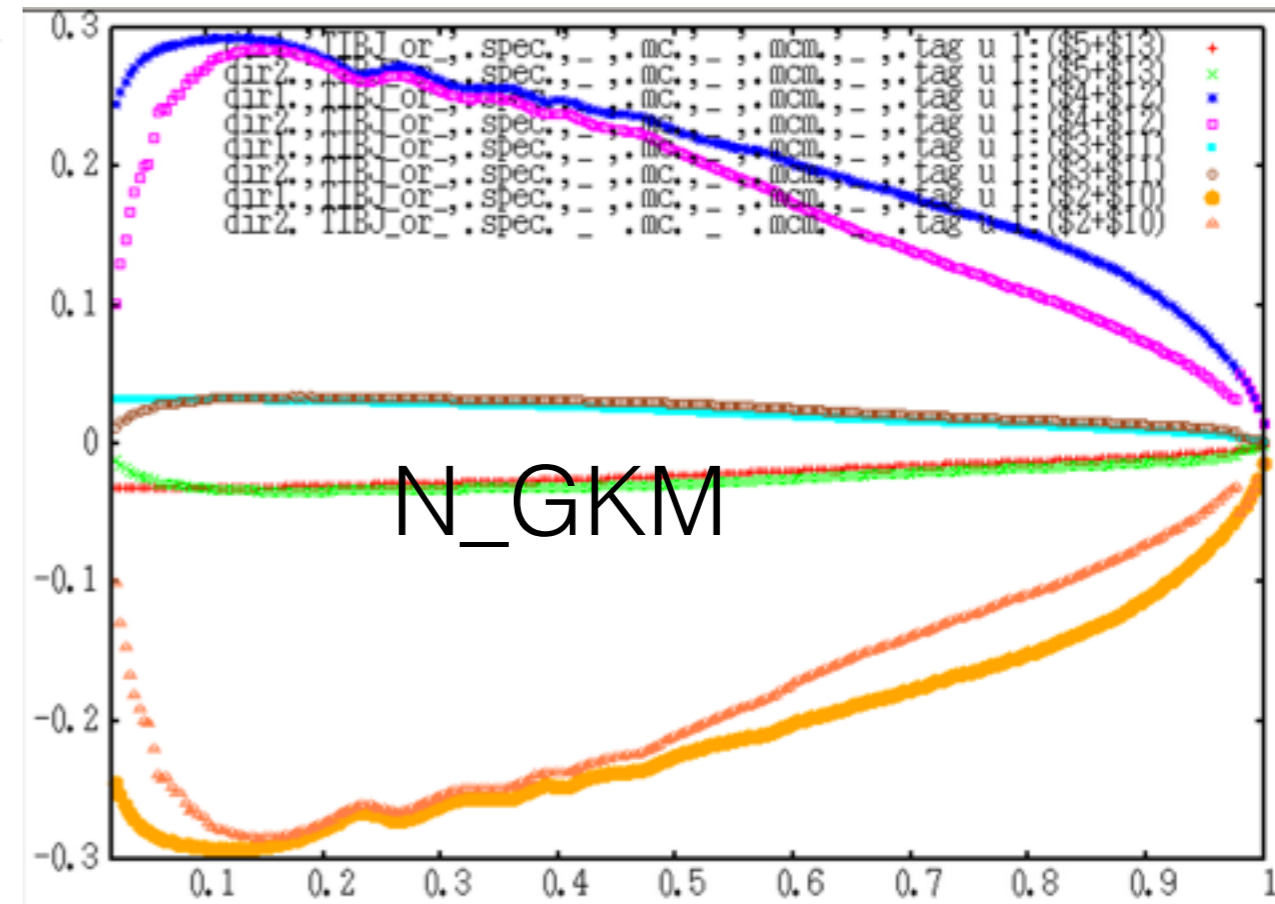
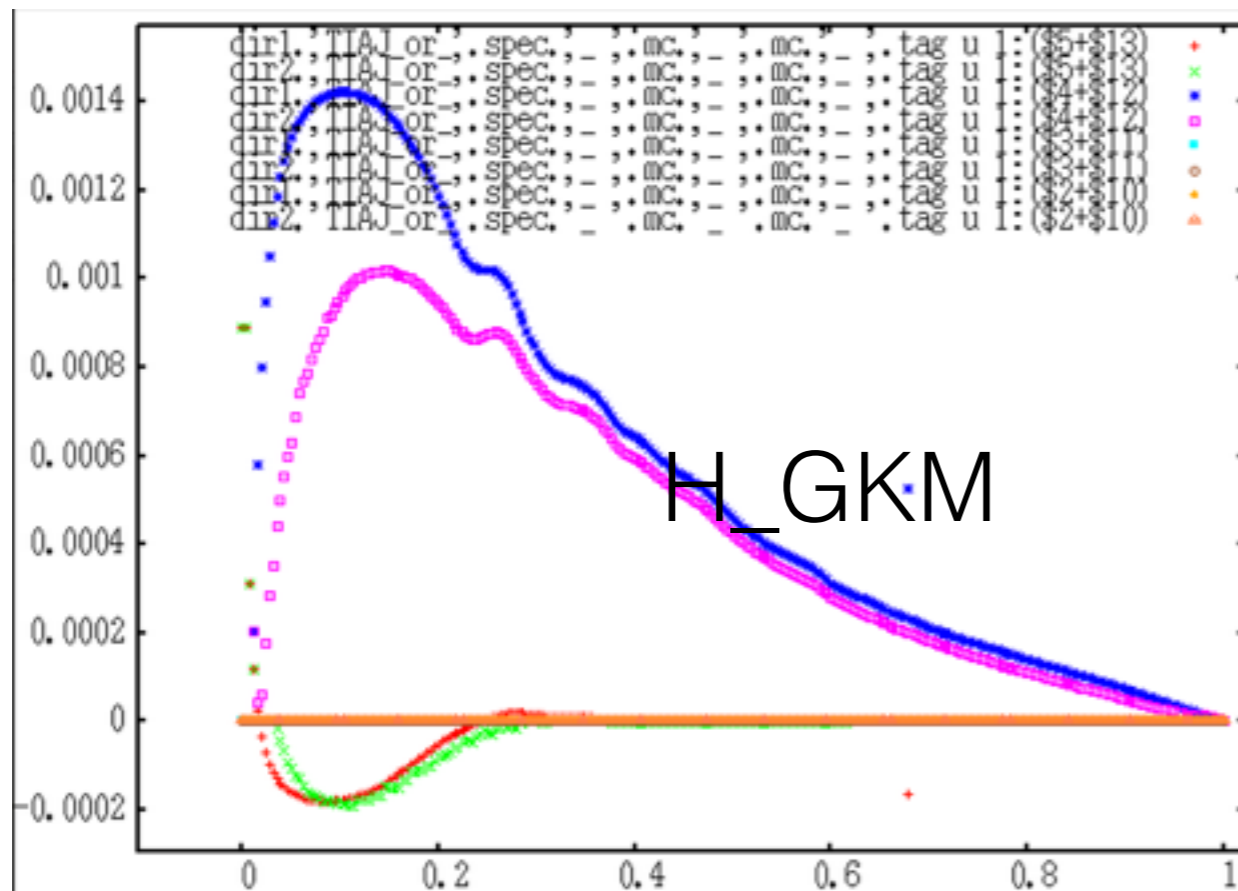
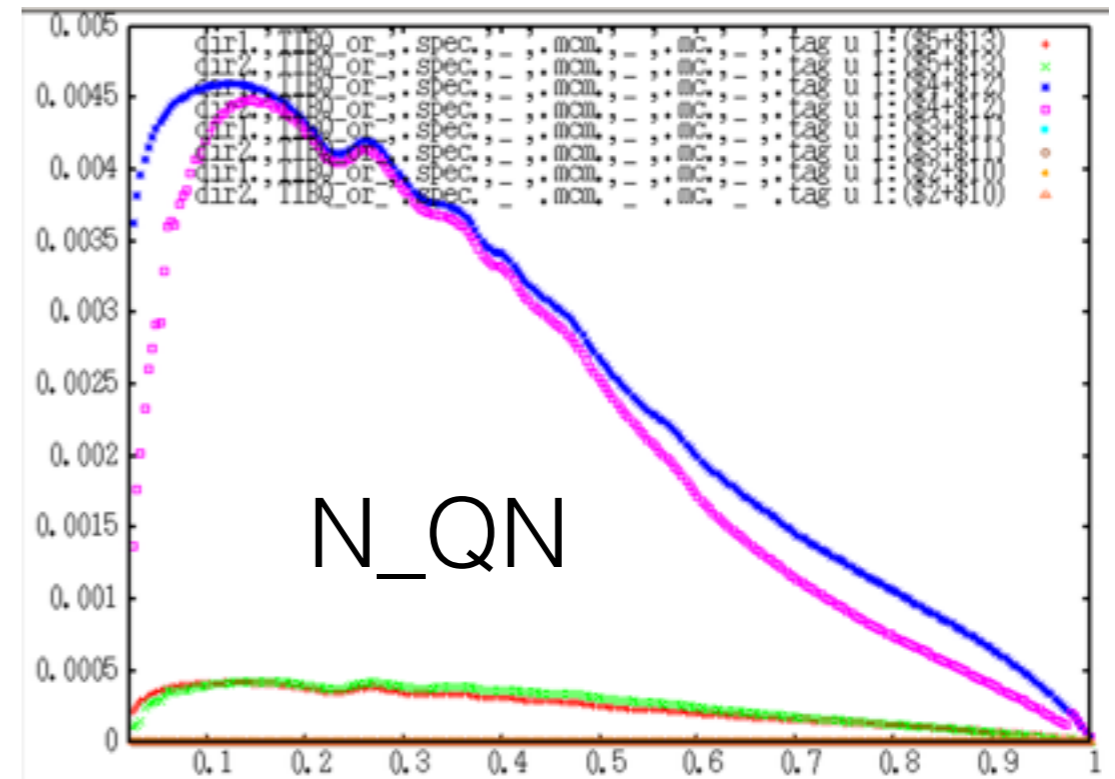
$$\omega = (0.25 - 0.025i) \omega_A$$

$$\omega_{th} / \omega_A = 0.07$$

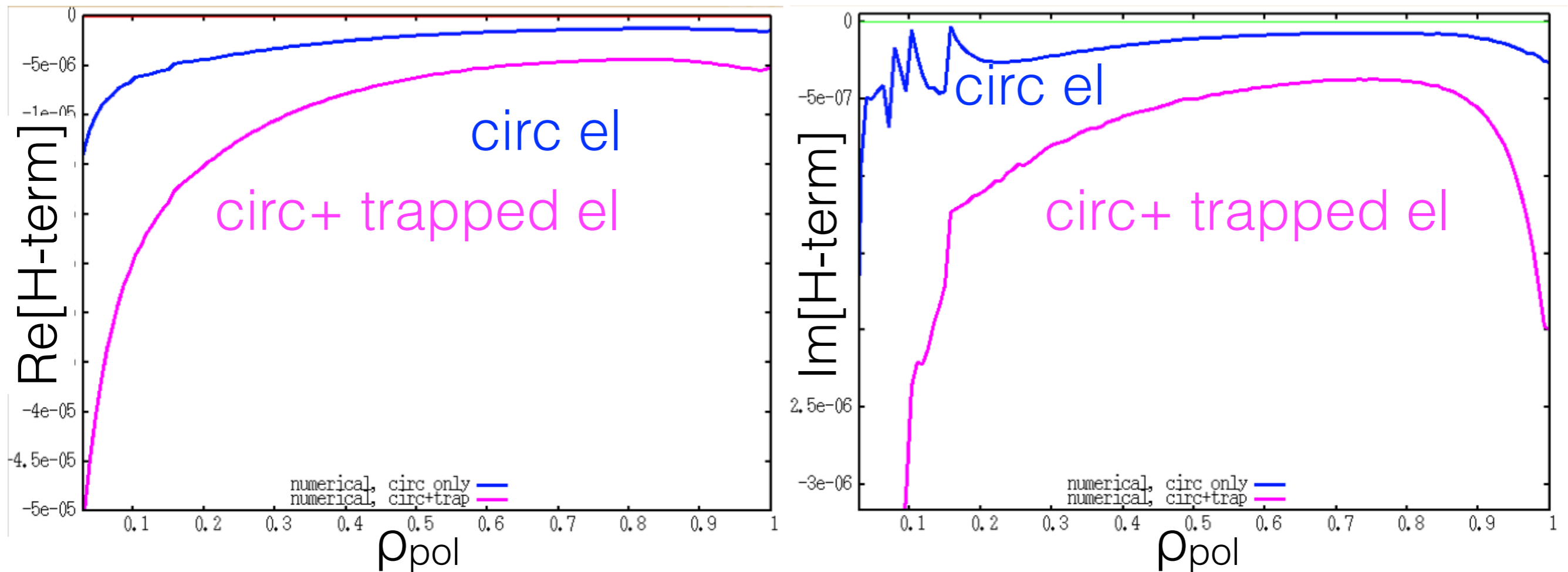
JT60U Eq, deuterium

ψ $n=3$

- analytical Re
- analytical Im
- numerical Re
- numerical Im



compare v-space integrals for v_{dr} moments:



main contribution comes from trapped electrons

$$\omega^2 \left(1 - \frac{\omega_*(1 + \eta)}{\omega} \right) - k_{\parallel}^2 \omega_A^2 R_0^2 = 2 \frac{v_{thi}^2}{R_0^2} \left(- \left[H(x_{m-1}) + H(x_{m+1}) \right] + \tau \left[\frac{N^m(x_{m-1}) N^{m-1}(x_{m-1})}{D(x_{m-1})} + \frac{N^m(x_{m+1}) N^{m+1}(x_{m+1})}{D(x_{m+1})} \right] \right)$$